# Design and Implementation of Small Satellite Inspection Missions

by

Michael Christopher O'Connor

B.S., Astronautical Engineering and Mathematical Sciences (2010)
United States Air Force Academy

Submitted to the Department of Aeronautics and Astronautics
in partial fulfillment of the requirements for the degree of

Master of Science in Aeronautics and Astronautics

at the

MASSACHUSETTS INSTITUTE OF TECHNOLOGY

June 2012





Author .....
Department of Aeronautics and Astronautics
May 24, 2012

Certified by .....
Alvar Saenz-Otero
Research Scientist
Thesis Supervisor

Certified by .....
David W. Miller
Professor of Aeronautics and Astronautics
Thesis Supervisor

Accepted by .....
Eytan H. Modiano
Professor of Aeronautics and Astronautics
Chairman, Department Committee on Graduate Theses

**Design and Implementation of Small Satellite Inspection Missions**

by

Michael Christopher O'Connor

Submitted to the Department of Aeronautics and Astronautics
on May 24, 2012, in partial fulfillment of the
requirements for the degree of
Master of Science in Aeronautics and Astronautics

## Abstract

For a variety of missions, vision-based navigation and similar architectures provide the advantage of detailed measurements for a fraction of the size and complexity of ground-based imagers. This thesis provides a simple navigation algorithm using no more than a visual centroid measurement to enable in-situ inspection of space objects.

This work evaluates those inspection maneuvers using the Synchronize Position Hold Engage Reorient Experimental Satellites, known as SPHERES. Evaluation of hardware performance was done using data from the International Space Station, in concert with ground-based simulations. Ultimately, this work is in preparation for future experimentation using the VERTIGO vision-navigation payload for SPHERES.

The first step presented is an analysis of the measurement capabilities of the SPHERES system and the predicted performance of the VERTIGO system. Using this analysis it is shown that tests run using the former system are applicable to the latter in terms of accuracy, precision, and observability.

The second step is an analysis of the tests run on the Space Station, a comparison to those predicted by simulation, and an extension of those results to simulations of more complex maneuvers. Further, a determination of the robustness of the control to disturbances is also performed.

Finally, this thesis reflects on the technical and programmatic challenges of developing the VERTIGO payload. From these challenges, lessons are drawn which may guide future developers and program managers, particularly in the university engineering environment.

Thesis Supervisor: Alvar Saenz-Otero
Title: Research Scientist

Thesis Supervisor: David W. Miller
Title: Professor of Aeronautics and Astronautics

## Acknowledgements

While this work may be of my own hand, there were many along the way who contributed: technically, emotionally, and even so far to make sure I didn't electrocute myself. I'd like to first thank my parents for their constant support throughout my educational journey, all the way to becoming an Air Force officer. You two are the ones who spent so much time in the air that flight seems to be the natural state for the family. Mom and Dad, thank you both for your guidance, my education, and starting me on this journey. To my sister, Jessica, thank you for keeping me honest and ensuring when I do something crazy, it's not *too* crazy. Here's to more years of that and more adventures around the world.

To Maria, thanks for making sure I didn't just study while at MIT, and for the support and understanding you've shown throughout my two quick years here. I have enjoyed so much more because of you. I'll see you in California.

To my advisors, Professor David Miller and Dr. Alvar Saenz-Otero, thank you for your support and advice about my research. More importantly, thank you for your leadership guidance. Whether I recognized it at the time or not, you kept me and the program on track. To Paul Bauer, thanks for making sure I never broke anything too expensive.

To Matt K., thanks for always having leftovers. You've been a great roommate and helped keep me sane through the whole MIT experience. To the VERTIGO team at MIT and Aurora, thank you for bearing with me as I learned how to properly manage an engineering program. Thanks for pushing to make VERTIGO a success. Brent and Konrad in particular, thank you for your help bringing the project to where it is today.

To Colonel Condit, thank you always for your support, kind words, and for enabling some of the great opportunities that I know lay ahead and for making sure that I always have the best role models as I go forward in my Air Force and engineering career. I still remember what you wrote those two years ago, and seek to be that professional. And in spite of the stress, I'd consider myself one of the happiest people I know.

To the SEA officers past and present, thanks for your friendship and everything else that comes with being a member of the SEA team. Thanks to Bruno and the rest of the SSL as well. And thanks to the MIT fencing team for letting me join you for the past two years. I'd also like to thank the individuals and organizations who have enabled me to further my education and research, from USAFA and FalconSat to DARPA and SMC.

THIS PAGE INTENTIONALLY LEFT BLANK

# Contents

THIS PAGE INTENTIONALLY LEFT BLANK

# List of Figures

THIS PAGE INTENTIONALLY LEFT BLANK

# List of Tables

THIS PAGE INTENTIONALLY LEFT BLANK

# Chapter 1

# Introduction

## 1.1 Motivation

Since the launch of the first artificial satellites over 50 years ago, there has always been a national interest in maintaining the high ground in every sense of the phrase. In resource constrained environments, certain advanced concepts provide value disproportionate to their costs. Vision-based navigation, especially on small servicing satellites hold the promise of being one such concept that delivers value in a way no other type of small system can.

### 1.1.1 Relevance of Spacecraft Relative Navigation and Inspection

Spacecraft design, launch, and operation are expensive and often risky undertakings. A major space-based observatory such as the Hubble Space Telescope, which has a lifetime cost estimated at $11 billion represents a significant investment of human and financial capital[1]. Hubble's successor, the James Webb Space Telescope is expected to cost even more[2]. In the latter case, as Lagrange point orbit puts it far out of the reach of current manned spacecraft and therefore would need to be serviced robotically if a problem were to arise. The signal delays associated with such an orbit, coupled with complex orbital dynamics about a Lagrange point preclude teleoperated systems. In order to effectively diagnose failures, a free-flying spacecraft must be able to autonomously inspect the damaged craft.

This ability to observe and repair a damaged spacecraft via a small inspector presents a risk mitigation strategy for future missions. Commercial ventures may also be more cost

effective in the case of servicing and attendant volume savings[3], while in-situ spacecraft salvage is currently an open research field[4]. In each case, solving the problem requires the ability to inspect a spacecraft of unknown condition from a distance that is far enough away to preclude a collision risk, but close enough to provide accurate resolution.

Long duration missions in earth orbit, such as those on the space station, lend themselves to human EVA to repair and maintenance. Missions travelling out of Earths magnetic field which require repairs would put astronauts at greater risk on two fronts: increased environmental risk to the spacewalker and an inability to return injured astronauts quickly to Earth. Autonomous inspector vehicles with the ability to identify problems through computer vision or other sensor systems provide a safer alternative for diagnosis, with the potential for follow-up repairs by crew.Before that can be realized, the inspection problem should first be solved in the relative safety of low earth orbit.

Large modern spacecraft are designed with significant redundancies as the forces of time and the space environment combine to cause part and system failures. Redundancy provides an element of reliability, but at the cost of increased mass and complexity as entire systems and subsystems must be duplicated. The ability to repair or replace single failed parts rather than design backup systems into a satellite has the potential to reduce costs by reducing the launch mass. Commercial systems on the ground often take this approach — after all, a car has but one engine. Even if redundancy is built in, the ability to install replacements, as was done during Hubble servicing missions can extend mission lifetimes many times the design lifetime for a fraction of the cost of a new system.

In each of the potential applications of in-situ inspection described above, the operating environments are very different. In each, however, the use of relative measurements between inspector and target are preferable to more global sensors or any earth-based observatories. In GEO orbits GPS measurements suffer from position errors on the orders of meters to tens of meters[5], errors which are compounded by solar fluctuations and their attendant ionospheric disturbances[6]. For close inspections such errors are unacceptably large, especially when collision avoidance is a high priority. Additional problems arise when an inspection target is uncooperative and GPS measurements or other global measurements are therefore unavailable[7]. Star trackers may be problematic in determining relative position to a target: if they are not overwhelmed by reflected solar light from the inspection target, their view of the starfield may be obstructed by a complex shape.

Ground-based radars are also of limited utility because of the distances and perspective involved. When the inspector eclipses the ground station, the problem is only further complicated. As mentioned before, using ground-based sensors also introduces time delays due to light-speed propagation and processing time[8]. In GEO this delay is on the order of seconds; for missions beyond that point, the delays grow significantly longer in proportion to the increased distance.

These physical constraints point to the need for space-based inspector vehicles using relative measurements to maneuver around a target object, and to do so safely (without colliding) and uncooperatively (no information passed from target to inspector). Furthermore, in contrast to other methods[9], the inspection should be performed with no *a priori* knowledge of the target.

## 1.2 Objectives

To satisfy the mission requirements for a space-based inspector, there are a handful of tasks which this thesis aims to address.

### 1.2.1 Develop Relative Navigation and Inspection Algorithms

The first objective is to develop algorithms to perform inspections of an unknown, potentially spinning and tumbling, target object in order to build up a 3D map of the target. This task is split into two parts:

1. **Relative Navigation** The ability to move about using measurements of a target object in the body frame of the inspector. These measurements must not be in reference to any "global" frame, but instead must be described as movements of the target in the inspector's field of view.

2. **Inspection** The movement of the inspector about the target object for the purpose of providing a vision payload with a view of the target.

An algorithm which combines these two approaches should enable an inspector to view all surfaces of a target object, and do so with no reference other than target itself, as well as onboard inertial navigation sensors like gyroscopes and accelerometers. The

combination of Inspection and Relative Navigation elements should allow for planning of paths around an unknown object.

Additionally, the algorithm should be as simple as possible to reduce the processing burden and make the algorithm applicable to as many space systems as possible.

Notionally, the algorithm should not require any information about the target object's rotation states. By discarding or not collecting this information, the algorithm should allow for inspections on a larger set of objects, including those that are rotating at high rates.

### 1.2.2 Characterize System Performance and Sensor Noise

This thesis must also develop a model of the vision system to be used and to compare that model with the existing SPHERES satellite system, both in simulation and in ISS testing.

Characterizing sensor noise allows for the application of the SPHERES system to the to-be-launched vision system that this thesis seeks to support. By comparing the noise sources and noise characteristics of the SPHERES metrology and inertial sensors to those predicted in a vision system, an understanding of the expected performance of the integrated inspection system can be gained.

### 1.2.3 Quantify Algorithm Performance

In order to apply the navigation and inspection algorithms that this thesis develops, the performance of the inspector system must be assessed with a number of characteristics in mind. The most significant of those performance characteristics are:

1. **Fuel Efficiency** Minimizing fuel use in an inspection maneuver is preferred. This will be measured in the amount of $CO_2$ fuel used by the test satellites.

2. **Time Efficiency** Faster inspections are desired, though more inspection time provides better coverage. Algorithms which minimize the time to complete an inspection are preferred.

3. **Coverage** Each algorithm must provide a full view of an unknown target object to the inspector satellite. This serves as a constraint on each maneuver. It can also be used to discriminate between inspection paths based on the quality of inspections — better inspections provide less oblique views of the target object's surfaces, and may provide multiple views of the same surface.

These factors will be quantified, and used to compare the performance of different algorithms against one another, as well as the reactions of the given algorithms to target object behaviors. Additional factors, such as the complexity of the algorithm, code size, and collision risk may also be taken into account, but only to discriminate when the three above qualities are insufficient.

## 1.3 Previous Work

Previous work done with vision systems has been used for purposes that vary from space station assembly (Canadian Space Vision System[10]) to autonomous rendezvous and docking (DARPAs Orbital Express[11], among others[12]). Relative navigation using vision sensors may also be the control of autonomous underwater vehicles, with applications in iceberg-relative navigation[13],[14] and benthic surveys[15],[16]. Research with application to vision is ongoing in rendezvous to a tumbling object[17], formation flight[18]. What is well understood is the use of vision and other sensing methods to safely approach a target prior to a rendezvous maneuver[19]. The success of these methods has been integral to the US space program, especially in the Shuttle/Station era. Difficulties, however, arise when the inspection target has an unknown form and no fiducials for easy reference in navigation. Studies addressing this problem often rely on pre-planned trajectories[20] around the object or are not easily adaptable to modification of the inspection path based on the tumbling motion of the target object.

This thesis will outline an algorithm for use in vision-based navigation applications to perform inspections while maintaining a safe keep-out distance. The algorithm makes use of range and bearing data which would be available to calibrated stereo cameras, along with a 3-axis gyroscope onboard the inspecting satellite. The approach will be based on a rotating inspector that maintains a body-fixed orientation with respect to a target object. Success will be evaluated primarily on the ability to maintain a safe distance, to maintain a closed planar path, and demonstrate robustness to certain disturbances. The algorithm is tested on the SPHERES satellite simulation and onboard the International Space Station (ISS). The ultrasonic, time-of-flight based navigation system is used on the ISS for truth measurements.

While more precise algorithms and optimal approaches exist[21], paper focuses on the

development of a simple inspection algorithm for use in a wide range of systems in which the control system may be computationally constrained and to experimentally demonstrate the effectiveness of that algorithm in a microgravity environment.

The first contribution of this thesis is the development of an algorithm for inspection that only requires a vision system to compute the range and range rates using a simple stereo algorithm that can easily be implemented in an embedded system with limited processing power. The computational simplicity of this algorithm is due to the fact that it does not need to compute the relative orientation[22], between frames. Instead, it dead reckons its position on a spherical surface surrounding the target object using its gyroscopes. The secondary contribution of this paper is an experimental validation of this algorithm in a microgravity environment (i.e. the International Space Station) using a gyroscope and simulated range measurements. This experiment showed that the amount of vertical drift during a 3 minute test was less than 10 degrees for a stationary target, with 25-minute simulations showing less than 12 degrees. The third contribution of this paper is an error analysis to compare the estimation accuracy between the simulated range measurements and what is expected of an actual stereo vision system.

# Chapter 2

# Relative Navigation

## 2.1 Vision System Outputs

Stereo cameras, LIDAR/RADAR, structured light systems, and other "vision" systems provide information about objects in their field of view that include depth, motion, and a host of surface properties. Each of these systems addresses the same problem using different hardware, but the principles are the same. Just as LIDAR provides relative distance measurements to a target's surface, a two-camera (or more) system will provide 3-dimensional measurements from a reference point to surface features on the target object that are in view. This is achieved by triangulating a feature which appears in the field of view of both cameras using knowledge of the distance between the two cameras and where the object falls on the focal plane of both imagers. Using trigonometric relationships, each feature can be assigned an estimated distance with respect to some pre-defined reference point. This reference point is customarily placed in the upper left of the leftmost camera, and range and bearing to a target are the set of 3-D measurements provided by the cameras. As they are later implemented in the relative navigation algorithm, this range and bearing is translated into range and horizontal translation measurements.

A typical stereo vision system provides synchronized images from each camera. Each camera and lens, however, distorts the true image. Therefore, in order to accurately determine the range and bearing to features, the cameras must first be calibrated. This is accomplished by providing a set of known features, most commonly a checkerboard pattern, and taking a set of images. Since the image of the checkerboard is distorted by the lenses and cameras, a recursive batch algorithm can be applied to the image set to provides

a least-squares estimate of the distortion parameters. After determining these parameters and creating matricies to undo the distortion, future images can be quickly adjusted to remove their effects. This process, the particulars of which will not be described in significant detail in this thesis, results in image pairs which are undistorted and rectified and are able to be used for the aforementioned ranging.

After the calibration, since distortions may be considered removed, the images can be treated as the output of a pinhole camera.

## 2.2 Simulation of Vision Measurements

Because of the launch schedule of the vision system hardware (described later, in Chapter 4), we do not yet have the capability to use the VERTIGO Goggles stereo cameras on orbit. Instead, the SPHERES global metrology system was used to simulate stereo vision measurements. It uses a time-of-flight ultrasonic ranging system system. Using measurements from a set of five ultrasonic beacons placed around the ISS test volume, the satellites are able to determine their position. Background telemetry over a wireless link allows each SPHERE to find the location of others in the test area. Differentiating (via an Extended Kalman Filter) provides velocity measurements, while the time of flight difference between faces of the SPHERE provides pointing information. To translate from the global to relative frame, there are a few steps.

The first step is to convert the global position measurements into the body frame. The process is illustrated in Figure 2-1, which shows the Inspector, Target, and the Inspector's body frame. The vector difference allows us to find the length and direction of $\mathbf{r}_B$ in the inertial ISS frame:

$$\begin{aligned} \mathbf{r}_{B(ISS)} &= \mathbf{r}_{A(ISS)} \\ &= \mathbf{r}_{TGT} - \mathbf{r}_{INSP} \end{aligned} \tag{2.1}$$

$$\begin{aligned} \dot{\mathbf{r}}_{B(ISS)} &= \dot{\mathbf{r}}_{A(ISS)} \\ &= \dot{\mathbf{r}}_{TGT} - \dot{\mathbf{r}}_{INSP} \end{aligned} \tag{2.2}$$

The origin of the coordinate frame, though not important to the relative state, is located at a point in the center of the test volume framed by the SPHERES ultrasonic beacons. Using the quaternion calculated by the ultrasonic metrology system, a rotation matrix from the

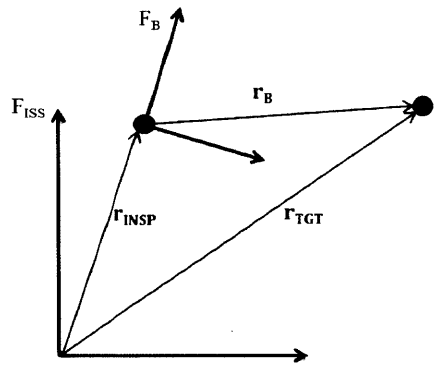


Figure 2-1: Inertial and relative frames

ISS (global) frame to the body, $\mathbf{R}_{G2B}$, places $\mathbf{r}_B$, which is the vector from the inspector to the target in the body-fixed reference frame of the inspector.

$$\begin{aligned} \mathbf{r}_B &= \mathbf{r}_A \\ &= \mathbf{R}_{G2B}[\mathbf{r}_{B(ISS)}] \end{aligned} \tag{2.3}$$

Since B is a rotating frame, the velocity measurement is not as straightforward, and again requires gyroscope measurements to measure the rotation rate. Using the rules for differentiation in a coordinate frame,

$$\dot{\mathbf{r}}_A = \mathbf{R}_{G2B}(\dot{\mathbf{r}}_{B(ISS)}) \tag{2.4}$$

$$\begin{aligned} \dot{\mathbf{r}}_B &= \dot{\mathbf{r}}_A - \omega \times \mathbf{r}_B \\ &= \mathbf{R}_{G2B}(\dot{\mathbf{r}}_{TGT} - \dot{\mathbf{r}}_{INSP}) - \omega \times \mathbf{R}_{G2B}(\mathbf{r}_{TGT} - \mathbf{r}_{INSP}) \end{aligned} \tag{2.5}$$

These measurements are then differenced with the desired states to determine the state error. A standard linear PD controller was then used to calculate thruster inputs for the position error, and a nonlinear PD controller was used to control only for the rotation rate (though the controller is effectively proportional as implemented). While more optimal controllers are available, the use of PD controllers allows the implementation of the algorithm on a wider range of computing platforms, achieving the stated goal of maintaining simplicity in implementation. An additional feedforward term was used to maintain the circular motion. This thrust, applied in the inspector's body +X direction (nominally to-

ward the target), provided the centripetal force to ensure a circular path:

$$\mathbf{F}_x = m\mathbf{r}_{x,goal} * \omega_{goal}^2 \tag{2.6}$$

Forces and torques were then mixed by the propulsion system, which schedules thruster opening times for a period of up to 200ms every during each 1-second control period.

Once the VERTIGO Goggles are launched to the station, the output from the cameras will be processed using the Goggles single-board computer. This computer will process the images and will output the range, $\mathbf{r}_B$, and range-rate, $\dot{\mathbf{r}}_B$, using previously developed thresholding and centroiding algorithms and eliminating the need for the transformations described in equations 2.1 through 2.5. Initial prototypes of this technique have demonstrated the capability to provide such relative measurements.

## 2.3 Relative Navigation about Unknown Objects

The nature of unknown objects means that they may have certain qualities that preclude simple tracking of features in order to navigate. Quickly rotating objects in particular pose difficulty to certain classes of algorithms. Systems which have a low framerate compared to the rotational rate of the target will have difficulty tracking a given feature from frame to frame. Take for instance, an image processing algorithm that can account for 10 degrees of angular motion between frames or less, and a system that operates at 10 frames per second. Since the maximum rotational speed, $\omega_{target}$, is defined by

$$\omega_{target} = (FPS)(\theta_{limit}) \tag{2.7}$$

An algorithm dependent on feature tracking for relative navigation will fail if the target object spins faster than $100°/s$, or about 17 RPM in a single axis. Of course higher framerates or more advanced tracking and estimation tools could be used, but to do so would be computationally intensive, requiring a larger, more complex system and all of the attendant support systems from thermal control to power storage and distribution. For complex motion, multifaceted or complicated shapes, unfavorable surface textures, or poor lighting conditions, processing requirements might push the maximum allowable frame-to-frame angular displacement far lower.

Alternatively, a tracking algorithm which does not require tracking of features from frame to frame could be used in order to move relative to the rotating target. This is the approach taken by the VERTIGO team.

First, operating at about 5 frames per second, the system identifies features in each image. Next, a filter is applied to the image to exclude those features outside of a set range (typically beyond 1m from the Inspector, while the size of the baseline excludes those too close to be observed simultaneously in both cameras). This is done to eliminate background features associated with testing in an enclosed volume like the International Space Station, a problem not encountered in an "outdoor" orbital environment where a starfield at effectively infinite distance is the only background. Next, features are blurred or blended together and a centroid is calculated. This centroid is then used to estimate range and translation to the target. The specifics are beyond the scope of this thesis, but the process unfolds as shown in Figure 2-2.

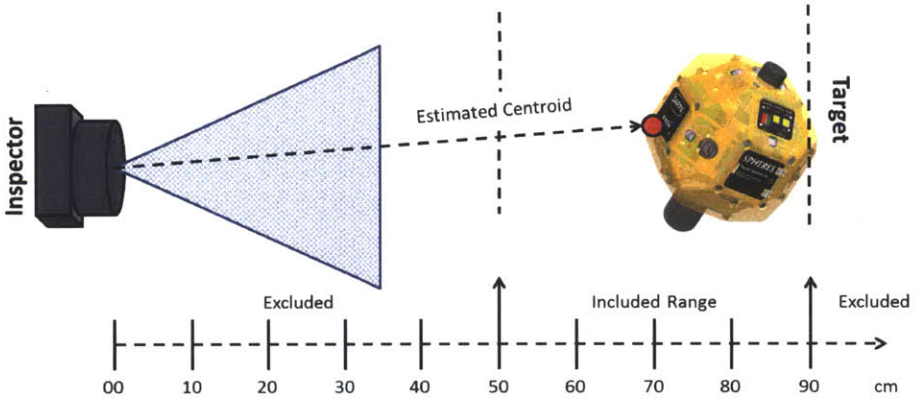


Figure 2-2: Filtering and Centroiding

### 2.3.1 Addition of Dead Reckoning

If the only goal of an inspection was to maintain orientation and relative distance, then processed vision information would be all that is needed. However, in order to perform maneuvers around a target object, dead reckoning is necessary. Single integration of gyroscopes is particularly useful when estimating the motion of the Inspector about the target. This is because if control is maintained with regards to range and pointing, calculating the rotation of the Inspector will provide an estimate of the location in an inertial frame whose origin is co-located with the center of the target object. This inertial location can be used to

develop paths which are most likely to provide global coverage of the target object.

The addition of dead reckoning is straightforward: as gyroscopes typically operate at a high frequency, measurements can be averaged or filtered over short periods. Given the estimation of the rotational rate of the Inspector, a simple integrator ($\frac{1}{s}$ in frequency domain, $\Sigma$ in time) may operate on the filtered rates to estimate the angular displacement. Since the rotational displacement is so closely related to the linear displacement in a well-controlled system, the motion in inertial space also falls out. A conversion from spherical to Cartesian coordinates shows this relationship:

$$\theta = \sum_{t=0}^{T} \omega_z \tag{2.8}$$

$$\phi = \sum_{t=0}^{T} \omega_y \tag{2.9}$$

$$x = r \cos\phi \sin\theta \tag{2.10}$$

$$y = r \sin\phi \sin\theta \tag{2.11}$$

$$z = r \cos\theta \tag{2.12}$$

Should the rotation rate about the body X-axis not be kept to zero, additional terms would need to be included to account for multi-axis coupling.

Inverting the relationships allows for planning of any trajectory in a coordinate frame that is body-centered and non-rotating with respect to the target object. This method, it should be noted, is sensitive to gyroscope noise, and will drift accordingly over extended periods of time. Tracking features on the target object may in some cases be able to augment gyroscope measurements, and be filtered to provide better accuracy over longer periods of time. The addition of target object rotations will allow for additional planning, but that is beyond the problem scope.

### 2.3.2 Addition of Target Rotation Information

The addition of the rotation of the target has two implications. The first is that by integrating the rotation of the target object and combining that information with the dead reckoning estimation from the Inspector's gyroscopes, maneuvers and navigation can be designed to take place in the target's body frame rather than in an arbitrary inertial frame.

This is of particular import for optimal design of inspections, as well as ensuring full coverage. Without the knowledge of the rotation of the target relative to the Inspector, there may be segments of the target which remain uninspected. Indeed, in certain cases where the inspection motion matches the target's rotation an inspection may fail to view more than a single side of the object of interest.

The knowledge of rotation can be two-tiered. A precise, accurate estimation of the rotation rates of a target are necessary if that information is to be used actively and continuously for the purposes of path planning. Such an approach is processor-intensive and decidedly not simple. It will not be dealt with in this thesis.

On the other hand, the use of a general estimation of the rotation of the target object can be used to improve efficiency of inspections (this will be discussed in a later section), as well as for insuring better coverage by fixing the inertial frame in a fourth degree of freedom, rather than just the original three.

THIS PAGE INTENTIONALLY LEFT BLANK

# Chapter 3

# Inspection

Inspection is the movement about an object for the purpose of observing its surface and developing an estimate of its form, function, or other qualities. For the purpose of the VERTIGO program, the goal of an inspection maneuver is to build a 3-dimensional map of the target by collecting, storing, and processing information about its surface features.

Four inspection maneuvers were developed for implementation on the SPHERES system (and later use on the SPHERES-VERTIGO combined system). Those maneuvers follow paths described by the following:

1. **Stationary** This maneuver holds the Inspector satellite stationary in the relative frame, only maintaining distance and pointing.

2. **Planar** This inspection is done by imparting a rotation in one axis, causing the Inspector to move in a plane.

3. **X-shaped** This maneuver requires integration of the Inspector's gyros to estimate movement about the target in an inertial frame. Rotations are imparted into inspector body axes one at a time, switching after 90° and 360° of rotation.

4. **Hemispheres** This maneuver uses gyroscopes onboard the inspector and an estimate of the target's rotation. Using the rotation estimate, the inspector aligns with the rotational axis, then performs inspections in the "northern" rotational hemisphere, followed by the "southern" hemisphere and equator, switching when the sum of the estimated rotation of the target and the Inspector indicates 360° of the target have passed in front of the camera.

While the first was developed merely for demonstration purposes and would fail to provide significant coverage unless the target satellite was rotating and tumbling between multiple axes, the latter three maneuvers are compared based on their performance according to coverage, fuel use, and time to completion metrics.

## 3.1 Coverage Quantity

Coverage is the measure of the surface of a target object that is "visible" to an inspector satellite. Given a surface mesh, we can therefore assign a binary 'coverage' state: 1 if the mesh section is visible, 0 if it is not. In order to determine if a section of the mesh has been seen by the inspector, we must check the following qualities:

**Viewing angle**: Test data from initial Phase II (image processing) algorithms shows difficulty matching features in consecutive frames if the feature lies on a surface angled more than 30 degrees from perpendicular relative to the camera boresight. Therefore, to be considered "viewed," a point should lie on a surface inclined less than 30 degrees (see Figure 3-1[23]).

**Obstruction**: Because we are working with the visible spectrum and solid, opaque objects, we should omit those which are behind another object. Fortunately, the SPHERES system does not have any self-occluding surfaces or geometries, save very small sections around the $CO_2$ tank and the regulator knob, which will be ignored for this thesis. For our purposes, this excludes only surfaces on the opposite side of the SPHERE from the inspector.

**In view**: Clearly, to be considered viewed, the surface should be in view of the camera. Given the camera and lenses selected for the VERTIGO project, as well as the loss of the edges of the images due to distortion, an assumption of a 30 degree field of view (half cone) is reasonable.

Because the goal of the VERTIGO inspection is to create a 3-D map of a target object, obtaining 100% coverage is desired. This requirement therefore determines when an inspection is completed. For the cost analysis, coverage serves as a constraint on the optimization. Considering the likelihood of some sensing and approximation error, an inspection shall be considered complete when 95% of the surface has been inspected.

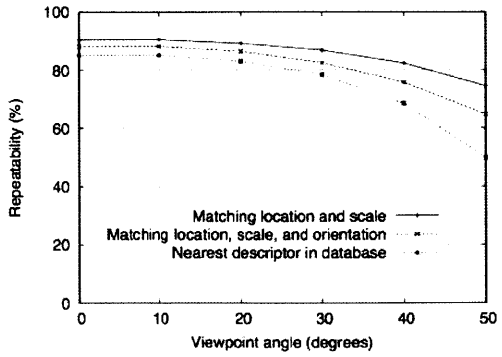


Figure 3-1: Feature Tracking and Reacquisition by Angle

## 3.2 Fuel/Time Tradeoff

In any satellite, fuel is at a premium, and so any evaluation of the efficiency of an inspection should take into account the fuel used for maneuvering.

In order to estimate the amount of fuel used in a particular inspection maneuver, there are two methods available. The first, most accurate way is to measure the amount of time a thruster is held open and how many thrusters are open simultaneously. Based on previous work[24], we know that the fuel used follows:

$$\dot{m}_{thruster} = (-0.033n + 0.5555) \tag{3.1}$$

$$\dot{m}_{total} = (-0.033n + 0.5555)n \tag{3.2}$$

Where n is the number of thrusters open simultaneously. Using this equation as well as the thruster firing times, we can get a good estimate of the total fuel used. For station tests, however, this data was not collected, and simulation does not normally collect this information. What is collected, however, is an estimate of the thruster firing times called "thruster counts" ($c$). With 1 count equivalent to a singe thruster open for 1ms, and a full tank approximately equal to 500,000 counts, we find that each count is equivalent to:

$$c = n_{open} * t_{\mathrm{ms}|open} \tag{3.3}$$

$$500000 * c = 170 m_{fuel|\mathrm{g}} \tag{3.4}$$

where $n_{open}$ is the number of open thrusters, $t_{\mathrm{ms}|open}$ is the time each thruster is open

(in units of ms), and $c$ is a count. Fuel mass, $m_{fuel|g}$, is the mass of fuel (in g) in a full $CO_2$ tank.

For the majority of the inspection, 3 thrusters are expected to fire at any given time, and we assume they operate for about 30% of their 200ms control period every second. This yields 2942 counts per gram of fuel. Counts are reported in both simulation and state of health data returned during SPHERES tests. Therefore, by tracking the thruster counts, we may estimate the rate of fuel use.

Fuel, however, should not be the only consideration: in two of the most applicable inspection scenarios, fuel for a small inspector spacecraft would be a small portion of the overall mission fuel. In "hosted" spacecraft inspecting a "host" spacecraft like the International Space Station or an exploration mission, the host would likely hold large fuel reserves compared to what is required for relatively simple inspection maneuvers of the inspector about the host and refueling might be possible. For missions requiring the rendezvous of one spacecraft with another from different orbits, the fuel cost required to attain and maintain a proper orbit would be significantly larger than maneuvering fuel needs. With inspections similar to those used for SPHERES, the total $\Delta V$ is on the order of centimeters or meters per second, compared to orbital maneuvers which may range in the 10s to 1000s of $\mathrm{m\,s^{-1}}$ depending on object size and inspection speed. In each of these cases, the criticality of failures that demand a close visual inspection may hint at an element of time-criticality. Indeed, in the case of the Space Shuttle, such maneuvering thrusters (RCS) were even used for attitude control during launch, implying on-orbit maneuvering fuel was a minor part of the fuel needs [25].

Therefore, time should also be taken into account alongside fuel use. After all, in most orbits, over an extended period of time, station keeping requirements would cause fuel use to grow. Furthermore, if an inspection is non-time critical, the use of orbital dynamics are more fuel efficient and better suited for most inspections than active inspection and navigation methods. However, if a spacecraft is damaged enough to require an inspection, or other mission requirements dictate an inspection to be completed before the completion of one orbit, the inertial methods presented in this paper are better suited than others. Certainly in missions requiring long-duration transfers, active control is the only option.

As time grows linearly and is always non-negative, conversion for a cost function is straightforward. Fuel use is also non-negative and monotonically increasing.

Combining the two, we get the cost function,

$$J(m_{fuel}, t) = Qm_{fuel} + Rnt \tag{3.5}$$

With the constraint

$$C(x, t) = 0.95 \tag{3.6}$$

Where $C(x, t)$ is the ratio of coverage of the target object to its total surface area. The constant $n$ is equal to $0.063\text{g}\,\text{s}^{-1}$ and is used to compare time and mass under the assumption that a typical SPHERES will finish a full tank of fuel in 45 minutes of test time.

Given $n$, weights $Q$ and $R$ are then selected to weigh fuel consumption and time, respectively. If both are equal to 1, then fuel use and time are equally weighted when compared to a typical SPHERES test.

## 3.3 Inspection of an Unknown Target

### 3.3.1 Expected Improvements using Rotation Information

Of the three inspection paths tested, only the last takes the rotational state information of the target into account. By doing so, it is expected that this path will minimize the cost function compared to the other options. Most of the efficiency is expected to come from the fact that the Inspector can actively take advantage of the rotation of the target rather than moving in potentially inefficient paths. For instance, if both satellites are have their body Z axes aligned, if the target rotates about its $+Z$ axis, if the Inspector rotates about its $-Z$ axis at half the rate, it will see the be able to observe the entire "equator" of the Target in a third of the time it would take should they rotate in the same direction.

Additionally, the Inspector will be able to use that knowledge to not only perform faster and more fuel efficient motions, but it may perform transitions quicker because it allows the integration of the target's rotation to estimate coverage rather than only the Inspector's gyro information.

As noted earlier, it should be emphasized that the use of rotation information from the target object is not, nor should it be, required for a successful inspection. Such information can only improve an inspection, and shouldn't be the difference between success and failure. Without the information of the rotation states, however, full coverage can-

not be guaranteed without additional precautions, especially in cases where the rotation rates of the two satellites match in direction, and particularly those where they match in magnitude. Such cases can be avoided by varying the inspection speeds in order to eliminate potential resonances between inspector and target. Those approaches and the trades which inform their selection are, however, beyond the scope of this thesis.

### 3.3.2 Path Optimality

The paths that were developed are unlikely to be truly optimal, but only improvements compared to the baseline planar inspection. Indeed, a maneuver designed to follow the shortest path[26] would likely follow one like the that shown in Figure 3-2[27] rather than the currently implemented paths.

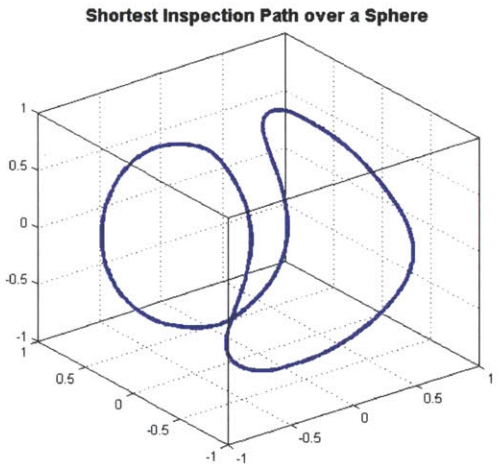


Figure 3-2: Shortest Inspection Path on a Sphere

Further complicating the solutions for true optimal paths are the rotation and nutation of the target object, which distort the "baseball seam" path, which is the shortest inspection course about a stationary target. Therefore, these results should only be considered first as relative value comparisons, and second as approximations of true optimal paths, not rigorously defined and derived fuel and time-optimal paths.

# Chapter 4

# Application to the SPHERES System

## 4.1 The SPHERES System

The Synchronize Position Hold Engage Reorient Experimental Satellites, or SPHERES for short, are the hardware upon which the navigation and inspection algorithms were developed and tested. To better understand the constraints of the research, as well as the realistic nature of the dynamics that are simulated, we first take a look at the current and future SPHERES program.

### 4.1.1 What is SPHERES?

The SPHERES satellite testbed was initially developed as part of a capstone design course in the MIT Space Systems Laboratory (SSL). Since its first launch in 2006 the system has been hosted aboard the ISS and as of May 2012 has conducted over 30 test sessions in such varied areas as formation flight, rendezvous and docking, online planning, and STEM education and outreach. In the 7 years of testing, SPHERES has provided valuable experimental data in a persistent microgravity environment and proven themselves as a valuable control and navigation testbed.

The system itself consists of ground and space segments, each able to operate independently of one another. Algorithms are first developed and validated in a high-fidelity simulation with a MATLAB interface. This simulation, which is constantly being improved and updated, allows for rapid prototyping of code for control and navigation algorithms. Based on the simulation results, scientists and engineers working on

the project verify and validate their code on a flat floor or glass table. After 2-D testing with the SPHERES hardware on ground, the code is packaged and sent for testing on the ISS. On ground and on station, up to three satellites may typically be used, each with internal gyroscopes and accelerometers, as well as an external ultrasonic time-of-flight measurement system[28][29]. The metrology system (Figure 4-2) provides time-of-flight measurements from five beacons with known locations, to microphones on six faces of the SPHERES. This data is used for position, velocity, and attitude estimation.


Figure 4-1: A SPHERES satellite

Each satellite has 12 cold gas thrusters, enabling full 6-DOF motion. As necessary, batteries and $CO_2$ tanks are changed by the operator. At a 5Hz frequency the satellite receives updates from the ultrasonic beacons, allowing it to determine its location in the test volume. At a frequency of 1Hz, the SPHERE may perform control actions for up to approximately 200ms. Throughout a test program, state data is sent from each of the satellites participating in a test over a wireless link back to a station laptop for post-test analysis.

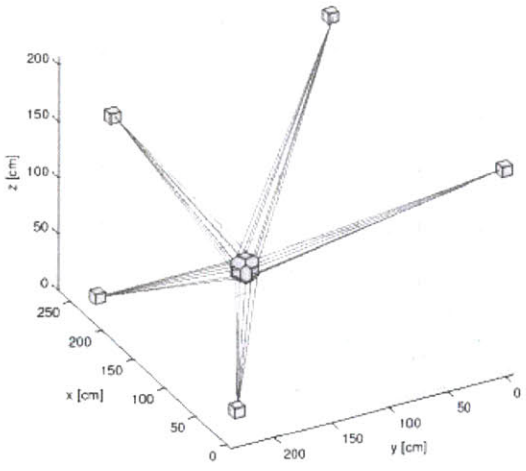


Figure 4-2: SPHERES Global Metrology System

During the design of the system, forward-looking designers added one important functionality: an expansion port. The expansion port allows for the physical mounting of additional payloads and provides adequate connectivity for communication between a payload and the host SPHERE. The expansion port also provides data lines for expansion of the metrology system as well as a handful of other health and status lines that a payload may use.

The software design is likewise flexible

enough to allow for payloads to interface with the satellite with minor changes to the core communication software.

These early design choices, particularly the ability to allow for expansion of the satellite capabilities were a critical enabling factor in achieving the vision-navigation mission that is discussed in this thesis. Much is owed to the design philosophy that nothing on the satellite should ever be a "terminator". The combination of this approach and past expansion experiments on SPHERES paved the way for the addition of the first flight-qualified expansion on the experiment: the VERTIGO vision navigation payload.

### 4.1.2 What is VERTIGO?

In 2010, DARPA began the InSPIRE program to upgrade the satellites to enable, among other things, vision-based navigation. As part of this program, in 2011 MIT and industry partner Aurora Flight Sciences began developing the Visual Estimation and Relative Tracking for Inspection of Generic Objects (VERTIGO) payload. Attaching to the expansion port built onto SPHERES, the VERTIGO Goggles Assembly consists of an avionics and processing upgrade, a set of stereo cameras, a high-bandwidth communication system and supporting elements (additional system requirements can be found in Appendix B). Due to launch vehicle and programmatic constraints, the Goggles will not be operational until the fall of 2012. The experiments described in this paper therefore use the SPHERES ultrasonic global metrology system to simulate range measurements that otherwise would be obtained from stereo cameras.

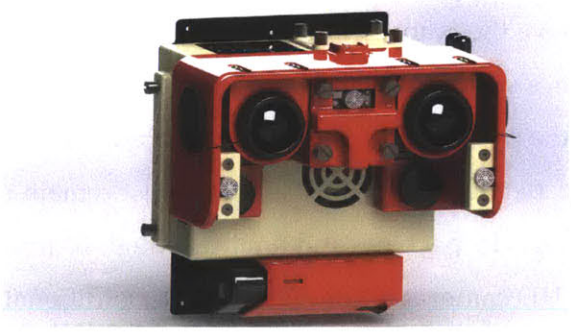

Figure 4-3: VERTIGO "Goggles" Assembly

At its roots, however, the VERTIGO hardware, however, is more than just a year old. Its roots lie in a program run in the MIT Space Systems Lab (SSL) one summer prior called

the Low Impact Inspection Vehicle (LIIVe). LIIVe prototyped many of the initial subsystem elements that would be inherited by VERTIGO, and served as a proof of concept for the project. A Naval Research Laboratory (NRL) project, it tested many of the critical trades, from power consumption to processing needs and architecture, allowing VERTIGO to proceed much faster. Without the LIIVe heritage [30], the VERTIGO program would not have been able to maintain the compressed schedule it was contracted for.

In the initial launch, two VERTIGO units will be sent to station. Each unit (Figure 4-3) is really two separate pieces — the avionics stack and the optics mount. In keeping with the design philosophy of expandability, the stack replicates nearly all of the connections provided to it by the satellite to enable other payloads to use the increased processing power granted by the onboard processor. The processor itself is a 1.2GHz single-core processor with a relatively low power draw for its processing capability. In order to take advantage of flight-qualified resources while still maintaining a low mass and realistic dynamics, the system has been designed to use onboard Li-ion batteries. These batteries provide between 1 and 1.5 hours of operational time, while keeping the mass below the limits which require significant changes to the SPHERES control algorithms. VERTIGO's thermal management system consists of a fan included on the single-board computer which forces convection across a heat sink. This cooling mechanism combines with motion-induced flow and thermal radiation to maintain a sufficiently low operating temperature for the electronics while keeping the package cool enough for astronauts to handle. The vent design minimizes disturbance torques from the airflow.

The optics mount, unlike the PEEK-encased avionics stack, is milled from 6061 aluminum designed to survive the launch vehicle vibration and acceleration loads with minimal distortion. The optics structure, purposely overdesigned, was built as such in order to reduce the chance of the cameras moving out of calibration between hardware delivery and on-orbit operations. Between then, the cameras must remain rigidly locked through shipping, handling, a train ride, packing, and finally, a rough 10-minute ride to the ISS. The structure hosts a pair of HD cameras, illuminating LEDs, additional metrology sensors, as well as the electronics required to run them and communicate with the avionics stack.

The two elements are designed for simple nominal operation by astronauts, with only power and reset switches available as well as an LED on/off switch. Should an anomaly present itself in development or on station, there are additional access panels for replacing

hard drives and a breakout connector which allows for mouse and keyboard inputs. Both wifi and ethernet connections are available for high speed communication between the Goggles and the commanding computer, bypassing the considerably slower SPHERES RF communications. This connection allows for real-time streaming video and download of large data files between the Goggles and the ISS computers.

That communication is managed, as are all operations, by a GUI running on a laptop on the ISS. The GUI allows for the astronaut operator to select, load, and operate test programs and monitor their progress. The VERTIGO plug-in to the SPHERES GUI also handles the aforementioned video feed to the astronaut crew. This provides additional feedback beyond what is typically available to ground observers, and provides a more interesting experience for operators.

Each of these design elements was built to achieve a two-fold mission. The first was to maintain the flexibility and usability of the SPHERES system as a student-usable, expandable testbed. The second, more particular goal, was to support the development of control, navigation, and other vision-based navigation investigations with space applications. With VERTIGO, MIT hopes to test out algorithms with application to on-orbit inspection, failure diagnostics, rendezvous and docking, assembly, and a host of other missions that vision sensors enable.

The profile for the current VERTIGO mission calls for three phases. The first phase (creatively named Phase I) includes an initial inspection of an unknown object which gathers information about that object from a "safe" distance with an expectation of near-global coverage of the target object. The second phase (Phase II) is a pause to allow the Goggles to process the inspection data to build a 3D map of the target using techniques such as bundle adjustment[31] or simultaneous localization and mapping(SLAM)[32]. The third and final phase (Phase III) consists of relative navigation using the 3D map to perform a closer inspection or to use the object as a stepping-stone or reference point to inspections further afield. This thesis primarily addresses the first phase.

The phase begins with the target object in view of the cameras of the inspector satellite (it is assumed that the lost in space problem has been solved on the SPHERES platform and is beyond the scope of the VERTIGO project). With the target in view, the inspector may make an estimation of the center of the object using thresholding and centroiding algorithms[33]. For now, we begin with an assumption that the target object is stationary;

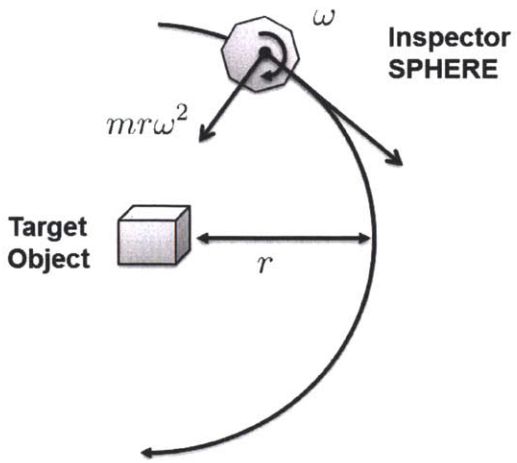


Figure 4-4: VERTIGO Basic Inspection Path

that is, it is not translating, though it may be rotating. The inspector, however, is rotating and translating as it expects to circumnavigate the target to build up a feature map of the object. The path taken by the inspector around the target object lies on a sphere with the target object at the center, and is ideally circular, as shown in Figure 4-4. The figure shows the constant radius that should be maintained by the inspector, which is equivalent to maintaining a constant range to the target.

This simple planar path forms the basis of the initial investigation into inspection paths. By examining the performance of the navigation algorithm to adjustments in the target object conditions, as well as modifications to the inspection algorithms, this thesis will make an assessment of the performance and robustness of those algorithms.

## 4.2 Measurement Fidelity

The block diagram formulation in Figure 4-5 describes the inspection estimation and control approach that will be taken by the VERTIGO Phase I inspection. In addition to the inspector rotation rate data coming from the gyroscope on the SPHERES satellite, the VERTIGO Goggles gathers images of the target object. From the images, the cameras can calculate X-, Y-, and Z-positions and rates of the target relative to the inspector. Because that hardware is not yet available on the ISS, the SPHERES ultrasound system is used to mimic the camera outputs. The use of a simple PD control law allows the algorithm to be used on nearly any system, regardless of computing capability.

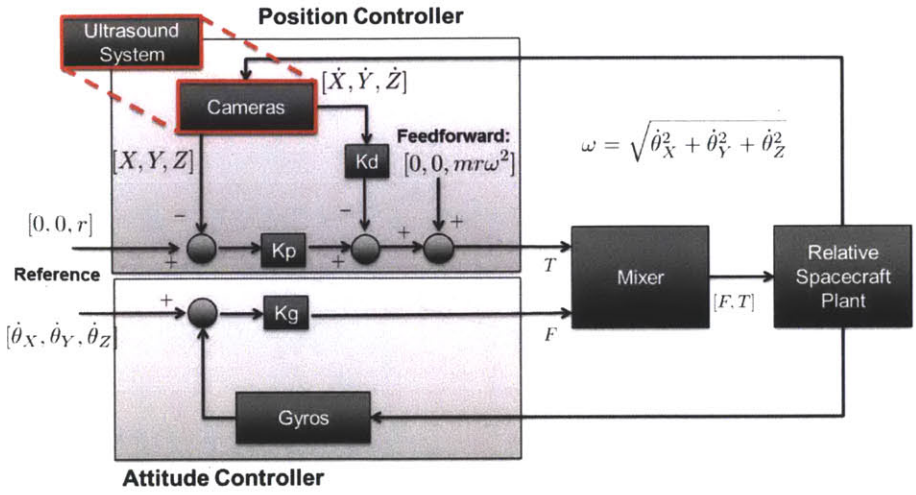


Figure 4-5: VERTIGO System Block Diagram

This section will compare the fidelity associated with the SPHERES ultrasonic global metrology system with that expected of the VERTIGO vision system. Such a comparison will address the differences in precision, causes for those errors, and describe and quantify expected causes of inaccuracies.

### 4.2.1 Vision System Fidelity

To ensure that the substitution of the ultrasound system for the cameras does not significantly change the performance characteristics of the total system, we must first compare the error of each system, beginning with the vision system.

Since the cameras will be calibrated during station operations, an error analysis can begin with the assumption that the cameras behave according to a pinhole camera model. As the pairs of cameras and lenses are identical, we will also assume that the focal length, $f$, of each cameras is identical. Calibrating the cameras undistorts and rectifies images, so that we may also assume that the focal planes of the left and right cameras are coplanar in X-Y, meaning that the focal planes are also collinear in X-Z. The distance between the centers of the cameras is defined by the baseline, $b$. The view of the X-Z plane of that setup is shown in Figure 4-6.

In Figure 4-6 the true position of the center of the target object lies at the point defined by ($x_0$,$z_0$) (note that the $y_0$) coordinate will be addressed below. The point ($x_1$,$z_1$) is where the VERTIGO Goggles believe the target to be when the error shifts the projected image on

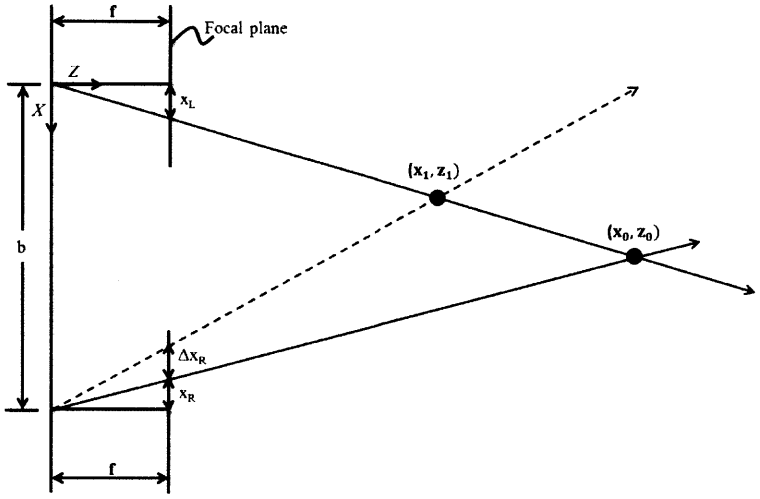


Figure 4-6: Pinhole camera model, X-Z plane

the camera in the x-axis by the distance $\Delta x_R$. We assume this noise to be Gaussian such that,

$$\Delta x_R \sim N(0, 1\ pixel)$$

Though an error of 1 pixel is conservative (previous experiments put the error at about 0.2 pixels[34]), it should provide a good upper bound on measurement error. Using the model and identifying similar triangles yields four relations:

$$\frac{z_1}{x_1} = \frac{f}{x_R + \Delta x_R} \tag{4.1}$$

$$\frac{z_0}{x_0} = \frac{f}{x_R} \tag{4.2}$$

$$\frac{z_1}{b - x_1} = \frac{f}{x_L} \tag{4.3}$$

$$\frac{z_0}{b - x_0} = \frac{f}{x_L} \tag{4.4}$$

From these relations, we can solve for $x_0$, $z_0$, $x_1$, and $z_1$. Combining equation 4.2 and equation 4.4 and solving for $x_0$, we get:

$$x_0 = \frac{b x_R}{x_L + x_R} \tag{4.5}$$

Placing equation 4.5 back into equation 4.2, we find that

$$z_0 = \frac{bf}{x_L + x_R} \tag{4.6}$$

Returning to equations equations 4.1 and 4.3, we can solve each for $z_1$, set them equal, and algebraically find $x_1$. A second substitution solves for $z_1$:

$$z_1 = \frac{x_1 f}{x_R + \Delta x_R} = \frac{f(b - x_1)}{x_L}$$

$$x_1 = \frac{b(x_R + \Delta x_R)}{x_L + x_R + \Delta x_R} \tag{4.7}$$

$$z_1 = \frac{bf}{x_L + x_R + \Delta x_R} \tag{4.8}$$

Using the typical inspection VERTIGO inspection position yields an ($x_0$,$z_0$) of (70cm, 4.5cm). With a pixel size of 6µm, the 1-pixel error yields ($x_1$,$z_1$) of (68.9cm, 4.57cm), for an absolute position error of 0.7mm in $x$ and 1.1cm in the $z$-axis.

The general form of the error is:

$$\begin{aligned}
\Delta x &= x_1 - x_0 \\
&= \frac{b(x_R + \Delta x_R)}{x_L + x_R + \Delta x_R} - \frac{bx_R}{x_L + x_R} \\
&= \frac{b(x_R + \Delta x_R)(x_L + x_R) - bx_r(x_L + x_R + \Delta x_R)}{(x_L + x_R + \Delta x_R)(x_L + x_R)}
\end{aligned}$$

$$\Delta x = \frac{b(x_L \Delta x_R)}{(x_L + x_R + \Delta x_R)(x_L + x_R)} \tag{4.9}$$

$$\begin{aligned}
\Delta z &= z_1 - z_0 \\
&= \frac{x_1 f}{x_R + \Delta x_R} = \frac{f(b - x_1)}{x_L} - \frac{bf}{x_L + x_R}
\end{aligned}$$

$$\Delta z = \frac{-fb(\Delta x_R)}{(x_L + x_R + \Delta x_R)(x_L + x_R)} \tag{4.10}$$

This, however, is only half of the story, as the X-Y plane also provides error sources. A similar approach can be used to approximate the position estimation error that results

from error in the y-axis. Once again, errors in the right camera are described by $\Delta y_R$ as we assume that the left camera perfectly captures the target location. Figure 4-7 shows the geometry of the relations. Note that the imagers are assumed to be identically oriented and facing into the page.

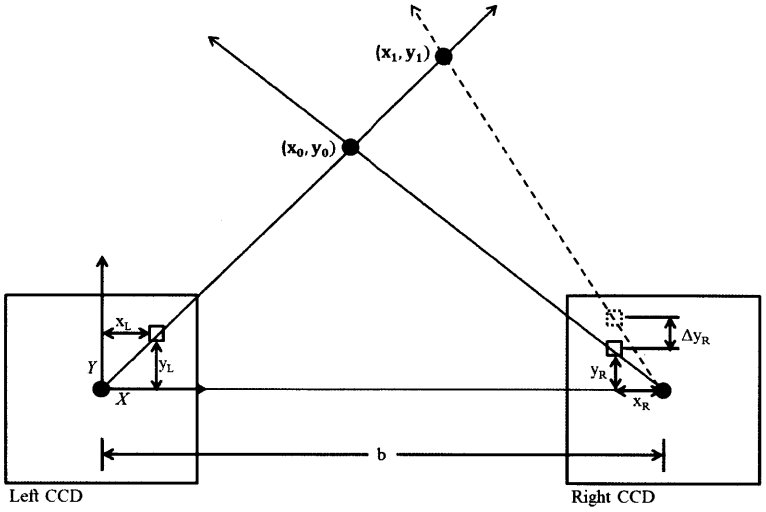


Figure 4-7: Pinhole camera model, X-Y plane

There are again four relations to account for:

$$\frac{y_L}{x_L} = \frac{y_0}{x_0} \tag{4.11}$$

$$\frac{y_1}{x_1} = \frac{y_0}{x_0} \tag{4.12}$$

$$\frac{y_0}{b - x_0} = \frac{y_R}{x_R} \tag{4.13}$$

$$\frac{y_1}{b - x_1} = \frac{y_R + \Delta y_R}{x_R} \tag{4.14}$$

Substitution of equations 4.11 and 4.13, combined with some simplification, yields:

$$x_0 = \frac{b y_R x_L}{y_R x_L + x_R y_L} \tag{4.15}$$

$$y_0 = \frac{b y_R y_L}{y_R x_L + x_R y_L} \tag{4.16}$$

while the combination of Equations 4.12 and 4.14 will give:

$$x_1 = bx_L \frac{(y_R + \Delta y_R)}{x_L y_R + y_L x_R + \Delta y_R x_L} \tag{4.17}$$

$$y_1 = by_L \frac{(y_R + \Delta y_R)}{x_L y_R + y_L x_R + \Delta y_R x_L} \tag{4.18}$$

Therefore, the combination of the two will yield an error that follows

$$\begin{aligned}\Delta x &= x_1 - x_0 \\ &= bx_L \frac{(y_R + \Delta y_R)}{x_L y_R + y_L x_R + \Delta y_R x_L} - \frac{by_R x_L}{y_R x_L + x_R y_L}\end{aligned}$$

$$\Delta x = \frac{bx_L x_R y_L (\Delta y_R)}{(x_L y_R + y_L x_R + \Delta y_R x_L)(y_R x_L + x_R y_L)} \tag{4.19}$$

$$\begin{aligned}\Delta y &= y_1 - y_0 \\ &= by_L \frac{(y_R + \Delta y_R)}{x_L y_R + y_L x_R + \Delta y_R x_L} - \frac{by_R y_L}{y_R x_L + x_R y_L}\end{aligned}$$

$$\Delta y = \frac{bx_R y_L^2 (\Delta y_R)}{(x_L y_R + y_L x_R + \Delta y_R x_L)(y_R x_L + x_R y_L)} \tag{4.20}$$

During an inspection, the target object is expected to be kept in the camera frame at approximately:

$$\begin{bmatrix} x_0 \\ y_0 \\ z_0 \end{bmatrix} = \begin{bmatrix} 4.5\text{cm} \\ -2.25\text{cm} \\ 70\text{cm} \end{bmatrix}$$

Additionally, the parameters of the cameras selected for VERTIGO include a focal length ($f$) of 2.8 mm, a baseline ($b$) of 9cm, and square pixels that are 6µm on a side.

By starting with these values, substitution allows us to find that as a result of pixel error in the X-axis,

$$\Delta x = 0.74\text{mm}$$

$$\Delta z = 1.15\text{cm}$$

while pixel error in the Y-axis gives

$$\Delta x = 0.78\text{mm}$$

$$\Delta y = 1.6\text{mm}$$

This leaves us with two values for the standard deviation of the x error. Because the probability of errors in the x- and y-directions can be treated as independent random variables, the total variance of x is the sum of the variances due to each pixel error:

$$\sigma^2_{x-total} = \sigma^2_{x|xError} + \sigma^2_{x|yError} \tag{4.21}$$

This works out to 1.7mm. This total error, as will be shown in the next section, is far below the error that will be introduced by the metrology system. Because of this, it is clear that any testing which uses the SPHERES metrology system does not provide accuracy that is unrealistic compared to vision measurements. Further research does need to be done to confirm this, especially when feature identification is put into the equation, but these preliminary results show that SPHERES is a valid way to test the vision navigation algorithms, and do so in a way that demonstrates a worst-case scenario for the sensors.

### 4.2.2 Metrology System Fidelity

The SPHERES global metrology system, which is made up of a set of 5 ultrasonic beacons, is triggered when an infrared pulse is emitted within the test volume. After a 10ms delay, this pulse causes each of the 5 beacons to respond at 20ms intervals, in sequence. Because the infrared pulse is propagated nearly instantaneously, the beacon locations are known, and the ultrasonic waves propagate at a known rate, a time-of-flight calculation can determine the range of each satellite ultrasonic sensor and each beacon. Onboard processing allows the beacons to determine position, velocity, and attitude of each satellite.

Errors can arise when additional light sources provide infrared pulses, though such errors are more likely to cause the processor to reset than to cause one-off errors in estimation. More common errors include variation in the positioning of the beacons themselves, as well as random noise in the sensors themselves, which may manifest itself as noise on the calculated satellite position and attitude.

Experience with the system shows that the uncertainty associated with the system has a precision no worse than 1cm and is accurate to within about 2cm. For position measurements, which require a difference, the variance is therefore summed, which means that the 1-sigma deviation of the metrology is expected to be accurate only to within 2.8cm in all directions, even before accounting for quaternion error associated with the metrology. This is significantly worse than the vision system is expected to perform.

## 4.3 Tests and Test Design

In order to evaluate the algorithms' effectiveness in a variety of settings, tests were developed which stressed the system. A subset of these tests was run in the 6 degree of freedom microgravity environment onboard the ISS, while the full set was evaluated in a simulation developed by previous SPHERES researchers.

By using the results from the ISS data and comparing it to the simulation output, it is possible to develop an understanding of how well the simulation approximates the real world system. Further, by identifying the differences, it is possible to determine the mode of the divergence.

The tests will evaluate the impact of the following variables on the behavior of the inspection system:

1. **Target Behavior** Movement of the target object toward, away from, and perpendicular to the field of view will demonstrate the robustness of the algorithm to uncertainty in the object's shape. More directly, it will also show the robustness of the inspection and relative navigation algorithms as implemented with SPHERES controllers to motion of the target.

2. **Vision System Noise** Vision system noise may impact the accuracy of the controller. The noise on the metrology measurements should provide an upper bound on the

vision system noise, but variation can be explored through by adding additional noise into the simulation.

3. **Motion Dimension** Initial movement is 2-dimensional. Tests should demonstrate the impact of introducing a 3rd dimension. An exploration of non-planar motion may also impact the optimality of the maneuver.

4. **Rotation Information** Taking the rotation of the target object into account may change the most efficient path.

Each of the variables fits into a test matrix which covers the target behavior, inspection motion dimension, and the use of rotation information. That table is shown below. Note that vision system noise is not shown because it is a factor which influences each test and can only be correlated to a baseline expectation from simulation. Each of the designed tests takes one element of from each row of the below table.

Each row of the table shows one variable that is being tested. Tests were developed which evaluated most combinations of the below variables. Necessarily, each test includes at least one element from each row.

| **Target Translation** | None | Toward | Away | Shear |
|---|---|---|---|---|
| **Inspector Motion** | Planar | 3D | | |
| **Target Rotation** | Use | Don't Use | | |

By comparing the tests against one another, we may determine the effect that each variable has on the effectiveness of the inspections, and ultimately, which algorithms perform better under the given conditions of a rotating target.

### 4.3.1 Target Translation

For the purposes of the VERTIGO program, the target object is considered to be uncooperative. In addition to the typical meaning implying that it shares neither state information nor provides fiducials, this can also mean that the target is moving in response to the inspector. This can manifest itself in evasive motion away from the inspector or motion perpendicular to camera plane. Aggressive motion toward the target will also require the inspector to react by moving away to avoid a collision.

The first motion was evaluated in two segments of an ISS test, while the latter two — shear and aggressive motion — was evaluated in simulation in addition to being prepared for later evaluation on station.

| **Target Translation** | None | Toward | Away | Shear |
|---|---|---|---|---|
| **Inspector Motion** | Planar | 3D | | |
| **Target Rotation** | Use | Don't Use | | |

### 4.3.2 Vision System Noise

Each test on ISS used the global metrology system transformed into a relative frame. Therefore, those tests can simulate noise only at or above the threshold that beacons provide. In order to test varying levels which are below that threshold, and hew more closely to the noise in a vision system, simulation-only tests can be run.

Though ISS tests do not provide a sufficiently low noise threshold to do more than provide an upper bound to the impact on the control system, they do allow for other analyses. Those analyses include a determination of how the noise impacts the control and determination and potential biases or instabilities, as well as a check to ensure that real-world hardware matches predictions of the simulation.

After a comparison of the ISS and simulation data, the simulation can be tweaked to introduce artificial noise into the simulation measurements, and to do so at varying levels. As there is no station test which allows us to isolate metrology noise during test conditions (including motion) without the addition of prohibitively complex hardware, there is not specific test that will be run to determine the noise level. Such data will instead be estimated from each of the below tests, with a particular emphasis on those highlighted:

| **Target Translation** | None | Toward | Away | Shear |
|---|---|---|---|---|
| **Inspector Motion** | Planar | 3D | | |
| **Target Rotation** | Use | Don't Use | | |

### 4.3.3 Inspector Motion

The initial inspection was first developed as a two-dimensional maneuver in order to make it possible to accurately test in a 1-G environment. With motion into a 3rd dimension, how-

ever, trades must be made to evaluate the paths which take the least time and fuel to complete, while still gaining full coverage. Comparing the 2- and 3-dimensional motions to one another also allows for an evaluation of the value of the additional coverage provided by a 3rd dimensional motion with time and fuel use.

The initial motion is evaluated in the first planar inspections. The planar inspector motion allows for the simplest trajectory design and does not require integration of onboard gyroscope to do more than to assess potential completion of the maneuver. It also provides a common baseline to compare all cases of target translation against one another without confounding variables.

The second category in this battery adds motion in the third dimension. This is achieved by changing the inspector's axis of rotation at certain points in the circumnavigation of the target: in order, about the Z-axis, Y-axis, and Z-axis once more. This occurs after the first 90 degrees and a subsequent 270 degrees. The determination of those angles are made by integrating the inspector's gyroscopes.

The tests comparing the dimensionality of different maneuvers are highlighted in the chart below:

| **Target Translation** | None | Toward | Away | Shear |
|---|---|---|---|---|
| **Inspector Motion** | Planar | 3D | | |
| **Target Rotation** | Use | Don't Use | | |

### 4.3.4 Use of Rotation Information

If the target object were static relative to an inertial frame, then the shortest path is well-defined, following a path similar to the seams on a baseball. A minimum fuel/minimum time path should be similar. If the target object is rotating, then the use of that information can provide a vastly different minimum fuel/time path. By changing the algorithm to account for this motion, the path can be optimized for fuel and time when compared to previously tested algorithms.

Previous work has shown that by differentiating the motion of features between frames, it is possible to estimate the rotational velocity of an object fairly accurately. To test the possible influence of taking the rotation of the target object into account, a test was developed to use that motion to inform the path of the inspector.

The maneuver begins with the assumption that the rotation is stable over the duration of the inspection maneuver (approximately 6 minutes) and has minimal nutation (less than approximately 20%). In the first portion, the inspecting SPHERE aligns its primary rotational axis (Z-body) with the rotation axis of the target. In the following portions, the inspector circumnavigates the target in thirds: the "northern" third, "southern" third, and "equatorial" third, respectively. During each of these latter portions, the inspector integrates its own rotation, as well as its estimation of the rotation of the target beneath it. Once the integrations sum to $2\pi$rad, satellite halts its circumnavigation and moves to observe the next third of the target. In all, this motion provides global coverage of the entire target object given a control range of 0.7m and camera field of view of 60° (full-cone).

In the case developed for testing on the ISS, a rate of 6 degrees per second about the Y-axis and a quarter of that about the Z-axis is used for the target object. These values should allow for the full inspection to be performed before the inspector completes a full circumnavigation. Further evaluation of these results should demonstrate whether this results in a more efficient maneuver than one which does not take the rotation into account.

In the test matrix, this covers the highlighted regions:

| **Target Translation** | None | Toward | Away | Shear |
|---|---|---|---|---|
| **Inspector Motion** | Planar | 3D | | |
| **Target Rotation** | Use | Don't Use | | |

## 4.4 Success Metrics

In order to quantify how well the inspection is performed, it is necessary to develop metrics which judge inspection performance on the basis of fuel use, time to completion, and total coverage.

### 4.4.1 Coverage

Because it is important to VERTIGO (and any other inspection mission for that matter), coverage will be dealt with first. First, the field of view of the cameras must be taken into account. Each camera is assumed to have a 60° full-cone field of view. Outside of this angle, light either does not fall on the sensor or is removed during the calibration process.

Since the inspector cannot determine range to a feature without the benefit of stereo vision, a location on the target will be considered *covered* if it is in view of both cameras. This implies that the covered area is defined by the area described by the intersection of the two cameras individual views, as shown below in Figure 4-8:

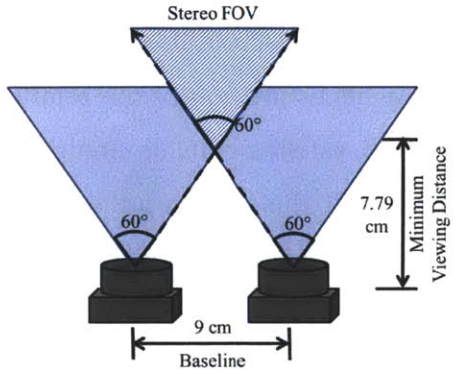


Figure 4-8: Stereo Camera Combined Field of View

Therefore, an area on the target object will be considered covered if it is in the area swept out by the Stereo FOV area (Figure 4-8), and the angle between the line of sight and the unit normal to that area is less than 45 degrees (as shown in Figure 4-9). This angular condition ensures that the area considered is on both the surface facing the cameras and is viewed at a flat enough angle that the cameras can resolve features.

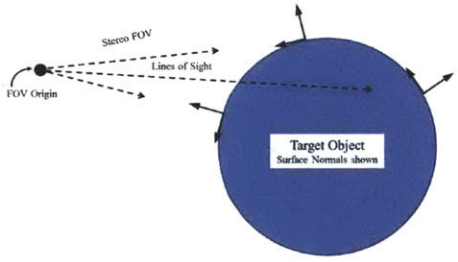


Figure 4-9: Target Object Surface Visibility

Using this metric, an inspection is considered complete once the coverage area reaches 100% of the target object's surface area or a sufficient fraction thereof (to account for estimation and other errors). For the purposes of this investigation, 95% coverage will be considered "full".

### 4.4.2 Fuel Use & Time

By beginning with inspection with similar coverage values, it is possible to compare the fuel use and time to completion of each inspection. Time to completion, which is simply the time to full coverage less any initial positioning, is simple to calculate.

A fuel calculation is slightly more complex when running tests on the ISS. This is because the opening of multiple thrusters reduces their effectiveness and changes their fuel use. Since the only measure of fuel use on SPHERES is the firing of thrusters, the opening of multiple thrusters must be accounted for in the fuel calculation. Previous work in this area will be used for those calculations [24, p. 135]. That work showed that mass flow rate ($\dot{m}$, in g/s) followed

$$\dot{m}_{prev} = -0.033 n_T + 0.5555 \tag{4.22}$$

where $n_T$ is the number of thrusters open at once. Since those tests were run with a higher regulator pressure, the constant term is higher than would be expected for station tests. On station, the regulator is set close to 25 psi rather than the 55 psi from the previous work. The same research showed that the massflow for a single thruster tends to follow:

$$\dot{m}_{prev} = 0.0058p + 0.1968 \tag{4.23}$$

where $p$ is in psi. A pressure of 25 psi yields a mass flow of 0.3418 g/s. That value can be used to replace the constant in 4.22. Therefore, the equation to be used in judging fuel consumption shall be modified slightly to read:

$$\dot{m}_{ISS} = -0.033 n_T + 0.3418 \tag{4.24}$$

In order to compare fuel use and time, an exchange between the two should be developed. Using a typical SPHERES test as reference, this gives an equivalence between a full fuel tank (170g), and 45 minutes of test time. This works to 63mg of fuel for each second of test time, which agrees with the earlier estimate of counts in a full tank. Therefore, the cost function to be minimized at the completion of an inspection is:

$$J_{ISS} = m_{fuel} + 0.063t \tag{4.25}$$

By comparing the ability of different algorithms against one another in terms of fuel use, we are able to characterize the relative effectiveness of each approach in providing near-global coverage in the uncertain inspection environment.

# Chapter 5

# Results

This chapter will discuss the data from both station-run tests and simulations. After a discussion of the performance characteristics of the inspector in both types of tests, a comparison will be drawn between the two. Overall, the chapter will examine whether the simulation is a sufficiently faithful model of the actual system, and what differences must be accounted for in simulation results.

Following the comparison, the chapter will analyze tests that were run only in simulation. Using the lessons from the comparison between station and simulation data, conclusions will be drawn about the expected performance of the simulation-only tests should they be run on station.

Finally, there are two additional elements which will be addressed. The first is an analysis of the gyroscope noise characteristics based on the small 2-test sample of station data. And finally, a brief analysis of the efficiency of various inspection methods will be conducted. This latter analysis will conclude which inspection path is the most fuel- and time-efficient method for inspecting a tumbling target.

## 5.1 Simulation and Station

This section will describe the results of the tests outlined in Chapter 4, with an emphasis on Section 4.3. To begin, the results from both station and simulation will be laid out, and then compared against one another. By comparing the two test methods, it should be possible to identify the differences and similarities between the two, and in particular the *reasons* why they agree or disagree.

### 5.1.1 Station Results

Due to limited testing time, the only cases which were run onboard the ISS were planar inspections (the code for those manevuers is in Appendix A.1). Those tests demonstrated a simple circular inspection maneuver about a tumbling target, first with the object stationary and then with motion away from and perpendicular to the camera line of sight. In each case the target object began with a rotational velocity which did not significantly slow throughout the course of the test though the axes of rotation did change as a result of the target's inertia properties.

As described in previous chapters, vision data was simulated using SPHERES global metrology measurements translated into an Inspector body-relative frame. The body frame for the inspection was aligned with the frame that the future VERTIGO payload will use: +X on the inspector body was the camera boresight, while +Y was parallel with the camera baseline, and +Z in the body frame ran perpendicular to the baseline. The center of the SPHERE served as the center for the coordinate frame.

One significant difference did exist between the setup that the code was designed for and what was actually run on station. That difference was the addition of extra mass on the target object in the form of a smartphone on the -X face. The smartphone was part of earlier tests in the session and was not removed for operational reasons. The additional mass was 300g, which changed the target SPHERE's mass properties as shown in Figure 5.1 (assuming wet mass values):

| Property | Old Value | Change (est.) | New Value |
|---|---|---|---|
| Mass (kg) | 4.33 | + 0.30 | 4.63 |
| CM offset from GC (cm) | <0, 0, 0> | + <0.65, 0, 0> | <0.65, 0, 0> |
| $I_{xx}$ (kg*m$^2$) | $2.83\times10^{-2}$ | $+ 3.2\times10^{-4}$ | $2.87\times10^{-2}$ |
| $I_{yy}$ (kg*m$^2$) | $2.68\times10^{-2}$ | $+ 3.0\times10^{-3}$ | $2.98\times10^{-2}$ |
| $I_{zz}$ (kg*m$^2$) | $2.30\times10^{-2}$ | $+ 3.0\times10^{-3}$ | $2.60\times10^{-2}$ |

Table 5.1: Mass Properties of Modified Target Satellite

#### Stationary Target

The ability of the implemented controllers to track the desired inspection path is apparent from the results. The first test run on station had the Inspector use a controller to maintain a constant 0.36m range to target, while keeping the target centered along the Inspector's

body X-axis. In order to create the inspection path a closed loop Z-axis rotation was commanded. The second test (discussed later) followed the same control and inspection profile. In this first test, the target object maintained its position in the ISS inertial frame, while freely rotating as the result of a commanded rotation during initial positioning which was left uncontrolled during the inspection. Figure 5-1 shows the positions of the Inspector and Target satellites in the ISS inertial frame.

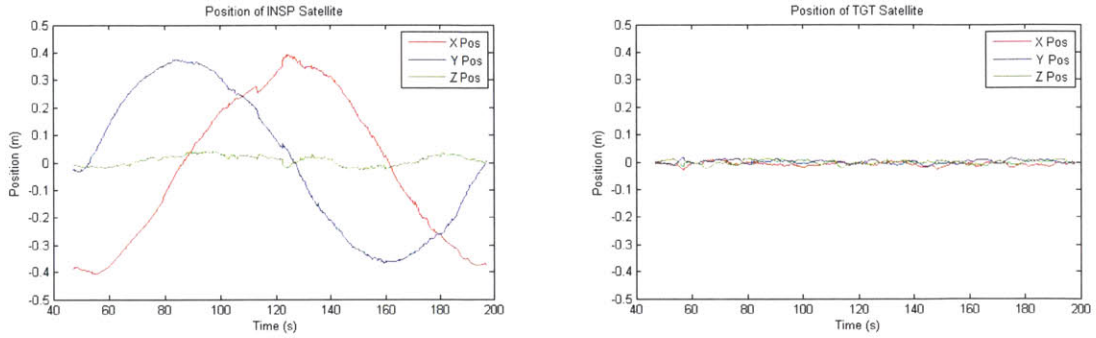


(a) Inspector Position

(b) Target Position

Figure 5-1: Planar Inspection: Position Data during Stationary Target Test

Using the Inspector's quaternion state, it is possible to convert the positions from the global frame to the relative one, as demonstrated in Figure 5-2.

Figure 5-2 shows the relative orientation target in the Inspector body frame during the inspection maneuver alone (disregarding the earlier initial positioning and estimator initialization stages). Here, an ideal motion would keep the Y- and Z-axis positions at 0 and the X-position at 0.36 meters.

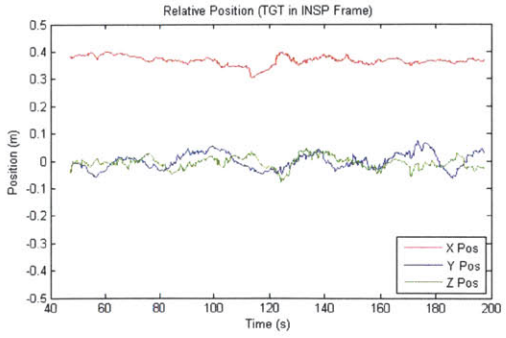


Figure 5-2: Planar Inspection: Relative Position during Stationary Target Test

Relative velocity should also be kept near zero in all axes. Figure 5-3 shows the performance of the Inspector in achieving such a state. During the course of the inspection maneuver the relative velocity never exceeds $1\text{cm}\,\text{s}^{-1}$ except for the beginning of the maneuver. This is due to the rotation command (visible in Figure 5-4) which begins at approximately 47 seconds. The rise time of the controller is 4.2 seconds with 12% overshoot. Furthermore, since that 12% overshoot works out to less than $2\text{mm}\,\text{s}^{-1}$, it is likely within the margin of error of the metrology system.

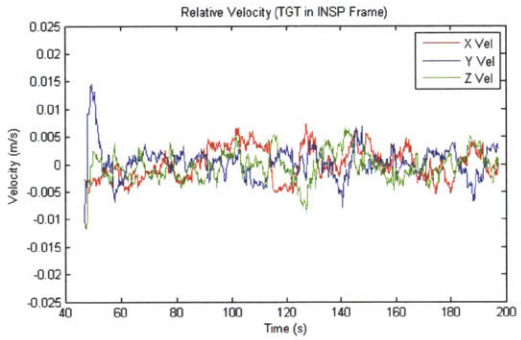


Figure 5-3: Planar Inspection: Relative Velocity during Stationary Target Test

In order to perform the inspection, a closed-loop rotation of the Inspector satellite is commanded to rotate at $0.0436\text{rad}\,\text{s}^{-1}$ ($2.5°\,\text{s}^{-1}$). The controller achieves a mean of approximately $0.0433\text{rad}\,\text{s}^{-1}$ and ranges from approximately 0.0411 to $0.0482\,\text{rad}\,\text{s}^{-1}$ ($2.76$ to $2.36°\,\text{s}^{-1}$). The sawtooth pattern is likely due to a loss of rotational energy due to fuel slosh and other dynamic forces immediately following thruster commands. As energy is lost the satellite's rotation slows. When this happens, the error goes uncorrected until it hits the deadband threshold, allowing the thrusters to activate and correct the rate. Since the state estimation filter does not take the thrusters into account when updating the rate estimate, it is unlikely the source is an estimation error alone.

Misaligned thrusters imparting rotations in other axes or misaligned gyroscopes measuring slightly off-axis are unlikely to be the cause of the sawtooth pattern since the difference between the rotation in the Z-axis and the sum of the rotation is on the order of $1.1\times10^{-4}$, peaking at $9\times10^{-4}\,\text{rad}\,\text{s}^{-1}$ (see Figure 5-5). At two orders of magnitude below the signal, this means misalignment is less than 1%. If thrusters or gyroscopes were misaligned there would be a significant component in the off axes as the thruster fired and imparted rotational velocity into X and Y. Additionally, during jumps in the Z-axis rota-

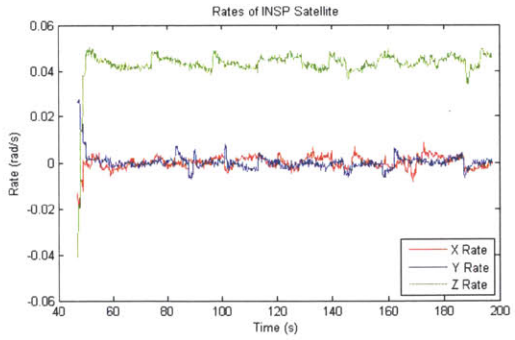


Figure 5-4: Planar Inspection: Inspector Rate during Stationary Target Test

tion rate, there is no significant corresponding increase in the X- and Y-axes, and certainly not within the precision of the gyroscopes.

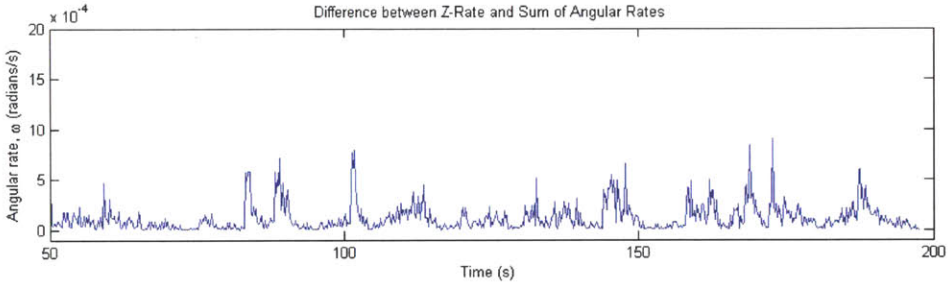


Figure 5-5: Planar Inspection: Difference between Z-Rate and Total Angular Rate during Stationary Target Test

During the inspection maneuver in this first test, the target satellite is rotating as the result of a controlled spin-up during initial positioning, as shown in Figure 5-6. As the target is rotating at about $0.1\text{rad}\,\text{s}^{-1}$ ($5.7^\circ\,\text{s}^{-1}$) in both the major and minor axes — Y- and Z-axes, respectively — control inputs to maintain its positioning, combined with some amount of fuel slosh cause the rotation to transition to an intermediate axis. This state, presumably temporary on the way to a minor axis rotation implies that there is at least some limited damping in the system. Controller overshoot is unlikely to play a major role since the same error is unlikely to result in the same absolute overshoot (rather than as a percentage) as is seen at approximately the 50-, 75- and 100-second marks. However, teasing out the exact contributions of each source of error is difficult in the absence of more data.

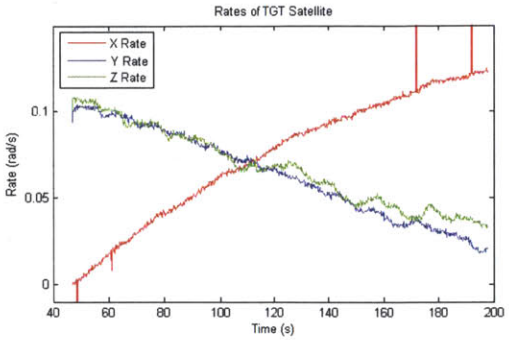


Figure 5-6: Planar Inspection: Target Rate during Stationary Target Test

### Moving Target

A second test run on station used the same relative navigation and inspection algorithm, with identical position and rate controllers, but added translational motion of the target object in addition to its spin. The resulting motion can be seen in Figure 5-7. Important to point out is that for all of the similarities with the first station test (and Figure 5-1), the inspector satellite does move in a different trajectory in order to compensate for the motion of the target. The different plot limits show as much. The motion of the target beginning at approximately 77 and 107 seconds appears as an 'L' shape in 3-space, and relative to the Inspector body frame appears to be a motion of the target away from the Inspector.

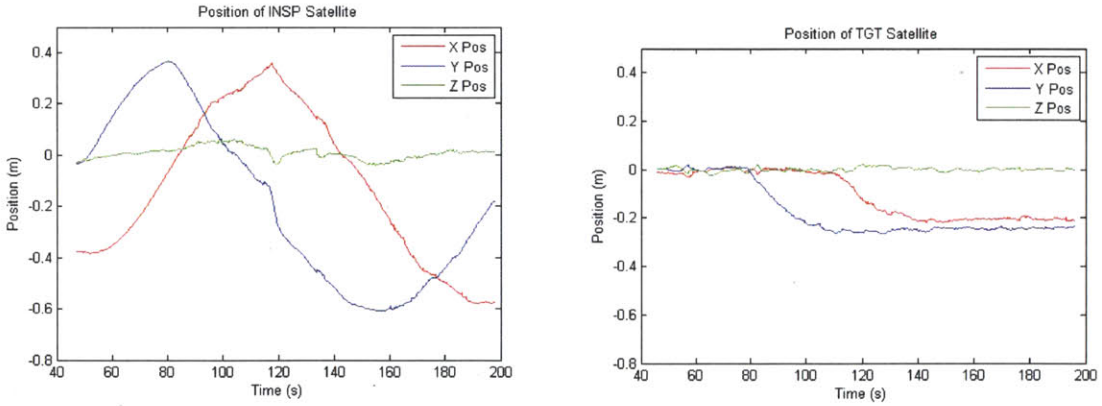


(a) Inspector Position

(b) Target Position

Figure 5-7: Planar Inspection: Position Data during Moving Target Test

As performance goes, the algorithm performs well in response to this motion. When

compared to the original maneuver with the non-moving target, the translation of the target at 77s is nearly indiscernible, particularly in the most critical measure — the relative range (X-axis). Because the primary objective of any inspector must be to avoid collision hazards, this result is promising. Likewise, the motion beginning at 107 s has an effect, but primarily on the translational error, not on the range. Even the Y- and Z-axis errors peak at 10 cm, which is crucially below the threshold which would drive the target SPHERE out of view since:

$$\tan(FOV) * x_{range} - R_{SPHERE} = y_{max} = z_{max} \tag{5.1}$$

$$FOV = 30^{\circ} \tag{5.2}$$

$$x_{range} = 36\text{cm} \tag{5.3}$$

$$R_{SPHERE} = 10\text{cm} \tag{5.4}$$

$$y_{max} = z_{max} = 11\text{cm} \tag{5.5}$$

Since the result of Equation 5.1 shows an allowable translation error above that observed, we expect the target object to remain in view of the Inspector, allowing the algorithm to maintain the inspection. Of note is the fact that this range is a stressing case, since the VERTIGO system will require an inspection distance that is at least 50cm, and preferably at least 70cm, which yields an allowable translation error of 19 and 30cm, respectively.

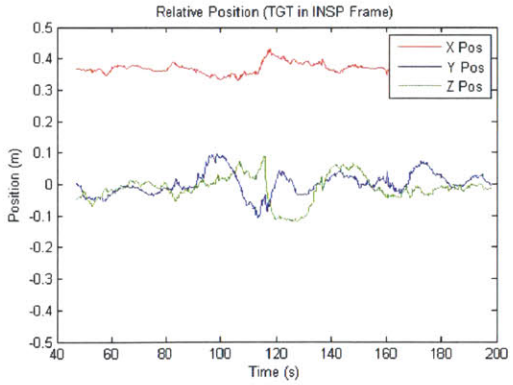


Figure 5-8: Planar Inspection: Relative Position during Moving Target Test

Likewise, the Inspector is able to maintain a relative velocity near zero for most of the test. Some velocity error appears during the first target motion (77s start) but is damped

out by the time the second motion starts (at 107s). This second motion, which is smaller in magnitude — 20 cm compared to 25 for the first motion — causes a large transient spike in relative velocity, which is afterwards not driven to zero. The implication is that the system is marginally stable or nearly so. Finer tuning of control gains will be necessary to address this shortcoming in future tests. If that is not possible, a thresholding condition may need to be placed on the algorithm which slows the rotation to allow it to regain proper position and velocity if those values move outside of desired bounds, as happened in this case. Especially with close inspections, a relative velocity error on the order of $3\text{cm}\,\text{s}^{-1}$ cannot be allowed to propagate for any significant amount of time, lest the target object drift out of view.

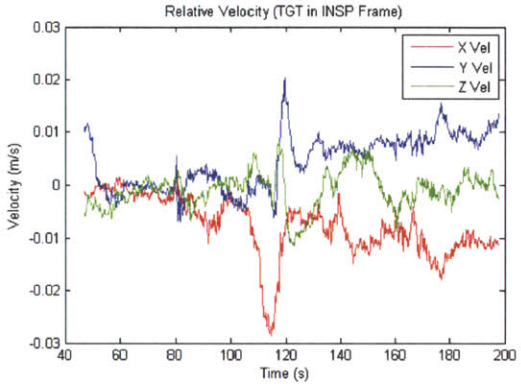


Figure 5-9: Planar Inspection: Relative Velocity during Moving Target Test

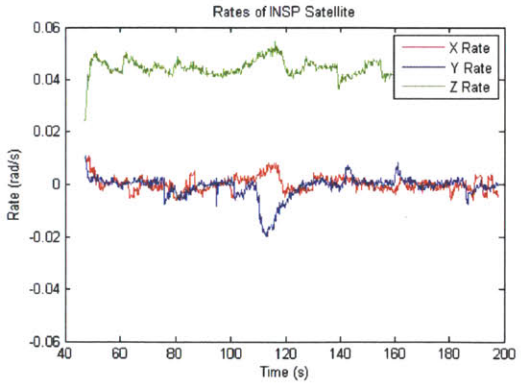


Figure 5-10: Planar Inspection: Inspector Rate during Moving Target Test

Once again, there is a significant difference between the stationary and moving target, but only following the beginning of the second motion. Here, there is an apparent jump in

the total inspector body rate compared to the Z-axis rate (Figure 5-11). This is attributable not so much due to a significant drop in the Z-rate — it actual grows about $0.01\text{rad}\,\text{s}^{-1}$ — but to a large rotation imparted in the -Y direction at over $0.02\text{rad}\,\text{s}^{-1}$ ($1.1°\,\text{s}^{-1}$).

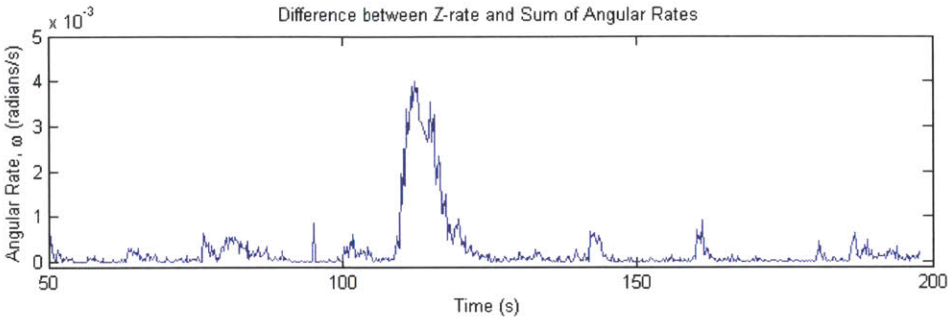


Figure 5-11: Planar Inspection: Difference between Z-Rate and Total Angular Rate during Moving Target Test

As significantly more control inputs are required of the target in the test with motion, there is more of a chance for those thruster firings to induce changes in the rotation rates. This is due to two factors: the first is that thruster firings to actuate the desired motion of the satellite are not impulsive actions, but have a pulse width. Since the satellite is rotating at a fair $0.12\text{rad}\,\text{s}^{-1}$ ($6.9°\,\text{s}^{-1}$) clip, this means a thruster firing will operate through a range of angles, imparting more than the pure, desired translation. This effect is small , however. The most important factor, is the fact that the target rotation rate is not actively controlled throughout the inspection maneuver. This means that any rotation which is either imparted or damped will not have a controller respond.

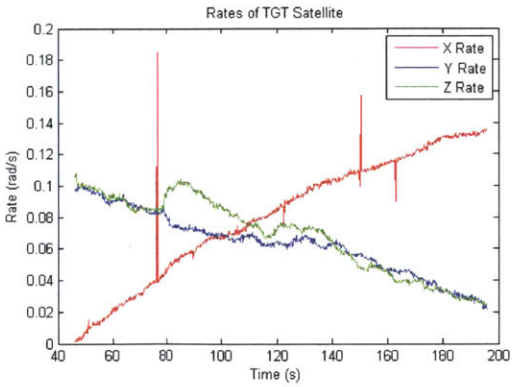


Figure 5-12: Planar Inspection: Target Rate during Stationary Target Test

### 5.1.2 Simulation Results

Prior to running the planar inspection maneuvers on the Space Station, they were composed and tested in a Matlab simulation environment. This simulation, available for all researchers working on the SPHERES system, allows the testing of code prior to launch. It mimics the dynamics of the satellites along with thruster misalignment and non-linearities (including hysteresis and deadband) and metrology system noise, among other factors, which provide a good estimate of potential disturbances from an ideal system. A simulation mode is also available which ignores sensor and thruster noise.

#### Stationary Target

The first maneuver with a stationary central target was run in the simulation. Figure 5-13 shows the inertial (ISS-relative) positions of the Inspector and target satellites. Here there is good tracking of the desired positions, with circular motion easily visible in the left image. Also noticeable is the fact that at the beginning of the inspection there is some small error in initial positioning with the relative range (Figure 5-14) being off by 2cm and Y-position off by approximately twice that amount This is the result of initial positioning taking longer than the 30s allotted. This is not particularly significant as the error is small and even when compounded by the initial angular acceleration to achieve the desired rotation rate, the error is removed by the controller after 40s.

Even after removing the initial error, there is still a consistent error in the relative position. Since the desired steady state condition is <36, 0, 0> cm in <X,Y,Z>, but the actual state value approaches <38, 0, 0> there is clearly a steady state error in the controller used, at least when a rotation is also commanded. Since the controller is PD on position, the position error is proportional to the control output. As it is implemented on SPHERES (and therefore in the simulation), it is likely that the deadband eliminates the small thruster forces associated with a 2cm error. A 10ms minimum firing time along with the steady disturbance associated with the rotation causes the error to stay fixed near 2cm. The addition of an integral term would likely resolve this issue, but at the risk of increasing the probability of the Inspector and target colliding. Such a decision should be made based on the mission at hand and the risk tolerance of that mission profile and the system operators.

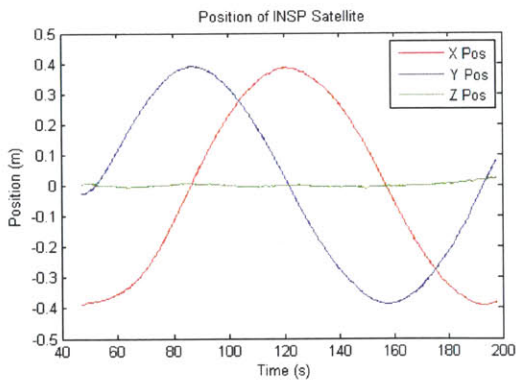


(a) Inspector Position

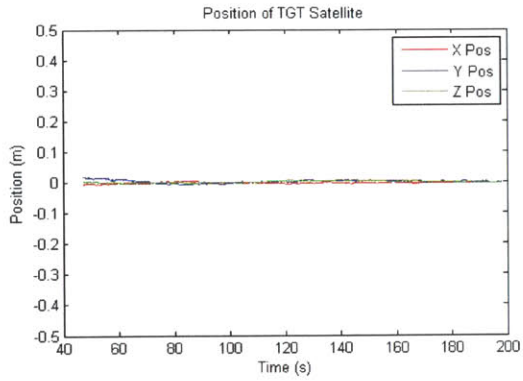


(b) Target Position

Figure 5-13: Planar Inspection: Position Data during Moving Target Simulation

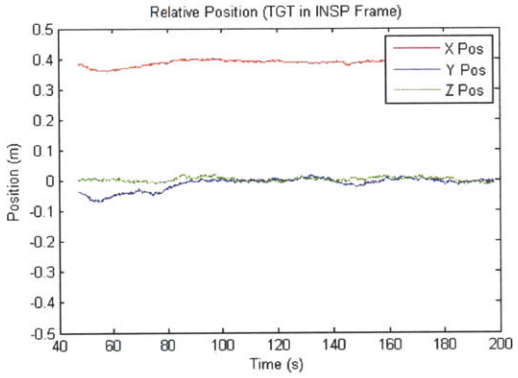


Figure 5-14: Planar Inspection: Relative Position during Moving Target Simulation

The relative velocity (Figure 5-15), as is to be expected, shows that the velocity of the two satellites with respect to one another is kept below $1\text{cm}\,\text{s}^{-1}$ throughout the maneuver. Indeed, after settling from the small transients associated with spin-up and correcting for initial positioning errors, the velocity never drifted from the desired state (all zero) by more than $5\text{mm}\,\text{s}^{-1}$ at a $2\sigma$ level. Notably, the estimate seems noisy in large part due to the way in which the measurement is taken; the estimate is the result of a difference between the two velocities transformed into the inspector's body frame. Since those measurements have a variance on them as a result of metrology noise, the difference has twice the variance. This will be important later when concluding the effectiveness and noise level associated with a camera system since its measure of relative position does not depend on this subtraction, and therefore is not affected by the doubling in variance.

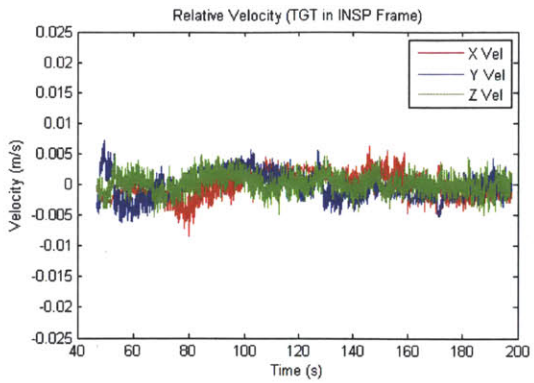


Figure 5-15: Planar Inspection: Relative Velocity during Moving Target Simulation

The Inspector rotation rate (Figure 5-16) is also well controlled and stable, with a standard deviation at or below $0.0045\text{rad}\,\text{s}^{-1}$ ($0.26°\,\text{s}^{-1}$). The mean of the measurement is also fairly stable, remaining within approximately $0.0018\text{rad}\,\text{s}^{-1}$ ($0.10°\,\text{s}^{-1}$) of the commanded rate of $0.0436\text{rad}\,\text{s}^{-1}$ ($2.5°\,\text{s}^{-1}$).

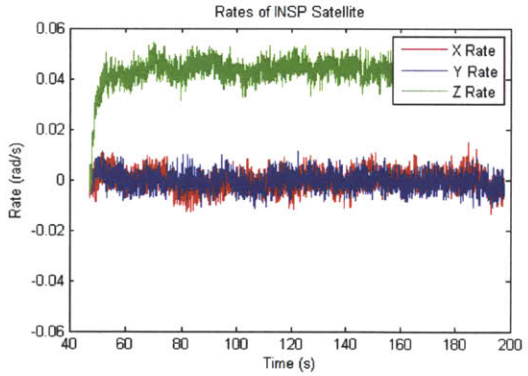


Figure 5-16: Planar Inspection: Inspector Rate during Moving Target Simulation

Critically, the off-axis rotations remain below 3.4% ($2\sigma$) of the total rotational rate of the satellite. Even at this level, error is likely due to noise that is the result of the implementation of the estimator in the simulation, and not from the actual state or from commanded inputs.

### Moving Target

The second test which incorporated a moving target was also run in simulation. Once again, the inspector and target satellites hew closely to their commanded paths. Some

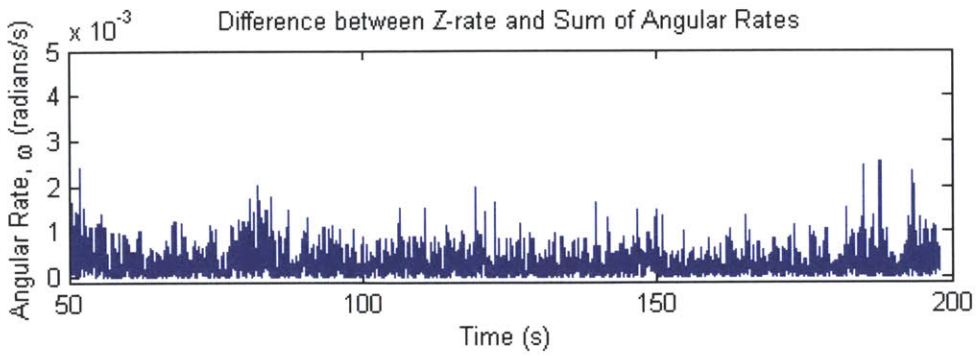


Figure 5-17: Planar Inspection: Difference between Z-Rate and Total Angular Rate during Moving Target Simulation

positioning error is seen at the target satellite during the beginning of the maneuver (Figure 5-18b), as it remains about 2cm away from the center of the test volume, indicating that earlier initial positioning may not have fully completed Similarly, the Inspector (Figure 5-18a) also has a 2cm error in the Y-axis, the result of an incomplete initial positioning which did not allow overshoot to be completely damped. Since the two satellites were deployed on opposite sides of the test volume, this error will compound itself at the beginning of the inspection maneuver rather than cancel out. However, because the maneuver is relative, such error is expected to be accounted for quickly. Figure 5-19 shows an initial error in the X- (range) and Y- body axes due to this initial positioning error, with expected Y-error near 4cm. Unfortunately, with the rotation of the Inspector beginning at 47s, the error begins to increase Y-axis for approximately 10s before the controller is able to recover.

The target SPHERE also shows overshoot of no more than 8% to the first commanded 25cm motion, and no more than 9% to the second 20cm motion. Variation in the two is likely due to sensor noise, as those measurements are the maximums observed by the system. The true overshoot likely lies between 7.5 and 8% based on an average of values near those extremes.

The simulation shows little to no out of plane relative motion (Figure 5-19), though some appears in the inspector inertial position (Figure 5-18a). Much like the initial error at 47s seen in the position of the two satellites, the Inspector's initial orientation was not complete at the beginning of the inspection maneuver. An error of about 0.056rad (3°) would be large enough to account for the 2cm above and below the inertial X-Y plane the Inspector moves. Also important is the fact that the error is bounded and consistent for

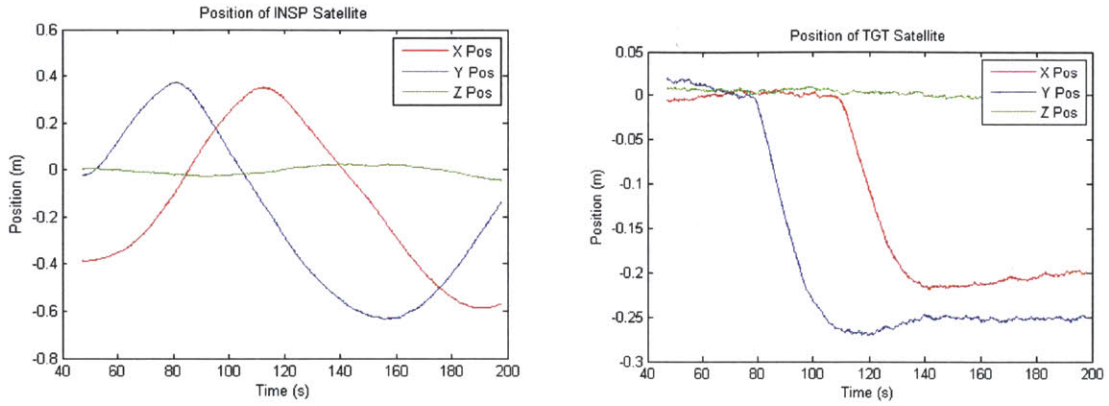


(a) Inspector Position

(b) Target Position

Figure 5-18: Planar Inspection: Position Data during Moving Target Simulation

the first 100-plus seconds of the inspection (through both a peak and a trough), implying that the error is causes only by the initial positioning and nothing more.

What is apparent is the range error that is caused by the target moving away from the inspector. The error begins growing immediately after the target object is commanded to move, which is to be expected. The Inspector is able to recover from the motion after approximately 25s, with error peaking after 10s into a motion which takes the target approximately 35s to complete. This implies that the algorithm using this PD controller should be able to perform an inspection of a moving object. An accelerating one, however, may be difficult, and especially so when both the inspector and the target satellite have the exact same amount of control authority. Also important to note is that the use of PD control allows the Inspector to recover from the motion without dipping below its original relative range. By not incorporating an integral element into the controller, the satellites remain at a safe distance from one another, meeting a critical safety threshold for any inspector.

The relative velocity (Figure 5-20) is not as well controlled as the position during this maneuver, much of which can be attributed to the motion of the target object. As the Inspector matches the velocity of the target as it moves away, the movement causes the former to build up momentum in the direction of motion. As the target completes its second movement and stops, the Inspector has now retained much of the momentum of the previous two motions by the target. This requires additional force from the controller which is already stressed by the need to move in a circular path and is unable to return to its

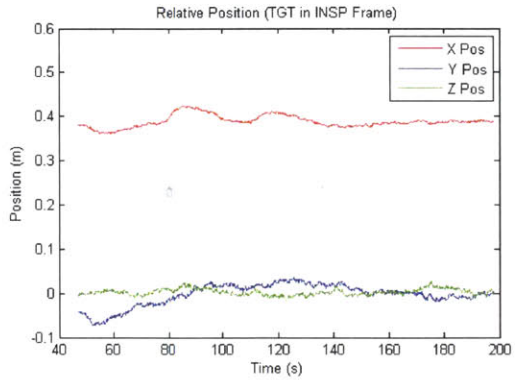


Figure 5-19: Planar Inspection: Relative Position during Moving Target Simulation

ideal path before it completes its inspection. This keeps the relative position approximately 2-3cm farther away than the desired 36cm range. Thought the signal is noisy, we can reach some conclusions about trends that appear in the data. Importantly, however, the error does appear to be bounded (not growing) for the final 60s of the maneuver, with the Z-velocity actually approaching the desired state (of 0cm $s^{-1}$). Once more, the implication is that the controller is working near its limits.

In a situation such as this, depending on the precision needs of the mission, it would be advisable to slow or stop the rotation of the Inspector in order to return to its desired relative position. Doing so would essentially mean a pause in the inspection algorithm in favor of the relative navigation one, a strategic pause which allows the inspector to remain within controllable bounds.

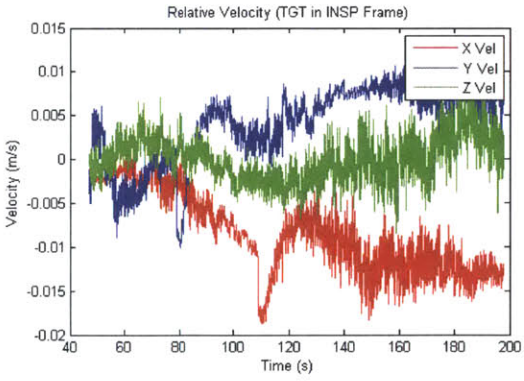


Figure 5-20: Planar Inspection: Relative Velocity during Moving Target Simulation

The Inspector is able to spin to its desired rotation rate of 2.5° $s^{-1}$ in the span of about

7s and is able to maintain that rate for the entirety of the maneuver (see Figure 5-21). During the course of the inspection, there is a slight variation in the satellite motion on the order of $0.005\text{rad}\,\text{s}^{-1}$ ($.29°\,\text{s}^{-1}$), though the noise level on the estimated rate is higher with a standard deviation near $0.009\text{rad}\,\text{s}^{-1}$ ($0.52°\,\text{s}^{-1}$). The variance is due to artificial noise placed on the beacon measurements used to estimate the state in the simulation. This noise is not found on the satellites as the estimator is differently designed, using only gyroscope readings to estimate rates.

Further, with the exception of a small rotation in the X- and Y-axes at the beginning of the test, and some small rotations at the 135 and 185s marks, the satellites maintain good control of the other body rates. The rotations which occur at the beginning of the test are a combination of some thruster misalignments and rotations that were imparted during the incomplete initial positioning (as we see in Figure 5-18a, there was still some positioning and pointing error being removed at the beginning of the maneuver). The misalignment problem becomes more acute when thrust needs approach the saturation limits for the thrusters with 200ms firing times. This is consistent with the previously mentioned hypothesis that the momentum imparted during tracking of the moving target has pushed the controller near its limits.

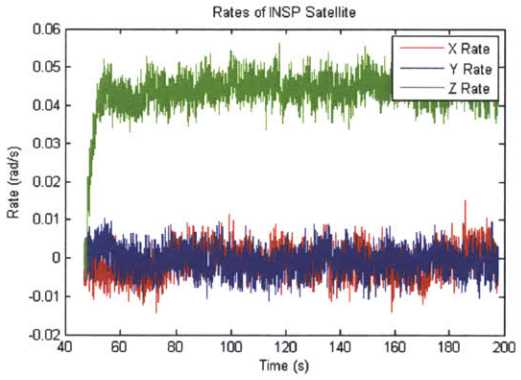


Figure 5-21: Planar Inspection: Inspector Rate during Moving Target Simulation

As a proportion of the total rotation of the Inspector (Figure 5-22), rotations in X- and Y-body axes are small, accounting for no more than 2% of the total rate at its peak, excluding those rotations which are attributable mostly to noise. Even accounting for the relatively large noise levels, at $2\sigma$ significance, the off-axis rotations never account for more than 4.5% of the total rotation.

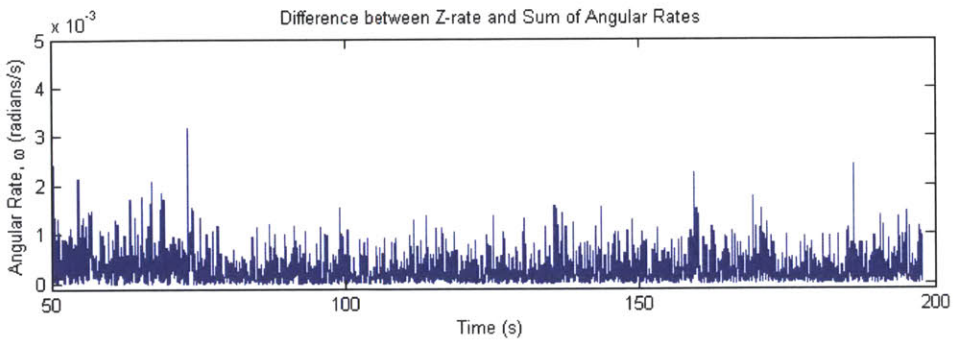


Figure 5-22: Planar Inspection: Difference between Z-Rate and Total Angular Rate during Moving Target Simulation

### 5.1.3 Simulation and Station Comparison

Because of the limitations on station testing time and an inability to test all inspection algorithms in the time before the launch of the VERTIGO hardware, it is considerably more productive to use the simulation to test out inspection maneuvers and run some subset of those maneuvers on station to both prove the concept as well as identify differences between the simulation and the real systems. The two tests described in subsections 5.1.1 and 5.1.2 were used for that purpose. These simple tests evaluated both the ability to maneuver using simulated vision and the differences between simulation and reality.

#### Stationary Target

In the ISS inertial frame the maximum difference between the simulation (Figure 5-13a) and the station data (Figure 5-1a) is 6mm in the +X direction, and 1.5cm in the -X direction. In the Y-direction the number is 1.7cm in the positive direction 2.3cm in the negative and in Z it is 1.7cm and 1.6cm in the positive and negative directions, respectively. Based on the variance in the measurements in Figure 5-1a, especially as the satellite drifts away from the center of the test volume, the variation between the simulation and station data is just slightly above the accuracy of the beacon system. At the extremes of the movement (peaks of curves in X- and Y-axes) beacon measurements become less accurate because the geometry of the satellite and beacons cause the angle between the two to become shallow, increasing measurement variance and decreasing accuracy. As the differences occur at these points and the measurement variation is on the order of 1-1.5cm (for Y- and X-axes, respectively), we conclude that there is a significant difference between the two paths sta-

tistically, but not practically.

Unlike the Inspector positions, the differences in the relative position are more substantial. Much of that difference, however, is likely due to the additional variance caused by the target object as well as the subtraction operation that is used to transform position from the ISS inertial frame to the relative one. In the simulation environment it is well-behaved with a zero-mean position (in all axes), with a standard deviation of no more than 1.7cm at a $2\sigma$ level. The station data however, shows slightly more deviation at 4.2cm, $2\sigma$. This deviation can partially be attributed to sensor noise, but only about 1.5cm based on the Inspector position variation. Other possible sources include disturbances like airflow in the module along with minor fuel slosh and thruster misalignment. Misalignment is compounded by the rotation of the satellite since that will cause the thrusters to create a force in the wrong direction up to about 1.2 degrees at a time. This is the result of thrusters firing based on orientation information which is at least 200ms old with a satellite rotating at $6°/s$ when used and which continues to rotate during the firing. The consistent lag in the system causes a zero-mean error but with some deviation, which the data shows to be up to 3 degrees.

The contribution of the two measurements should give a deviation near 2cm since

$$\sigma_{rel}^2 = \sigma_{INSP}^2 + \sigma_{TGT}^2 \tag{5.6}$$

$$\sigma_{rel}^2 = (1.5\text{cm})^2 + (4.2\text{cm})^2 \tag{5.7}$$

$$\sigma_{rel}^2 = 4.5\text{cm} \tag{5.8}$$

$$\sigma_{rel} = 2.1\text{cm} \tag{5.9}$$

which is observed in the relative state plot of the station data. The deviation, however is not the only difference. Of more concern is the relative motion which is attributable to the actual motion of the satellites rather than sensor and actuation error. There are two things which stick out in comparing the two datasets.

The first is the periodic oscillation in Y- and Z-position, and the other is the drop following the 110s mark in the X-position.

In addressing the first concern, we first observe that many oscillations in the translations correspond to variations and jumps in the rotation rate of the Inspector (Figure 5-4). Varying rates about Z should affect the Y-axis relative position. When the Inspec-

tor increases its rotation rate quickly, system lag causes the horizontal (Y-axis) component to grow, pushing the Y-relative position positive until the position controller is able to catch up to the new rotation rate. Furthermore, the design of the controller may be lightly damped in the presence of disturbances. Fine-tuning of the controller gains for future development efforts would solve this problem. That said, with the current design, it is expected that there may be error in the Y- and Z- directions up to approximately 5cm and has the same period as the jumps in rotational velocity.

To address the second, it is important to refer back to the inertial position of the Inspector satellite (Figure 5-1a). That measurement ha s similar drop of nearly 4cm over the period of 200ms. Therefore, this drop is likely an artifact the metrology system, possibly due to a bad ultrasound reading that the internal state estimator (an EKF) is not able to completely disregard and which then persists in the state estimate for the next 4-5s. Such outliers are possible with the vision system, but since the implementation of the controller with the vision system does not currently filter its data, outliers will be transient events that do not effect the position controller beyond the current frame. Future vision estimators and outlier detection that should be included on the vision system can be tuned to eliminate the occasional large jumps like what is seen in Figure 5-1a large jumps.

From these two differences we make the following two claims about the differences between simulation and ISS tests:

1. Y-/Z-axis errors are linked to variations in the rotation rate.

2. At a range of 36cm, variations are up to 5cm in Y/Z.

Since the position errors are so closely coupled with the rotation rates, it is those rates which we shall next examine. Referring back to Figure 5-4, we observe that the Z-rate has a $2\sigma$ deviation of 6.7mrad $s^{-1}$ ($0.39° s^{-1}$) about the commanded mean of 0.0436rad $s^{-1}$ ($2.5° s^{-1}$). The X- and Y-rates have a similar distribution, but around a commanded mean which is instead zero.

The peaks in the Z body rate come approximately every 20-21s. This is likely the result of large thruster inputs that is the result of a fairly wide deadband in the controller that comes from the relatively small control gain that is placed on the angular rate. Coupled with the dynamics associated with rotation about a minor moment of inertia, this causes the rotation to reach a peak slightly above the desired rate, then decay (as is visible in the

target rate decay in Figure 5-6) until the controller can once again provide enough control authority for another thruster firing.

Unlike the simulation, however, the rate has far less noise on the measurement as a result of the different measurements used in the simulation and in the SPHERES standard estimator. Since the standard estimator uses the gyroscope measurements as truth, the variation in the rotation measurements is equivalent to the sum of the movement of the satellite itself and the noise of the measurements. An estimate of the variation which subtracts the variation due to the satellite motion (itself an estimate of the decay of the satellite rate) yields a standard deviation around 1.395mrad $s^{-1}$ (0.080° $s^{-1}$) at a $1\sigma$ significance. That estimate, using the data from the first 50s of the maneuver, is liable to drift over the course of the test. However, with random noise in that range, the angular random walk is expected to be about 7.66mrad (0.44°) after a 150s maneuver. The random walk is derived as follows[35]:

$$\sigma_{ARW} = \sigma_{gyro}\sqrt{\Delta T * T_{total}} \tag{5.10}$$

$$\sigma_{gyro} = 0.080°/s \tag{5.11}$$

$$T_{total} = 150.4s \tag{5.12}$$

$$\Delta T = 0.2s/measurement \tag{5.13}$$

$$\sigma_{ARW} = (0.080°/s)\sqrt{(0.2s) * (150.4s)} \tag{5.14}$$

$$\sigma_{ARW} = 0.44° \tag{5.15}$$

These results actually exceed the specification sheet for the gyroscopes, which give a resolution of 0.0407° $s^{-1}$, with a noise ceiling of 0.05, which works out to a 1-$\sigma$ error up to 0.35 ° $s^{-1}$ at 50Hz[36].

Prior to moving onto an analysis of the inspection with motion it is important to note a few remaining items about the gyroscope measurements based on the target object's rotation estimate. The first is that the standard deviation approaches the same value with a sample showing approximately 1.42mrad $s^{-1}$ (0.081° $s^{-1}$) of standard deviation at $1\sigma$ significance. This level is exceptionally close — within 1.3% — to the estimate given by the Inspector satellite, providing another check on the value. The second is that the somewhere along the line the gyroscopes will occasionally provide outliers, particularly in the X-axis

of the target satellite. Over the course of a 150s maneuver, there were 3 exceptionally significant outliers (100s of % error) and a fourth which is still significant error (at 60% deviation from the immediately preceding and following measurements). Though these errors did not cause any significant problem during the course of the inspection since the rotation of the target was not actively controlled, it may be worthwhile to avoid using the satellite used as the target in this test as an inspector in future operations.

### Moving Target

Once the target adds motion the path in inertial space matches up well with the simulation, even better perhaps, than in the previous test with a stationary target. The overshoot of the target satellite was approximately 3% in the inertial frame (Figure 5-7b vs 5-18b).

Station results from the Inspector's inertial position (Figure 5-7a) also track well with the simulation data (Figure 5-18a). With the exception of the maximum observed in the X-axis, all other peaks (X-min, Y-max and Y-min) occur within 1s of the predicted time. The exception occurs 5s later, though that may be the result of noise on the metrology system. The overall error in those same peaks is 1.6% for an average of 7.7mm error in positioning.

The relative position is more important than the inertial one, however. Refer back to Figures 5-8 and 5-19. In those plots, as well as the supporting data, we observe that there is significantly more noise and variation on the relative positions when compared to an inspection with a nearly static target object (Figure 5-2). Control in the X-axis (range) actually maintains itself fairly well with error staying within approximately [-3,7]cm of the desired 36cm range. Much of that error in the negative direction is cause by lag in the controller as it tries to bleed momentum acquired by matching the target object's speed. In the positive direction, the adjustments being made by the controller in order to deal with the slowing target work against the Inspector as the target then begins motion away once more.

Compared with the simulation, the general shape of the Inspection matches well — there are peaks near 85 and 120s as the Inspector reaches its maximum distance from the target, as well as a trough near 107s as the second motion begins. The timing agrees well, but it is the magnitude of these which is incorrectly estimated in the simulation. Relative to the commanded position of 36cm, the peaks and troughs exceed this in simulation by 6.3, 2.8, and 4.9cm, while the actual data shows errors of 2.9, -3.1, and 7.0cm. The implication

for future tests is therefore the following:

1. The actual system maintains an average range to target better than predicted in simulation by up to 2cm, or 6%.

2. A single target motion in simulation which causes up to 1.7cm in error may cause up to 3cm in hardware, or roughly double.

3. A second motion will cause error to compound, creating a peak up to 2.5 times larger, where simulation may predict no growth in error relative to previous motions.

Examining the Y- and Z-axis errors, we observe that both simulation and station data shows that it is zero-mean but that the magnitude of that error is much higher when run on that hardware. This, however, appears to be the result of poor control in the angular rate of the satellite rather than the position controller itself (see Figure 5-10). This is also partially to blame for the error in the Inspector's body X-axis. This allows the error to change by 20cm in the span of 4s, as does somewhat noisy position relative position data that sees very large variation throughout the test and does so at a rate that the satellite cannot achieve by translation alone.

The conclusions that may be drawn from the data is this:

1. There is no bias in the simulation with Y- and Z-axis positions.

2. Pointing and metrology errors causes the error in these axes to be approximately twice what is predicted in simulation (5cm in simulation, 10 on station).

To close out the comparison, we next examine the rates of the Inspector satellite. As with the inspection with no target motion, we see significantly less noise in the station data (Figure 5-10) than with the simulation (Figure 5-21). This has the same cause, which is the different methods used to estimate the rate — the simulation uses the beacons and their attendant noise where the satellites themselves use their more accurate gyroscopes for measurements. The error in measured vs. commanded rates is zero mean, but the simulation noise is on the order of $0.01\text{rad}\,\text{s}^{-1}$ ($0.57^\circ\,\text{s}^{-1}$), where the real data shows variation no greater than half of that, at $0.005\text{rad}\,\text{s}^{-1}$ ($0.29^\circ\,\text{s}^{-1}$). While the noise is much lower than in simulation, and the X- and Y-rates match well, there are some differences which are less beneficial. When the controller is stressed, as is the case following the second motion

of the target, rate errors may grow to 0.018rad $s^{-1}$ (1.0° $s^{-1}$) in off-axis rotations, though only 3.9mrad $s^{-1}$ (0.22° $s^{-1}$) in the Z-direction. In less than 10s, however, those errors are expected to damp out.

Critically, the most important fundamental difference between the simulation and the station data is damping in the system which causes rotation about the minor axis to slow consistently until thruster activity respins the satellite and controls rotation in the off axes. This damping, which is uncontrolled in the target (Figure 5-12), would cause the rotational axes to slowly change over the course of an inspection if left alone. This means that for a successful maneuver the rotation of the Inspector must be closed loop rather than the initial spin up that is used for the target.

Ultimately, these data points allows us to draw the following conclusions:

1. Simulation and station rate data show error that is zero mean, but the standard deviation of the simulation is double what is to be expected on station.

2. Damping is present on station that is not accounted for in simulation.

### 5.1.4 Simulation Only

The previous two subsections described tests which were run on the International Space Station following simulations which demonstrated their ability to control an Inspector performs a circumnavigation of a target object. The targets also demonstrated that the maneuver is robust to limited movement by the target object. Based on the comparison of the predicted and actual maneuver performances, we may analyze four additional tests that were developed and run in simulation. Those tests are (the code for which is included in Appendix A.2):

1. **Additional Motion** This test is a continuation of the motion test that was run on station, but with movement perpendicular to the inspection plane as well as motion of the target toward the Inspector.

2. **3D Inspection** This test finally moves out of the planar inspection and attempts to get full coverage of the target object.

3. **Long Duration Planar Inspection** This inspection is identical to the first, stationary target test, save for a duration of 10 minutes rather than 4. This is done for two

purposes: on station this would allow a better characterization of gyroscope drift while in simulation it potentially allows for greater coverage while remaining in a planar motion.

4. **Inclusion of Rotation Information** The final test uses rotation information in order to build a more fuel- and time-efficient inspection path, as it takes measurements of the rotation rate of the target satellite in order to estimate its own coverage performance.

Further, each of these tests is designed to be run at 70cm range rather than 36cm. While this makes it more difficult for the inspection to fit within the space station test volume, it more closely fits the range at which the VERTIGO system is designed to operate. To compensate for the additional distance that needed to be travelled for a similar angular rotation, the satellite rotation rate was dropped from 2.5 to $1.5° \, s^{-1}$.

### Additional Motion

In this test, we aim to determine the reaction of the Inspector satellite to motion by the target, but rather than having the target satellite move away, *a la* the second station test, it will move toward the Inspector, and then in a shear direction to it. During this test we aim to characterize the motion by determining the closest approach, overshoot, and stability. The primary objective will be to quantify these values in the relative frame, though looking at the inertial frame is also useful, especially for visualizing the motion.

For this test, the satellites begin slightly offset from the center of the volume in order to ensure that there is sufficient room for maneuvering. At the 60s mark in this maneuver, the target moves first in the Y-direction toward the Inspector. 60s later, the satellite moves once more, this time in the negative Z-direction. In both cases, the Inspector adjusts, chasing its target. Figure 5-23a shows the former's motion, while Figure 5-23b shows the latter.

The simulation shows the motion is well controlled. The overshoot of the target satellite is at or below 10% for the both motions. The more interesting motion, however, is that of the Inspector. In this maneuver, the Inspector begins to react to the motion of the target within 2s in both directions. Such a reaction matches fairly well with what was observed in the station tests. What differs, however, is the Z-location of the Inspector, which appears to have set up a periodic motion. This change is not easily detectable in the gyros because

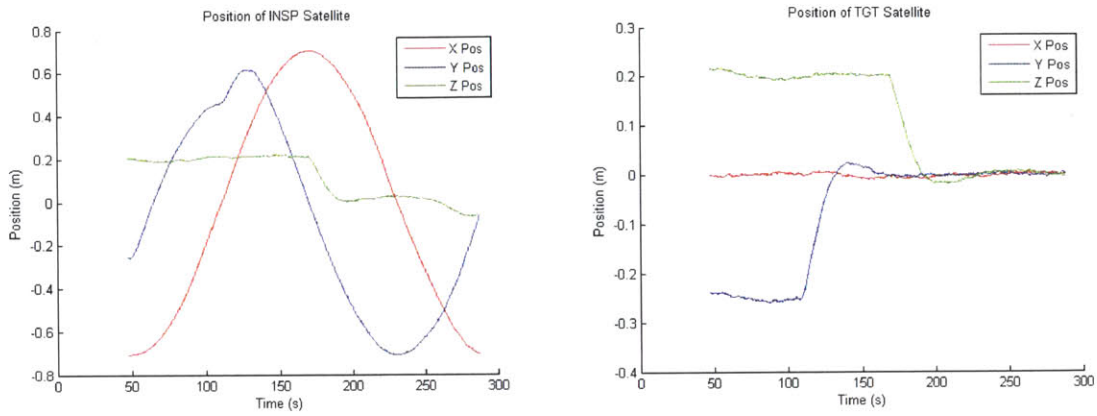


(a) Inspector Position

(b) Target Position

Figure 5-23: Planar Inspection: Position Data during "Additional Motion" Simulation

of the simulation noise (see Figure 5-25), but a cursory examination suggests that this is caused by a misalignment that happens during the vertical motion that is maintained. This can probably be attributed to thruster simulated misalignment, as a similar angular error is seen during initial positioning (not plotted).

Nevertheless, the inspection does maintain the proper distance, never approaching closer than 68cm on the desired 70cm range (see Figure 5-24). This minimum comes 5s after the motion of the target toward the inspector begins. On the whole, proper distance is maintained within a centimeter of the commanded range excluding the peak due to the motion.

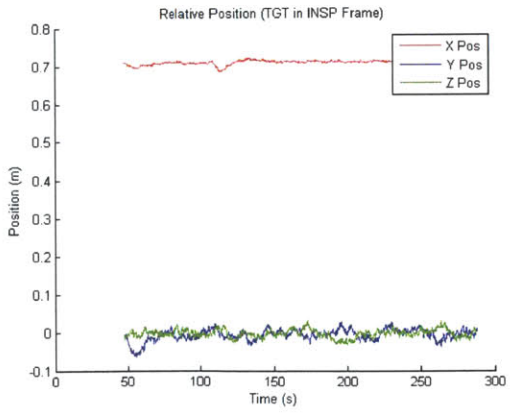


Figure 5-24: Planar Inspection: Relative Position during "Additional Motion" Simulation

At this range, however, slight misalignments in the inspector can cause large displacements in the relative Y- and Z-measurements, which is visible in the 6cm maximum displacement near the beginning of the maneuver. Given the station results compared to simulation results, a safe assumption is that errors will be no greater than twice that amount. Thus, the expected translation error should be below 12cm.

It should be noted that this doubling is based on data collected from a 36cm inspection, which stresses the control authority more than the 70cm distance. To simplify the model, we assume that the added pointing sensitivity is equivalent to the increased control authority, and thus they cancel one another out.

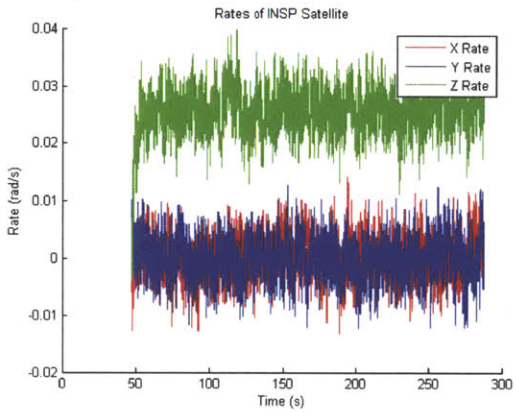


Figure 5-25: Planar Inspection: Inspector Rate during "Additional Motion" Simulation

Finally, we also observe during this test that the inspector satellite maintains its constant rates (Figure 5-25), with the exception of a small spike in the Z-axis during the target satellite's first motion (toward the Inspector). This motion may be the result of a combination of control saturation and thruster misalignment during the maneuver, since the same thruster used to maintain the rotation may be used for translation to try to maintain the correct pointing. The resulting spike is small, however, and without confirmation with station data, it remains to be seen if it is significant at all.

### 3D Inspection

This maneuver is the first foray of VERTIGO into the Z-dimension in a way that is meaningful for the purposes of inspection. Since the inspection path is managed by the rate of the Inspection satellite, a glance at Figure 5-28 shows the motion well.

The inspection begins as all the previous ones, with an X-Y planar motion. After 90 degrees of rotation, however, the inspector changes rotation axes and pitches over while it moves around the target. In order to better fit the maneuver into the ISS test volume, the target is commanded to move in the Z-direction, as shown in Figure 5-26b.

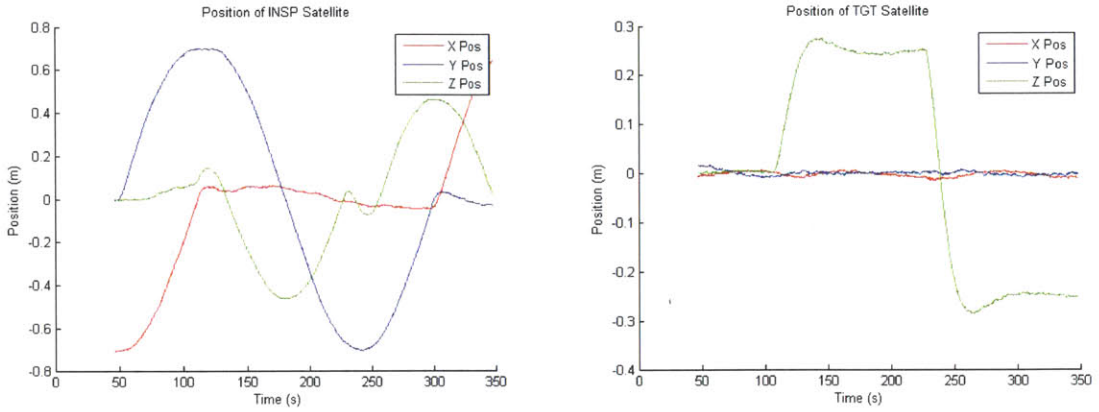


(a) Inspector Position

(b) Target Position

Figure 5-26: Planar Inspection: Position Data during 3D Inspection Simulation

The overshoot and steady-state error matches that from previous tests in the inertial frame. Likewise, the error in relative position (Figure 5-27) is minimal, with translation error keeping at or below 6cm. In range, the error is even smaller since the target is not moving toward the Inspector. Unfortunately, because of the volume constraints, the target must move in a way that is favorable to the inspection, and the maneuver isn't fully representative of what would be encountered in the "outdoor" space environment. Nevertheless, the coverage — which will be discussed later — should be very similar.

In Figure 5-28, the rates are held steady throughout the maneuver, though Z-rotation is replaced with Y-body-axis rotation 90s into the maneuver. The the target readjusts its position halfway through, and then the Inspector Y-rotation is replaced with the original Z-rotation at the 300s mark, as it finishes its circuit about the target.

This inspection appears to be controlled and maintain good control, remaining at a safe inspection distance, and doing so within a 2cm margin. With the simulation results, it is expected that a station test would perform well, as there are no significant disturbances that would be expected to perturb the motion. Even though the motion takes advantage of a third dimension, the separation of the movement into discrete axes means that the

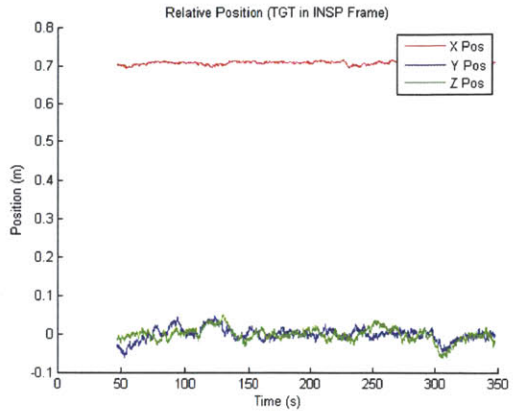


Figure 5-27: Planar Inspection: Relative Position during 3D Inspection Simulation

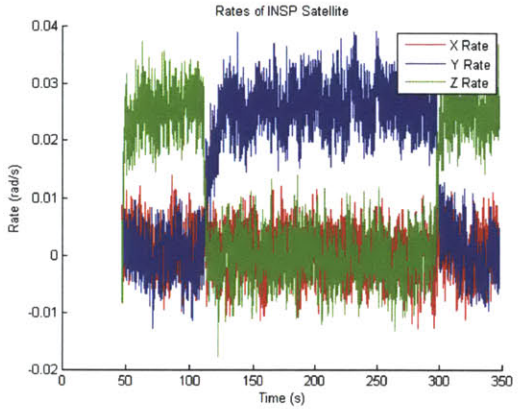


Figure 5-28: Planar Inspection: Inspector Rate during 3D Inspection Simulation

performance should be similar to that in the tests run on station.

### Long Duration Planar Inspection

This inspection is fairly simple, and consists of the first station-run test run for a longer duration in order to gather a larger sample of data about the rate gyros on station, their biases, and their noise characteristics.

For most of the inspection, there is little in the way of disturbances which show that thruster misalignment or gyro error affects the inspection by tilting the plane of movement. After approximately 400s, however, that is no longer true, as the satellite reaches a peak near 6.5cm above and below the X-Y plane (Figure 5-29a). This peak does not correspond with any peak or motion by the target (Figure 5-29b). The disturbance implies an angular

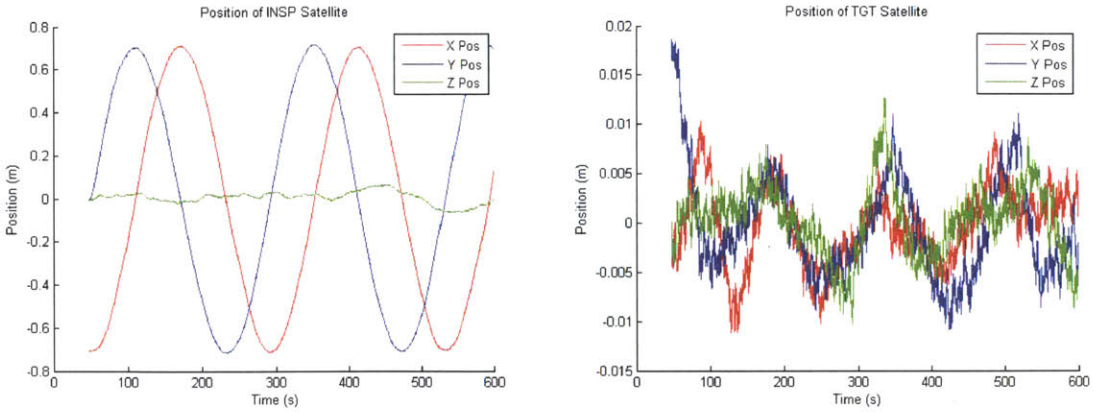


(a) Inspector Position

(b) Target Position

Figure 5-29: Planar Inspection: Position Data during Long Duration Simulation

walk of 0.093rad (5.3°) over 10 minutes, which implies combined error from the gyros and thruster misalignment of 8.4mrad $s^{-1}$ (0.48° $s^{-1}$). Since the test objective is to identify the noise on the gyros and what the actual random walk, the test in itself is only particularly valuable when compared to station data.

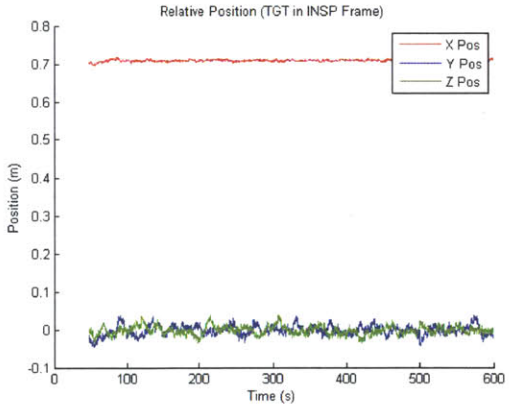


Figure 5-30: Planar Inspection: Relative Position during Long Duration Simulation

Nevertheless, the maneuver does appear to hew closely to the desired relative position, with translational error remaining below 5cm for the duration, and no significant errors in the range measurement (Figure 5-30). Based on the shorter-range, shorter-duration test run on station (see Figure 5-2 for comparison), we would expect no more than approximately 5cm of error, below 10%. Likewise, the noise level on the gyros as seen in Figure 5-31

is expected to be far lower than the simulation output, though it should remain equally steady.

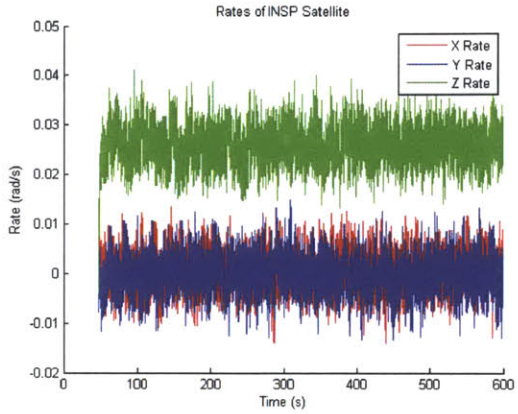


Figure 5-31: Planar Inspection: Inspector Rate during Long Duration Simulation

### Inclusion of Rotation Information

This is the most complex motion that was developed during the course of the maneuver development. The first part of the motion finds the Inspector rotating about its X axis in order to align with the rotation axis of the target. After the alignment is completed, the inspector moves to a position in the "northern" hemisphere of the rotating target object, where it begins a multi-axis rotation to maintain pointing toward the target while maintaining itself in the same relative orientation. The inspection would follow an equal line of "lattitude" were the target to remain stationary.

This motion is repeated in the "southern" hemisphere and along the equator, with a switching function defined when the entire target has moved through view, based on the sum of the rotation of both objects.

This motion is best understood by looking at the motion of the Inspector in Figure 5-32.

In spite of the complexity of the motion and the increased potential for rotational rates to influence the relative position error (since the motion is in two axes), the motion is relatively well controlled. Error in range (see Figure 5-33) remains within 2cm, and translational error peaks around 6cm, which is consistent with previous motions at this range.

Once more, the simulation falls victim to large amounts of noise on the rotation rates that the ISS system is unaffected by. Regardless, with the exception of small increases in

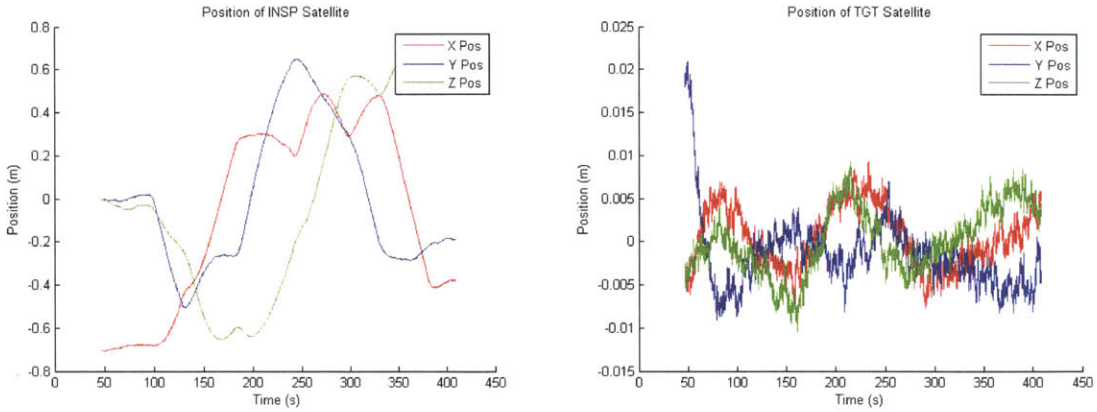


(a) Inspector Position

(b) Target Position

Figure 5-32: Planar Inspection: Position Data during "Rotation" Simulation

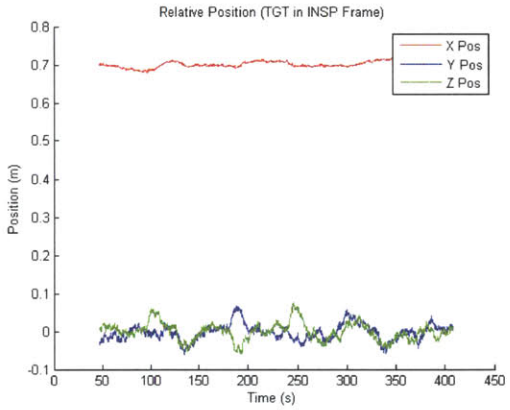


Figure 5-33: Planar Inspection: Relative Position during "Rotation" Simulation

the variability of the Y-rate around 225s (Figure 5-34), the inspection shows stable rates.

The behavior of the simulation-only maneuvers is not exceptional compared to the motion that was simulated and run on the Space Station. Since the motion of the Inspector satellite in simulation data matched with the station data within a margin of about 10%, while remaining stable with bounded error, we can trust the simulation-only inspections to perform similarly well.

The significant differences between the station and simulation data included the result of an additional mass placed on the target object, which exaggerated the effects of rotation about a non-major, non-minor axis. Also significantly, the simulation did not track the

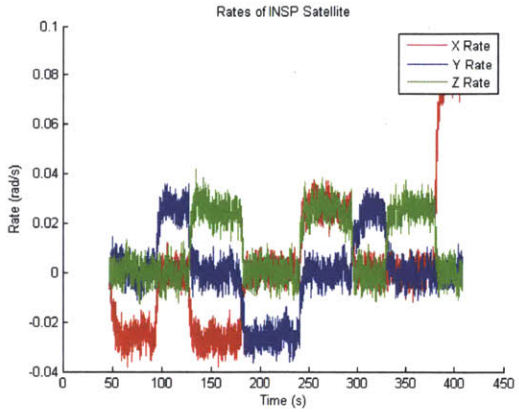


Figure 5-34: Planar Inspection: Inspector Rate during "Rotation" Simulation

rotation rates nearly as well as the gyros in the SPHERES satellites themselves do.

## 5.2 Maneuver Comparisons and Inspection Performance

This section will focus on the results of the tests called out in Sections 5.1.1 through 5.1.4. It will identify the effect of test variables that the station tests and simulations, and attempt to isolate those effects. Particular focus will be paid to the lessons learned in the previous section in order to extrapolate into the real world those results which were from simulation alone.

### 5.2.1 Target Behavior

Taking the Stationary Target test that was run on station as the reference maneuver, to determine the impact that motion by the target has on the inspection, it must be compared to the Moving Target test also run on station and the Additional Motion test run in simulation only.

The best measure for how well the inspection responded to this unexpected motion is to compare the perturbation to the range measurement (X-axis measurement in relative frame).

In the Stationary Target test (Figure 5-2), the desired range is 36cm. With the exception of a 20s time period that may be attributable to an outlier in the metrology system, the Inspector maintains that range fairly well. Nevertheless, the total variation is between 31

and 41cm, for a range error of 5cm.

In the Moving Target test (Figure 5-8), the situation is much the same, with an approximate 5cm range of error, but this time with a bias away from the target, with a range from 33 to 44cm. From this data, it appears that motion of the target away from the inspector does not significantly altered the performance of the inspection, and certainly does not affect the collision risk based on the point of closest approach.

Because of the need to develop tests that more closely approximate the inspection capabilities of the VERTIGO system, especially the need for a greater inspection distance, an additional confounding variable was added to the Additional Motion test. However, the test appears to show very similar results, though even more favorable. At a desired range of 70cm, the extent of the range varies from 68 to 72cm, for an error of $\pm$2cm. At this greater range, the stress on the control system is less, as the maneuver requires much slower rotation of the inspector satellite (the error is likely closely related to the feedforward term, which is about 1.5 times larger at the closer distance). Therefore, the two errors, while different, are comparable.

The results across these three tests suggests strongly that motion of the target satellite — provided it has no more control authority than the Inspector — is not significant. Translational error also shows only a small increase in error as a result of target motion, even in the case of shear motion, as in the Additional motion simulation.

Coverage should also be examined to determine the effect of the motion on the total coverage and how quickly the maneuver approaches full near-complete coverage.

The first two maneuvers that were tested on station show striking similarities, in both the amount of coverage at 89 and 87%, respectively, but also in the pattern in where that coverage is accomplished. This is understandable, since the two maneuvers are nearly identical in duration and in the relative motion of the two bodies. The coverage is not global, though the trend in the data suggests that a longer inspection, where the target has the opportunity to rotate through a larger angle would allow for the areas which are currently unobserved to be seen. This data, however, shows no significant impact to the coverage by target motion.

With the simulation-only data, there appears to be significantly better coverage, with effectively full coverage. Like the station-evaluated maneuver, the poles of the satellite are unobserved, though it is less pronounced with the station group because the target changes

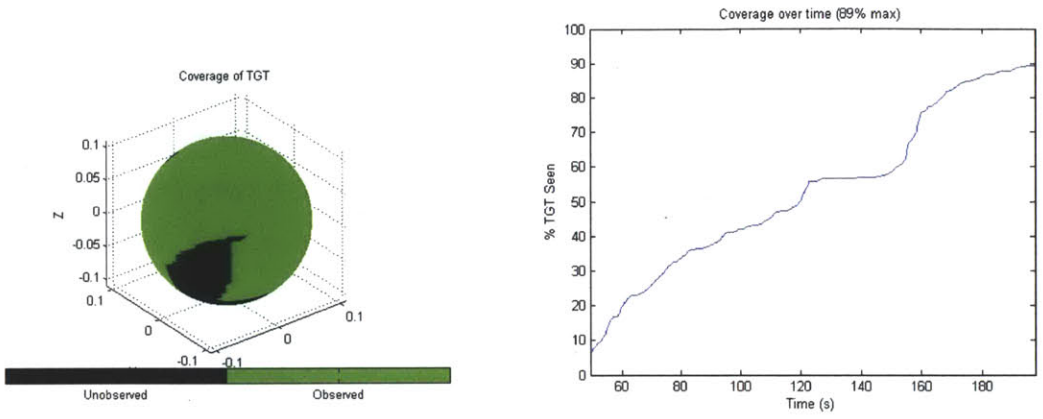


(a) Final Coverage on Target Surface

(b) Coverage over Time

Figure 5-35: Coverage: ISS Stationary Test

its axis of rotation throughout the maneuver, allowing for better diversity in coverage. The fact that observation is being done at 70cm rather than 36, however, is much more significant that the effect of the motion. When compounded with the fact that the Inspector is travelling at a slower angular rate, making the inspection take longer, this means that a comparison between the two has little significance. It does, however, suggest that the maneuver, when run with the actual camera system at a range of 70cm, will be well-suited to full coverage.

Coverage, like the inspection maneuvering error, shows independence from the motion of the target object, though it is closely bound to the range and rotation rate of the two satellites. Additionally, at the range and rates demanded by the actual vision system, coverage should be nearly global for a planar inspection, though certain rotation rates by the target can interfere.

### 5.2.2 2- and 3-D Motion

As motion of the target was examined, so too should variation in motion by the Inspector. Similar analysis may be done on the basis of the relative position error as well as the coverage provided by the inspection. Again, the baseline for this inspection will be the ISS test with a stationary target, though supplemented with the long-duration inspection simulation data. The maneuvers which will be compared to that baseline are (aptly) the

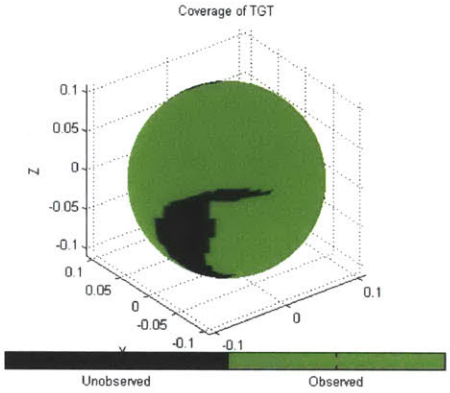


(a) Final Coverage on Target Surface

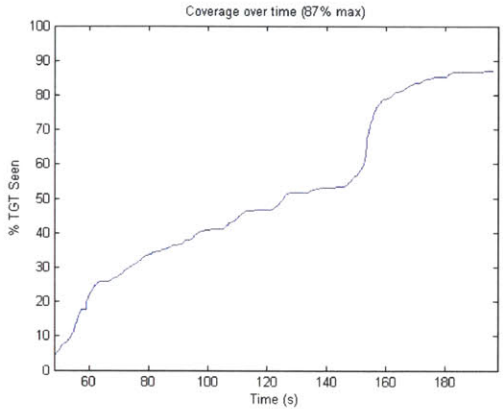


(b) Coverage over Time

Figure 5-36: Coverage: ISS Motion Test

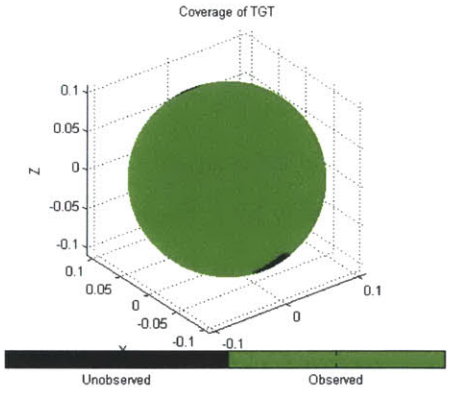


(a) Final Coverage on Target Surface

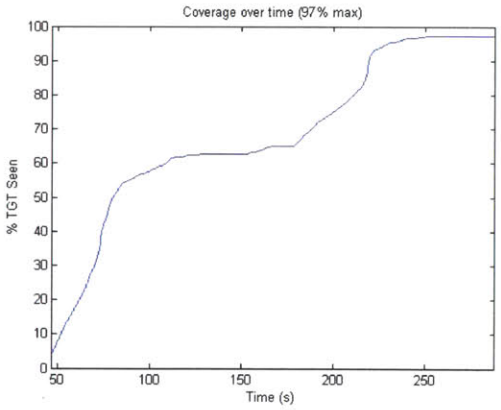


(b) Coverage over Time

Figure 5-37: Coverage: Simulated Additional Motion Test

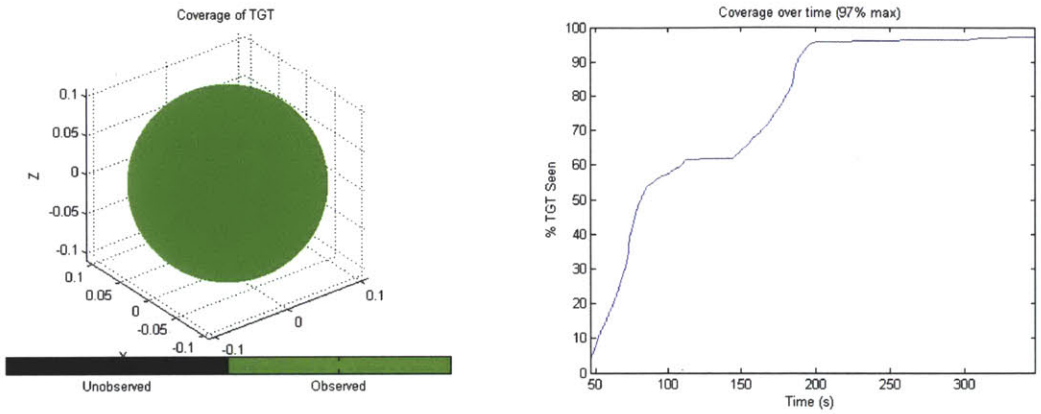


(a) Final Coverage on Target Surface

(b) Coverage over Time

Figure 5-38: Coverage: Simulated 3D Inspection Test

"3D Inspection" and the "Inclusion of Rotation Information" maneuver.

Figure 5-39 shows the coverage that is experienced by the long duration test. As would be expected with an Inspector that make a planar motion for 10 minutes with a rotating target, the coverage is nearly global. Surprisingly, this takes only 150s out of the total 600s of the inspection, suggesting that much better coverage is possible merely by using the increased inspection distance.

The risk associated with this inspection is that the rotation rate of the target may interact with the path of the Inspector. Should the two have matching or near-matching rotation rates, the field of view will be constant, and coverage will be minimal. Even if the path of the inspector shows resonance (in the orbital sense) with the rotation of the target, then there are likely to be areas which remain covered no matter how long the inspection is.

In order to reduce or eliminate this possibility, the estimation of the target's rotation rate is of great use. Furthermore, in spite of the relative accuracy that vision algorithms can determine the rotation of an object in view, the algorithm requires only an approximate knowledge of the angular velocity. This allows the inspection to take advantage of the rate to plan more efficient paths. Given a stable rotation (as seen in Figure5-40), this gives effectively global coverage, with less than 0.5% unviewed.

The way that this maneuver uses the rotation information of the target is to align its inspection planes with the plane defined by the rotation of the target. To best take advantage of both cameras, the Inspector rotates so that its body Z-axis is parallel with the

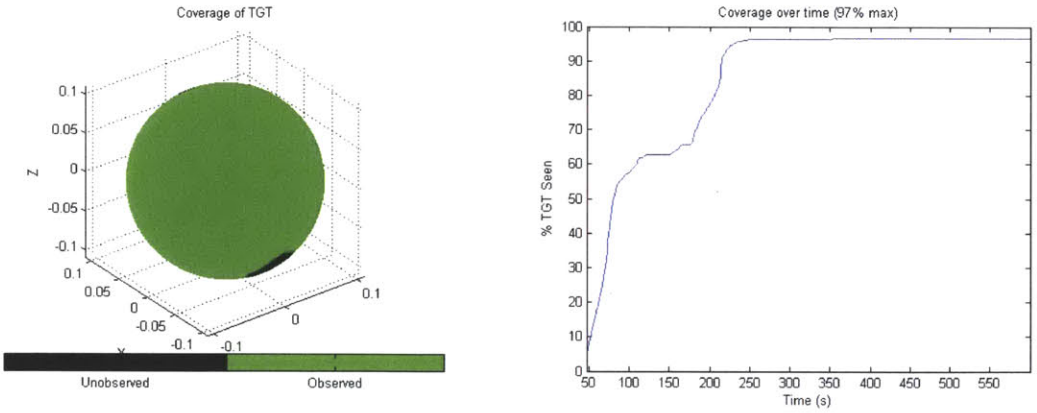


(a) Final Coverage on Target Surface

(b) Coverage over Time

Figure 5-39: Coverage: Simulated Long Duration Test

target's angular velocity. This places the camera baseline parallel with the plane defined by the angular velocity. The Inspector then moves to scan the upper, lower, and middle thirds of the target, all the while integrating the sum of the target's rotation and its own to determine when to switch.

As a result of the alignment of the inspection planes with the rotational planes, the inspection avoids the potential pitfalls of an inspection which depends on the target not having a certain set of undesireable rotations.

### 5.2.3 Use of Rotation Information

Because of the numerous confounding factors in comparing the use of rotation information to the original stationary target baseline, with a desired range of 36cm, the long-duration inspection will be used instead. Additional comparisons can be drawn through comparison to the "3D Inspection" maneuver as well. This allows for an evaluation of tests of similar duration, with an without the third dimension taken into account, and with the use of rotation information.

What the analysis looks for is the performance of the inspection; time to full coverage, fullness of coverage, and fuel use are the discriminating factors.

As noted in Figures 5-38, 5-39, and 5-40, all maneuvers do eventually approach full coverage, though only the rotation information test is able to effectively provide 100%

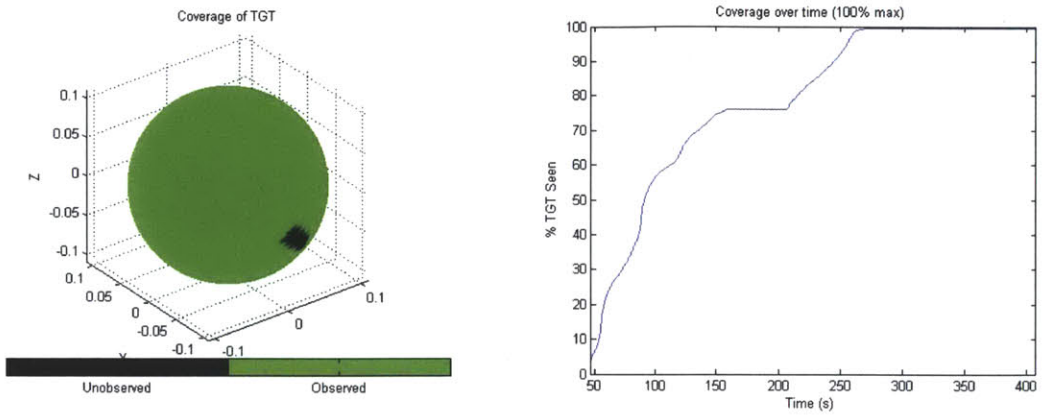


(a) Final Coverage on Target Surface

(b) Coverage over Time

Figure 5-40: Coverage: Simulated Using Rotation Information Test

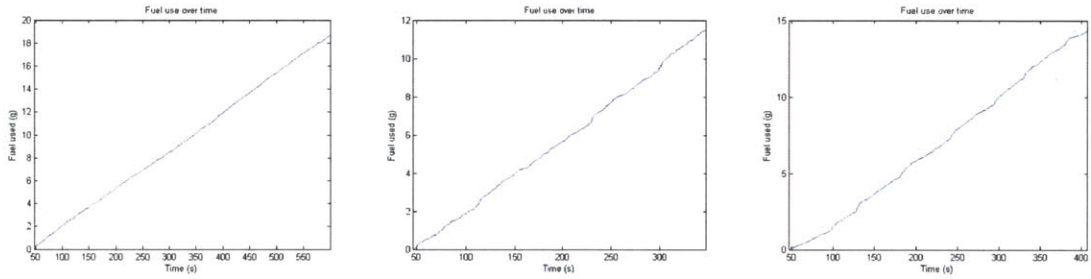


(a) Long-Duration

(b) 3D Inspection

(c) Rotation Information

Figure 5-41: Fuel Use: Rotation Information vs Baselines

coverage compared to the former pair's 97%. If full coverage is a hard requirement for the maneuver, then it is clearly necessary to either use the latter approach or run the 3D Inspection or Long Duration algorithms for much longer than they are currently designed to run.

If, however, 97.5% is an acceptable coverage ratio, then the discriminating factor in determining the preferable inspection for the mission at hand comes down to a weighting of the time and fuel used by the Inspector satellite to perform its maneuver. The fuel use for each can be seen in Figure 5-41.

Fuel use, however, is essentially flat across each of the maneuvers at an estimated consumption rate of 1g of fuel for every 30s of test. The difference, therefore is not in the rate of consumption, as the different maneuvers have nearly identical fuel needs, but rather in

| State/Quantity | Value |
|---|---|
| Gyro Random Noise ($1\sigma$) | 0.080° |
| Gyro Angular Random Walk ($1\sigma$) | 0.44° |
| Relative Range Overshoot | <12% Error |
| Closest Approach (% Desired Range) | 94% |
| Farthest Approach (% Desired Range) | 106% |
| Largest Vertical Error | 12cm (at 70cm range) |
| Largest Horizontal Error | 12cm (at 70cm range) |
| Fuel/Time Efficient Inspection | Planar, Nonaligned Rotation Axes |

Table 5.2: Estimated Navigation Accuracy

the time until full coverage is obtained.

Using the earlier definition of full coverage as 95% of the surface having been viewed, the time-to-completion for the various maneuvers is 196.7, 229.9, and 255.3s for 3D motion, Long-Duration motion, and Rotation Information inspections, respectively. Fuel consumption at those time points are 5.545g, 6.303g, and 8.130g, respectively. Given the cost function,

$$J_{ISS} = Q * m_{fuel} + R * \frac{t}{15.87}$$

with equal unity weights $Q$ and $R$, the values of the cost function for the respective inspection methods are 17.94, 20.79, and 24.22. Therefore, the most effective inspection in terms of weight and time for 95% coverage is a simple 3D inspection that does not use the target rotation information. One caveat remains however, and that is that the situation applies only to this particular rotation of the target. Further, it also only applies if 95% coverage is acceptably considered "full".

## 5.3 Conclusion

This chapter provides a comparison between the simulation results and station data, and also provides an estimate of expected performance of the inspection and navigation algorithms as implemented on the SPHERES Satellites.

From this analysis, it is claimed that the performance parameters of the design inspections are as described in Table 5.2. It should be noted that since these measurements were made using simulated vision data that those listed values (with the exception of gyroscope noise) represent upper bounds on the navigation error.

The consequences of the data is that inspections will be able to be conducted without significant risk of collision. Further, the best estimate of the gyroscope random noise suggests that 50Hz data has a deviation of 0.080°. Whether or not that meets performance requirements for a vision system is dependent on the camera algorithms, but the low value suggests that they will work for most situations. The low translational errors also bode well for VERTIGO, since they suggest that it will be able to maintain pointing toward the target object even if the target begins to move during the inspection. Further, since a 3-minute inspection does not move out of plane by more than 10cm, when combined with image processing tools, it will be possible to build an accurate 3D map — and achieve the VERTIGO mission.

# Chapter 6

# Project Management of the VERTIGO Payload

The story of the VERTIGO Program is one that will be familiar to many who are involved in the development of spaceflight hardware. This chapter will delve into some of the challenges and successes that the program experienced and analyze the program from the point of view of your author, the MIT Program Manager.

Throughout the chapter we will follow the program through two points of view: the Product and the Process. We will examine how technical problems and approaches fed back into the program management, and how the same management in all its forms informed the final product in fabrication.

We will also show the initial timeline of the program and its evolution as it met the realities of the engineering, scheduling, and other technical challenges. It will also cover feedback on the program model — that of a fast-paced technical development program designed to mature ground hardware up the technology readiness ladder. And finally it will provide lessons learned for future student program managers, and military officers as a part of the Space Engineering Academy program within MIT's Space Systems Laboratory.

We begin with an exploration of the eight guiding principles which were used to guide the development of the VERTIGO product and the leadership and engineering process to develop that product. Figure 6-1 shows the two elements side by side, and how the different legacies of the LIIVe and SPHERES Programs worked together with VERTIGO on the way to delivery of flight hardware. This figure will guide the discussion throughout.

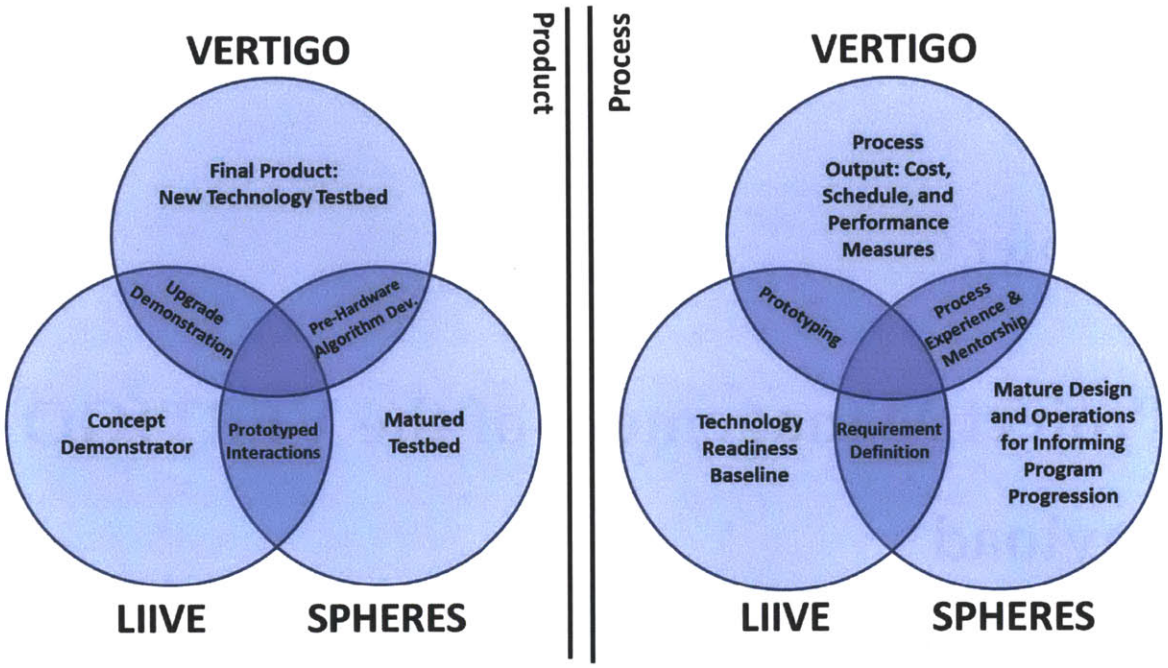


(a) Product

(b) Process

Figure 6-1: Project and Process for Successful Design

## 6.1 Design Principles

For the successful management of a small, flexible design team, there are a number of principles to keep in mind. While the list that follows is by no means exhaustive, it provides the necessary framework for leading the team through the systems engineering process.

Those principles are infinitive and imperative: to *Understand*, to *Build*, to *Try and Test*, to *Grow*, to *Advocate*, to *Fail*, to develop *Depth*, and to maintain *Margin*. Each contributes to the success of the product design or to the process which allows the design to be delivered on time, on-budget, and as promised.

We first address those principles that influence the design of the end product.

### 6.1.1 Product Design

The ultimate goal of designing spaceflight hardware and associated peripherals is to deliver a product with some value to the customer, which can work moderately autonomously, and which needs minimal maintenance. The VERTIGO Goggles must fulfill all these needs,

in spite of the atypical access that operation on the International Space Station grants operators.

In light of the restrictions that the operational environment places on the end product, we examine those principles which enable successful delivery and operation.

### Understand

> *The first principle of designing the Product, in this case the VERTIGO hardware and software is to understand the technical and program requirements of the project. Without this understanding, no schedule or resource allocation can be realistic.*

Coming into the VERTIGO program at its inception had both benefits and disadvantages. As the program manager, this allowed me to see the product through its entire design cycle - from requirements through design, test, and eventually fabrication. Such an experience is the exception for most engineering that a military officer may expect, but yields many of the same lessons, in particular because the VERTIGO design was informed so thoroughly by the lessons learned from its heritage in the LIIVe and SPHERES programs. Those lessons, however, were institutional, and not fully known or understood to your author. Of course, there is always a learning curve to every project, especially when integrating with a team that is more experienced, but a concerted effort can shorten the transition from team member to active contributor.

Two examples highlight the difference that a full grasp of the engineering problem makes. For the first example, we should examine the schedule and its evolution as the understanding of the software requirements increased.

| Action | Milestone | Due Date |
|---|---|---|
| SW 1 | SPHERES Software Updates | 12 Jul 2011 |
| SW 2 | VERTIGO Core Software Completion | 19 Aug 2011 |
| SW 3 | Visual Navigation Algorithm Prototype | 19 Aug 2011 |

Table 6.1: VERTIGO PDR Software Schedule

As shown by Table 6.1, at the Preliminary Design Review, held on the 8th of June, there were three identified software deliverables, each expected to take no more than 2 months to complete, and to be completed prior to the critical design review. Of note is the fact that algorithm prototyping and core software development was believed to be able to be

done fully in parallel, as demonstrated by the simultaneous delivery dates. Though there is an element of truth in that belief, in hindsight such scheduling was clearly unreasonable. To get a better perspective, Table 6.2 shows that by CDR (held on 8 September 2011) the dates have shifted by 2-4 months, and an entirely new deliverable had been identified — updates to the GUI that astronauts use to operate the SPHERES on station. Such a shift was the result of the program manager not fully grasping the magnitude of the project and more importantly, the number of peripherals associated with operation of the hardware.

| Action | Milestone | Due Date |
|---|---|---|
| SW 1 | SPHERES Software Updates | Late Oct 2011 |
| SW 2 | VERTIGO Core Software Completion | Nov 2011 |
| SW 3 | Visual Navigation Algorithm Complete | Mid-Oct 2011 |
| *SW 4 | SPHERES Flight GUI Updates | Late Oct 2011 |
| | *indicates new deliverable | |

Table 6.2: VERTIGO CDR Software Schedule

By the beginning of December 2011, when external deadlines began to constrain schedule slips, the software schedule had grown to include 19 individual deliverables, with the major ones identified in Table 6.3. Some of the schedule shift and new deliverables can certainly be attributed to the fact that early designs were just that — preliminary. However, at CDR and beyond, schedules were consistently underestimated; two were 2 months late, while the other pair took four additional months to complete beyond initial estimates.

| Action | Milestone | Completion/Due Date |
|---|---|---|
| SW 1 | SPHERES Software Updates | Dec 2011 |
| SW 2 | VERTIGO Core Software Completion | 16 Feb 2012 |
| SW 3 | Visual Navigation Algorithm Complete | Nov 2011 |
| SW 4 | SPHERES/VERTIGO Flight GUI | 16 Feb 2012 |

Table 6.3: VERTIGO Revised (Dec. 2011) Software Schedule

Understanding the problem that is set in front of the team give the team the advantage of being able to plan ahead and dedicate necessary resources to solving technical issues. By having a realistic schedule, it is possible to identify areas that need additional resources to solve technical issues rather than being dismissed as poor time estimation. Dedicated study of the existing systems and technology which the product will be based on gives the manager the understanding that is prerequisite to managing realistically and properly.

Understanding the existing technology is the basis for the second example of how dedi-

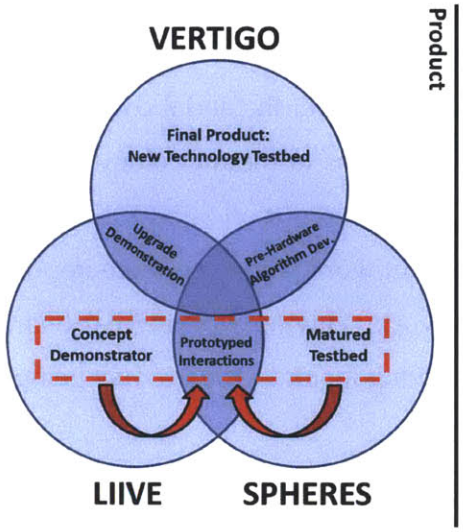


Figure 6-2: Understanding your Design

cated study and preparation make for good design. This area is one in which the VERTIGO team performed exceptionally well — that of synthesizing knowledge from previous technical efforts, understanding their interplay, and applying that to the VERTIGO product.

Figure **??** provides a visual description of the products of the LIIVe, SPHERES, and VERTIGO projects, as it relates to the development of a vision navigation testbed.

We begin by examining the influence that the LIIVe hardware and software design had on the VERTIGO product. As a concept demonstrator, LIIVe demonstrated the general form of the flight package, from the use of a single board computer, to the user interface panels, to the integration of cameras as a modular attachment. It also presented the general form for image processing algorithms and a basic model of the noise and system performance that such a system can achieve. From that program, we can answer the question of *what* VERTIGO should be.

In contrast to the LIIVe program, which was very much a technology demonstrator, the SPHERES program represents maturity as a testbed for 6 degree-of-freedom control and navigation studies. Experience with SPHERES gave the team familiarity with the NASA requirements for payload development and launch, as well as operation in a station environment. From procedures, to pre-launch testing, to informing the design philosophy, SPHERES provided many answers to *how* VERTIGO should be built with operations and program requirements in mind.

As important as the two projects were on their own, the interplay between the soft-

ware and hardware of each gave the VERTIGO team insights and understanding of how the VERTIGO hardware should interact with SPHERES. Without the prototyped interactions between the two sets of hardware, the serial communication protocol would have been set back, as would modifications to the metrology system. Because those major elements had been developed and tested out on SPHERES-LIIVe, SPHERES-VERTIGO was able to learn what did and did not work, and even more importantly (for a short-duration project), know what did not work. Having working hardware that could be built upon and modified was the key enabling factor in the product being delivered within the short 15-month timeframe.

Those elements that were prototyped or otherwise studied on SPHERES-LIIVe that informed the design of the SPHERES-VERTIGO product included:

1. Serial communication between the payload and the host SPHERE (later matured with development of other payloads in addition to VERTIGO)

2. Mechanical fitting and interaction

3. Thermal management and component temperature limits

4. Component selection and shortcomings of certain parts, including reduced lifetime at operating conditions

Had the system been started from scratch without being developed in a simple ground-based system prior to launch, there would have been no way for the relatively small team assigned to VERTIGO to complete its task in the time allotted. The benefit was that both the team and its managers understood the lessons learned from the previously-developed hardware.

**Build**

> *Build early and often. If you build it, you will understand it better, and the deadlines associated with hardware build will motivate engineers to move from paper to product. If you wait to build, you will have fewer chances to identify and fix those problems which inevitably occur. Even worse, those that do crop up will be much more complicated than those which appear early.*

There is always a time for careful paper design and analysis that mostly eschews working in hardware — that time is before the critical design review. This is especially true under the conditions that the VERTIGO project was contracted and developed: a hardware predecessor had demonstrated many of the concepts that were to be made flight-ready, and hardware delivery in a compressed (15-month) schedule.

The existence of working hardware implies that the technology has reached maturity as a ground demonstrator, and is ready for advancement up the technology readiness level ladder. As acknowledged during the requirements and preliminary design process, much of the typical background work had already been done in the course of the development of LIIVe.

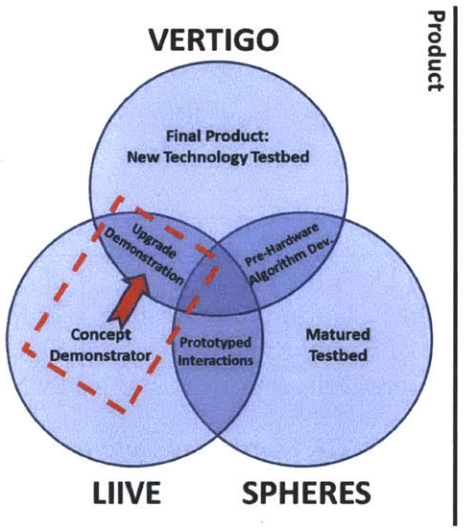


Figure 6-3: Building your Hardware

Figure ?? demonstrates the transition from the existing concept demonstration hardware (LIIVe) to the flight deliverable (VERTIGO). What the upgrade demonstration represents practically was the implementation of design changes that had been identified at the preliminary design level and before.

The reason to make the changes begins with the fact that the existing hardware had demonstrated its worth as a vision platform, but only in a certain configuration. Changes included a processor change, wireless card changes, voltage converters upgrades, LED drive electronics, and new optics and batteries. This represents a huge redesign, where the only components that remain unchanged for all intents and purposes are at the board-level. Without actually making configuration changes there is no way to understand the

2nd- and 3rd-order effects that hardware modification can have. The decision was therefore made that all avionics changes that were to be built into the VERTIGO flight unit were to be made on the existing "flatsat" version of LIIVe prior to CDR. This provided a pair of benefits.

The first benefit is that the prototyped changes were made early in the process. This means that when there were inevitable hang-ups or failures, such problems could be identified within the first 6-7 months of the program. If such changes remained on paper, there would have been little substantive difference between PDR and CDR. Instead, an avionics flat-sat version of the VERTIGO hardware was complete by the latter milestone.

Following the CDR presentation, the next pair of deliveries ended up being an early March software GUI submission deadline and electromagnetic interference/coupling (EMI/EMC) testing which would eventually come due in late March. A quick examination of the hardware delivery date (Table 6.4) shows just how little room there is for schedule slip past those dates.

| Action | Milestone | Start/Due Date |
|---|---|---|
| 5 | Critical Design Review | 08 Sep 2011 |
| 8 | EMI/EMC Compliance Testing | 22 March 2012 |
| 9 | Phase III Safety Review | 5 March 2012 |
| 10 | Hardware Delivery | 09 May 2012 |

Table 6.4: Post-CDR Hardware Delivery Schedule

By the end of December, however, no additional hardware existed beyond the flatsat that had been completed in September. The implication is clear — with four months left before contract delivery all schedule margin had essentially dried up. The consequences were also clear — with flight GUI delivery in 2 months, there was no hardware with flight-like boards, which created technical challenges for the team.

One of those challenges was the development of high-speed USB lines for synchronized video data transmission from cameras to the single-board computer (SBC) for processing. As the result of a hard-and-fast vibration testing date that was added on the 1st of February, the optics mount, with cameras, LED, and support electronics were put together over the month of January. When the optics were connected to the SBC via a new prototype board, there were repeated failures to capture images. In an optical payload, this is obviously unacceptable.

Over the course of testing with the upgraded flatsat, a number of USB cables of questionable manufacturing quality (and varying lengths in some cases) had shown that they could impair image capture. Because of the previous work, when the problem cropped up in the prototype board, it was much more easily identified. When the solution — better length matching and more discriminating cable selection — was implemented, the cameras worked once more.

The lesson from this example is two-fold. On one hand, had the prototype board been fabricated and tested before the December/January timeframe, the USB issue would have been addressed outside of the schedule-constrained environment that can lead to mistakes. On the other, however, the insistence to test changes to the hardware prior to CDR very clearly led directly to the positive outcome when problems did eventually crop up during the build of the vibration test article (which would also be used later for usability testing).

**Test and Try**

> *"One test is worth a thousand expert opinions" — Whatever technology you are maturing should have a solid prototype. Prototype and test out any changes you plan to later implement into the final hardware.*

Demonstration of the upgrades that would turn the LIIVe hardware into the flight-qualified VERTIGO units included more than just modifying hardware and running the same software. In reality, there were really three elements (highlighted in Figure **??**) that needed to fall into place, of which the upgrade demonstration were only one. Development of the initial flight algorithms as well as the communications architecture and software have also taken place in advance of the launch.

The development of the initial inspection algorithms ("Pre-hardware algorithm development") took place over the summer of 2011, even before the completion of the critical design review. Testing of the basic versions of those algorithms was completed in early November, just two months following the review. Those results — described in later chapters — were the direct result of a test-heavy approach that sought to prove that the VERTIGO payload would work as proposed.

Testing provides one particular advantage, especially applicable when in a schedule-constrained environment. Because testing necessarily involves a demonstration of capa-

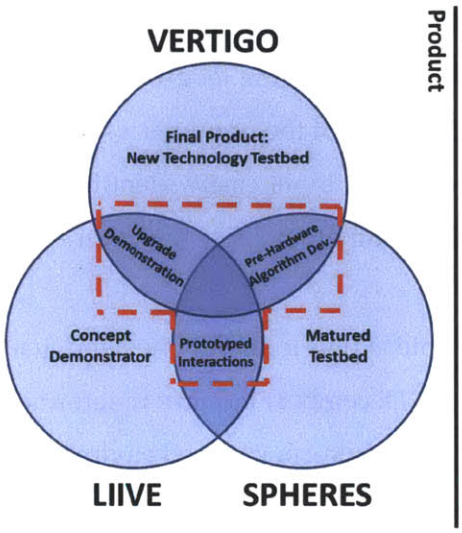


Figure 6-4: Testing the Product

bility in place of a purely paper analysis, it shows confidence. Prior to the inspection algorithm tests, the SPHERES gyros had not been used much for dead reckoning, and not with the precision that vision-navigation prefers. The behavior and drift of those gyros after years on orbit was not well-understood or studied. They had certainly not been used for pose propagation from one camera frame to another, which requires fairly low noise. By demonstrating the constraints on the random error and random walk, and physically demonstrating the maneuver in a microgravity environment, confidence was built in the SPHERES hardware to accomplish the missions prior to even launching the VERTIGO payload.

Furthermore, that basic testing established a simple maneuvering algorithm which could then be built upon without concerns that the basic premise was somehow flawed. For future revisions, if the inspections do fail, then the problem is likely to be in the new code, or in the hardware. Overall, by trying and testing the code on the original SPHERES hardware, confidence was built. Expected performance was also established, and performance was able to be baselined from it. Beyond the establishment of functional confidence and a performance baseline, it also provided code that could be used to more accurately test the hardware when it was completed.

During the course of the GUI testing from the original delivery date on 5 March until an update delivery in early May, elements of the algorithm code were combined with code which would handle communication between the SPHERES and VERTIGO. The develop-

ment of that code also followed the "Try it and Test it" approach to hardware, though that was delivered with less lead time. Software was developed first with basic functionality, and tested while adding additional functions. Its development followed the hardware build. By usability testing, the software was functionally complete, but still somewhat buggy, with some changes still needing to be implemented. By developing the GUI in this piecemeal approach, it was possible to test while working to implement new pieces of code, and allowed for the required feedback from the approval authorities reviewing the software for NASA's Payload Display Review Team (PDRT).

### Grow

> *In everything you do, start with a known, be it working hardware/software or even a full program, and then increase complexity.*

All elements described in Figure 6-1a followed the motto to always grow — in system knowledge and product capability. Though there is something to be said for parallel development, a product developed for space cannot afford to have components designed and developed in isolation for too long.

VERTIGO did this well, in part because the team was small, team members had relatively well-defined areas of responsibility, and project forces demanded close cooperation.

The immediate project team, as it was first constituted post-CDR consisted of a program manager, lead scientist, GUI programmer, two avionics (electrical) engineers, mechanical engineer, and two software developers, in the form of 7 people (the first two roles were student-filled, the remainder, professional engineers). By having 7 people fill 6 distinct roles, there were few questions about where responsibilities lay for most tasks which came down the pipeline. Later, when manufacturing began, another member was added with responsibility for that task.

Forces within and external to the project also played a role. Once more, the compressed timeline required quick, yet accurate decision-making. Schedule pressure forces changes to be made through all elements. This forces team members to interact with one another almost daily. While the scope of the project makes this a burdensome requirement for larger projects, and not for VERTIGO, the project could not keep to schedule without it. Almost no time is lost to design changes trickling through the systems engineers because that re-

sponsibility on VERTIGO was held by all members. For instance, when manufacturing of the prototype optics mount discovered difficulties routing cables and mounting boards, solutions were found jointly between all team members, led by the mechanical engineer and the assemblers.

Similarly, when modifications needed to be made to the electronics to fit within the mechanical fixtures, the changes were made in a day by the two team members tasked with that role, with the assemblers watching.

The program as a whole also followed the rule of growing from a known before moving to an unknown. LIIVe itself was a known quantity from which VERTIGO could evolve. The inspection software began first as a simple circumnavigation maneuver, and then added different paths to the inspection planner. Serial communication between the SPHERES and the Goggles was first prototyped with the CSAC experiment and expanded upon with simple message parsing and passing built into the SPHERES guest scientist code. After that element was tested, it was combined with more advanced inspection algorithms that were in turn tested on the ground and in simulation. Each element fell into place after gradual steps.

This approach has two significant advantages over others. If subsystem interaction is largely on paper, once the designs are implemented, they must be integrated. After fully designing a subsystem, designs are not partiularly malleable. Furthermore, since most problems arise at interfaces, most time is then spent to combine subsystems. By constantly integrating, improving, and reintegrating, the design process is more responsive and fast.

The downside to this approach is that it depends on the ability of a design to be able to evolve from one state to another. Such an approach must either accept the possibility of non-optimality in design (as the design evolves, the need to always be operable constrains the nature of changes of design) or be willing to keep some elements from integrating until project completion.

On the balance, however, the approach is beneficial in maintaining a rapid design-to-flight schedule, while minimizing the chance for significant miscommunication which hamstrings the project until a full redesign can be accomplished. In this manner, the lessons are applicable even to larger projects, particularly at the subsystem level where different components much some together.

The design and evolution of the VERTIGO product, however, is not the only reason

for VERTIGO's success thus far. Just as technical design and product implementation followed four principles, so too did the design and implementation of the management and systems engineering process. Those themes — Advocate, Fail, Depth, and Margin — are described below.

### 6.1.2 Process Design

The process of hardware development and engineering leadership is as important in the resulting end product as the engineering of that product itself. In order to develop the best process, there are four principles to keep in mind.

#### Advocate

> *In an environment where individuals have more than one task in front of them, you must advocate for your project to get done. If no one advocates for your project, it will never be a priority and all the margin you have built in will quickly slip away.*

As a project manager, many times you will not have direct control over those who are working on your project, but instead must encourage buy-in and work to have resources directed your way. One of the early lessons of VERTIGO is the difference in the leadership necessary for such situations versus for direct reports.

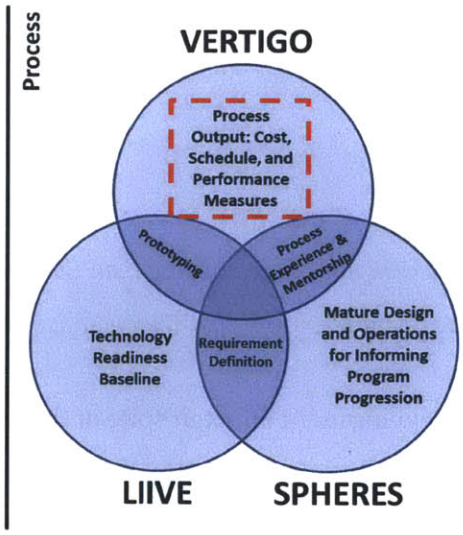


Figure 6-5: Control Measurable Performance through Advocacy

The lack of direct influence can initially be frustrating for those who are unused to managing without it. Instead, management must become about gathering resources and close cooperation as much as giving direction.

Advocacy as it relates to VERTIGO meant that when initial oversight created a large reporting burden that hampered work efforts that an agreement was worked out for unified updates. Under the project, there were a number of stakeholders — DARPA, NASA, and the Space Test Program (STP) all wanted to be appraised of project progress. By engaging senior project leadership, it was possible to combine the communications between those players.

Advocacy also meant that when team members were over-scheduled that the project management team again sought to make VERTIGO a priority, especially in light of the schedule of the project. At times this meant once again engaging senior leadership to ensure human resources were sufficiently applied to meet the program needs. It also required working closely with other team members to develop and adjust schedules so that other projects weren't completely ignored. In some cases, this was directive in nature, but in most cases the nature of the leadership situation required participative styles.

Advocacy also requires listening to the team and their concerns. If the team needs resources that are not available, they need to be made so. In the development of the VERTIGO Flight GUI, this required bringing additional personnel onboard, while also adding team members for the purpose of hardware assembly. It also involved making MIT team members more readily available to work alongside the other project engineers in all areas, from project management to software development to assembly.

**Fail**

> *Identify where you are wrong early and often. New technology means that you missed something because it hasn't been done before. More than that, you will make mistakes. They can only be overcome if you recognize that they will happen.*

VERTIGO is very much a development effort in spite of the fact that it traces its heritage to SPHERES, which has been operating for the better part of a decade and to LIIVe, which proved the concept of a SPHERES vision payload was possible. Because it is still a program under development, there are inevitable stumbling blocks along the way. Those temporary

failures provide lessons for future operations, and for future programs.

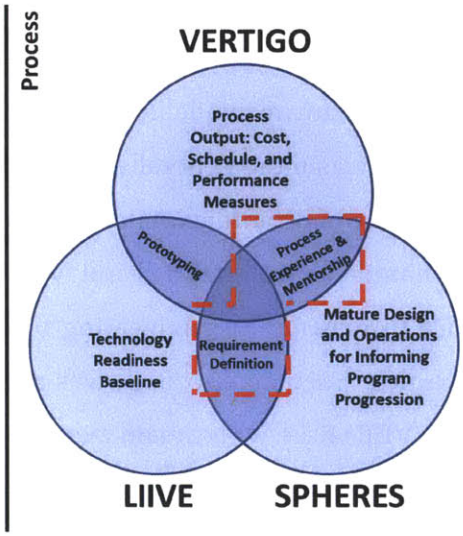


Figure 6-6: Improving the Process by Learning from Failure

We will focus on two specific failures which improved the process by which your author managed his team members. The first is a failure to fully define the system requirements and the second is a lesson in engineering leadership which project mentors and reflection provided (see Figure **??**).

During the requirements definition process, it is understandable that a feature here and there will be missed. The programmatic failure by your author to identify in-depth operational requirements beyond "VERTIGO must be able to be operated by astronauts working on the International Space Station" (see Appendix **??**) was significant. This failure resulted in overly optimistic schedule predictions early on in the program, which influenced the amount of resources that were dedicated to accomplishing that task.

Learning from that failure took the better part of a year, as it became clear that the dedicated time of a single programmer might not be enough to code, test, and interface with other software architectures. More directly, the failure to accurately identify requirements for the software development means that those requirements were assembled piecemeal as the project progressed, often requiring changes after a piece of code already demonstrated that it worked capably, but not in the way that the project now needed. A better up-front understanding of software needs may have avoided the delays and changes which followed. That lesson having been learned, the team rectified the situation by spending time in a handful of meetings in late summer and early fall of 2011 developing requirements

and design choices so that the GUI development could proceed with more direction.

The second failure of project management was really a failure of leadership at the project manager level. By December of 2011, with the first major delivery about two and a half months away, there was no hardware available to test software on. This was the result of a leadership strategy which was more generally suited for a situation more closely tied to those for which your author had more experience: those with military chains of command in which the task at hand was well-defined and which all members had directly applicable previous experience (it was not an engineering project, each of which has its own nuance) and few other duties. Such an approach was not suited to the open-ended engineering challenge posed by VERTIGO, where team members had other responsibilities and where resources could only be mustered in an indirect way. That difference meant that a hands-off approach was not the best option, and instead closer teamwork was needed.

This failure was overcome through mentoring and guidance provided by those MIT managers who had been through the engineering leadership challenge previously with SPHERES. The solution was multifaceted.

First, additional resources were sourced (indirectly) so that software development had additional resources to meet their deadline. The additional manpower allowed VERTIGO to meet its software deadlines. Additional team members were brought on board with expertise in assembly to speed up the build process.

Second, the project management team began to advocate more strongly for those resources which were already assigned to the team. Previously, other projects had been given priority over VERTIGO, which meant that the total man-hours spent were not enough to match what was needed. By working with over-scheduled team members to prioritize project-related work in light of fast-approaching deadlines. Perhaps most importantly, the MIT team began to work heavily in the industry partner's own facilities, providing faster feedback and interaction. By speeding up the communication loop by orders of magnitude, as well as bringing MIT resources directly to bear, work was able to quickly pick up. Waiting times shortened. Without the closer interaction and resultant improved communication, there was little chance that the early delivery deadlines would have been met.

The final factor which was able to influence the course of the project was the addition of a vibration testing deadline a month in advance of the software delivery. Though it increased schedule pressure considerably, the hard-and-fast date associate with it pushed

the team to develop working optics and support avionics. The hard deadline compelled the manufacturing of boards and mechanical fixtures, rather than remaining in assembly and CAD layouts. By manufacturing (see Subsection 6.1.1), the team was able to identify problems in the design. Perhaps just as importantly, by having working hardware ready in advance of the software deadline, that software was able to be tested on flight-like hardware rather than only on simulators alone.

As these two examples show, failures need not doom a project. Instead, take the lessons from those failures, adapt, and use them to improve the process by which the program is managed.

### Depth

> *Your development team will have some area in which there is no "reserve" to call upon. Find that shortage and fix it.*

For the process by which you build hardware and software to be successful, you must create depth in your team. Different approaches are possible, but all require an investment of financial or human resources.

Though it is by no means exclusive to the software development side of VERTIGO, the team had a single member working on the payload-specific GUI from conception until about two months before initial delivery. Combined with an underestimation of the software tasks early in the design process, as well as software modifications which were implemented later than desirable, this pushed the software delivery date from its original October 2011 date (Table 6.2) to February 2012 (Table 6.3), to an eventual initial delivery in March 2012 with a final delivery in early May 2012.

The team members were more than competent at their tasks, but it was up to program management to provide the necessary resources for those members to achieve the schedule. Quite literally, there were just not enough hours in the day for a single person to accomplish the tasks that were being asked of them. At that point, it is incumbent upon the program manager to provide those additional resources in concert with those who control the financial and personnel resources. This is a shift in the "Iron Triangle" of Cost, Schedule, and Performance, but one which must be made when one of those elements has fallen out of balance, as discussed in Section 6.2 of this chapter.

Furthermore, those resources must be applied in a manner and with such timing that they neither detract from the current efforts nor require so much extra up-front investment that the benefits of additional team members is null. In the case of VERTIGO, this was achieved by bringing in the programmer of the original SPHERES GUI (from the 2006 launch delivery) about two-and-a-half months prior to Flight GUI initial delivery to help with integration and coding support. Doing so allowed both of these conditions to be met — the training burden was minimal, and the resource was applied with just enough time to make a difference before the only time remaining had to be devoted to testing.

Adding depth to the team in places where it needs it most also provides an added benefit: returning margin to the schedule. When unexpected issues appear, from illness to additional projects, a team which has depth can absorb the impact of the lost team member much better. During the EMI unit build, the loss of one member to illness would have been catastrophic save for the fact that when it occurred, the team was able to very quickly adjust because each member was familiar with most other project elements. As a result, the team did move slower, but was still able to manufacture and test boards and integrate the units before shipping them out for testing.

Such an experience also implies that developing depth does not necessarily mean an influx fo resources beyond those that are already available. On the VERTIGO team, though each segment of the project (Mechanical, Electrical, Software, Algorithms, etc) are nominally separate entities, with separate team members, as noted in Subsection 6.1.1 ("Grow"), the team knew well the tasks and concerns of others. This meant that some depth was built into the team, though responsibilities were very specifically divided. In many instances, though the mechanical engineer is responsible for assembly/disassembly of the package, during protoflight (EMI/EMC unit) assembly, both your author as program manager and one of the electrical engineers would fill that role. Likewise, during assembly of the optics mount, which behaves temperamentally, requiring fine alignment of a number of different parts, there were three or four team members on a team of eight who became competent in performing the job. As a caveat, this does not imply that team members are not indispensable in their own roles, but only that as engineers it is often possible for a group that works very closely with each other to supplement each other. With this approach, the responsibilities do not disappear, but the tasks can be filled by a team that is flexible, with sufficient knowledge and preparation by other team members.

Depth, therefore is achievable in at least two ways: by assigning additional resources, be they financial or human, to achieve a task, or by developing team members to be able to complement one another and support each other when internal and external demands require it. The first is the preferable when significant resources are required which demands very specialized skills or experience, while the second approach is acceptable when in a constrained environment that demands project-specific experience and engineering skills.

### Margin

> *If you're a hardware engineer, your software estimates are off by at least 100%; Not only in how long development will take, but in how much software is needed. Recognize what you don't know and add margin for that.*
>
> *Then add some more.*

One of the most difficult elements in managing the process by which a project is completed is estimating the time that it will take for each part to be completed. Managing margin and schedule is what enables the rest of the process elements to fall into place. Without a good handle, it is much more difficult to muster the proper depth and advocacy for the project.

An understanding of the project (see subsection 6.1.1) is what contributes most to successfully managing this process element. Figure **??** shows those elements which played a significant role is growing, shrinking, and generally informing schedule margins over the course of the VERTIGO project.

As has clearly been demonstrated previously (Tables 6.1, 6.2, and 6.3), accurately scheduling software was your author's most difficult part of maintaining schedule. That estimation ability increased as the process itself became more concrete. Two elements played a role in that: prototyping of the changes required, and learning lessons from the SPHERES experience.

To address the former, we start with the LIIVe program, with all of its working electronics and software. The results of that program were not flight-ready, but did demonstrate a technology readiness near TRL 5. By making modifications to that hardware and prototyping the new boards, the effects of those changes became more pronounced. For the sake of identifying particulars, let us focus on the changes necessary in developing the optics to

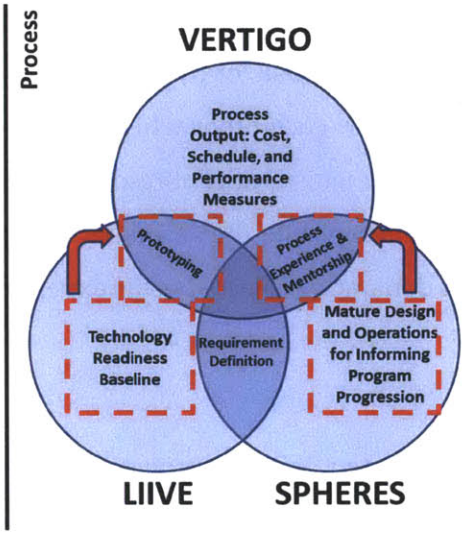


Figure 6-7: Developing Project Margin Estimates

support the mission.

Because camera synchronization in software was not accurate enough for the science needs, it was necessary to develop hardware cabling which could accomplish that task and to write the software to support that objective. Space constraints also required that optics be split into two boards rather than one, necessitating inter-board connections. Finally, prototyping of an Ethernet connection also turned up problems with lost communications.

Prior to prototyping changes, these problems were unknown, and certainly not accounted for — after all, LIIVe was well-understood with months of heritage and operation. Making judgements on schedule based on that experience therefore suggested that the transition to flight-ready hardware would only require small independent changes and a few months of development.

Prototyping, however, suggested otherwise. Identifying the need for specific Ethernet cable types, along with component changes from the original specification (adding magnetics) added at least a month to the completion of the optics board. Inter-board connections proved to be temperamental, necessitating mechanical and avionics design changes. These changes added another month to the redesign. Finally, the development of supporting hardware and code for camera synchronization took many months of parallel work with the supplier on driver development for what seems to be a simple technical task.

Some of these challenges were apparent at the outset of the project — most were not. Not until the prototype units were built for vibration testing and later modified for us-

ability testing were many of these issues identified and resolved. Early expectations were that hardware would be complete months ahead of the contract delivery date. Experience showed that such estimation was optimistic. From this, there are two approaches to dealing with this uncertainty:

1. Build the schedule to a "horizon". The best information you have at any given time gets less accurate the further into the future you try to predict. To counteract the growth in uncertainty, predict only to the point you can make reasonably accurate judgements. That may be to the next deliverable or only to the next two months. This allows for more accurate predictions, but completely ignores long-term planning.

2. Develop increasingly large margins over time, and decrease them not based on the maturity of the design, but an estimate of the uncertainty that you have in the project. While this aids in long-term planning, it may unfortunately give a false sense of security, as a lack of knowledge about potential challenges with a technical problem can cause an underestimation of the schedule risk.

Combining the two, by predicting accurate dates in the short-term, and putting margin for both expected design issues and unexpected challenges on longer-term deliverables will provide the best estimation of future schedule performance.

We now move to discuss the latter element, that of the applying the lessons learned from the development and operation of the SPHERES satellites. As opposed to informing the process for developing hardware, those lessons instead provide an understanding of the operations development process.

Most satellites are in some way operated using human input rather than fully autonomously. SPHERES-VERTIGO is no exception, and indeed, as a testbed operated on the ground by students and on the ISS by astronauts, there are set procedures used to control those interactions. From SPHERES, the MIT team has learned a number of lessons, a few of which follow:

1. Simplify interfaces — Astronauts are necessarily time constrained when they learn to operate their payloads, and with training often happening months in advance of a launch, it is likely that much of the training may be forgotten. From SPHERES, the lesson was clear: keep design simple and clear and as a default present only the information that is needed for nominal operations. From the beginning of GUI and

hardware design, this concept was kept in mind. The VERTIGO GUI presents no additional options to the SPHERES GUI aside from the capability to load a file, perform a shutdown, download data, and if desired to switch the camera view seen. Only three switches are immediately visible on the hardware: Power, reset, and LED enable. By keeping the design simple, it simplifies the procedures, and streamlines test sessions, as additional complexity in science and design does not transfer significant complexity in interfaces to the astronaut operators.

2. Provide debugging tools — Nearly everyone in the chain from those who provide funding to astronauts who operate the payload to those who review paperwork submissions want to see the mission succeed. By providing those tools in an easily accessible format, when things inevitably go wrong, much more data will be available much faster, with much more accuracy and detail. Just as various debug tools within the SPHERES software allows for large amounts of data collection and transmission, the use of which inspired and informed VERTIGO's design. The flight GUI was given a dedicated "maintenance mode" in order to run maintenance scripts and change settings, while providing feedback to astronauts and ground scientists as to the state of the Goggles. The development of these tools aid in on-orbit operations as well as ground testing, providing easy access to the most relevant information for developers. Additional debug options were also built into the design from the beginning.

3. Hard-code nothing — While *nothing* may be a slight exaggeration, the ability to modify parameters for a GUI or test code is easier both procedurally, as it avoids multiple code compilations, as well as programmatically, as far less paperwork is required for software change approval.

Each of these lessons was taken into account in developing the procedures and design for the system. As a result, when the first prototypes were in production (and especially after the protoflight units were built), debugging was far simpler than it otherwise might have been. Extracting performance data allowed the development team to identify faults as varied as communication errors, camera synchronization errors, and much without having to disassemble the entire system for every problem. More directly, by designing simplicity and flexibility into the design from the beginning, NASA approval was far easier to

gain, as changes were minor, few, and far in-between.

Proper margining and scheduling is the result of a good understanding of uncertainty, knowing the limits of uncertainty estimates, and building debugging capabilities into the project from the beginning. VERTIGO has been evidence of all three.

## 6.2 Timeline and Earned Value Analysis

At the time of contract signing the VERTIGO Project was designed to be a 1-year undertaking beginning in January 2011 and ending a year later. After some delays in contracting, the schedule eventually began with the following timeline of critical milestones on the way to hardware delivery, a 15-month start-to-finish timeline:

| Action | Milestone | Due Date |
|---|---|---|
| 1 | Program Start | 15 Feb 2011 |
| 2 | System Requirements Review (SRR) | 12 Apr 2011 |
| 3 | Preliminary Design Review (PDR) | 07 June 2011 |
| 4 | Phase II Safety Review | 01 Nov 2011 |
| 5 | Critical Design Review | 08 Sep 2011 |
| 8 | EMI/EMC Compliance Testing | 8 Feb 2012 |
| 9 | Phase III Safety Review | 23 Mar 2012 |
| 10 | Hardware Delivery | 09 May 2012 |

Table 6.5: VERTIGO Initial Delivery Schedule

As conceived and contracted, the program was designed to be fast and relatively cheap, with development times and costs comparable to a ground testbed. As such, in the "Iron Triangle" of Cost, Schedule, and Performance (Figure ??), the balance was weighted heavily toward those elements, while performance was judged to be a best-effort approach.

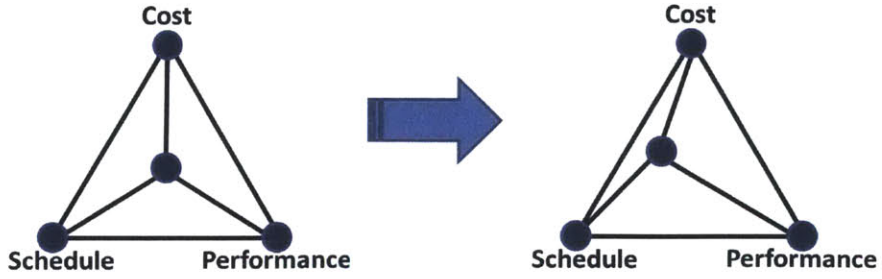


Figure 6-8: Cost/Schedule/Performance Weighting at Contract Start

### 6.2.1 Initial Design Period

Such a schedule was aggressive, especially with a small (yet motivated and competent) team. Indeed, in many areas the development team was a single individual — one mechanical engineer, one electrical engineer, one vision researcher, one software developer — though some relief was granted, by bringing engineers who had worked on the project in the past to create depth in the software and avionics areas, and bringing outside researchers to work on the vision algorithms and libraries which would inform the software design.

Also critical to note is that the schedule gives just shy of 15 months from Program Start to Hardware Delivery, with 2 months of development time given to SRR and PDR, and 3 months for preparation for CDR. The 7 months of preparation for flight hardware had positives and negatives attached to them. On the positive side, that meant that changes to the already existing precursor hardware (from LIIVe) were able to be experimentally checked out, with technical issues being sorted out before they were implemented into in the flight hardware development path. By dedicating 7 months to developing changes to hardware which would not fly, significant time was spent which may have been better spent on more flight-like hardware. On the balance, the dedicated development time was advantageous to the team because it allowed two things to happen:

1. Changes could be compared and baselined to a working vision system.

2. Technical issues could be better isolated before they became intertwined on an untested flight system.

Additionally, it allowed most changes to be identified prior to the CDR presentation.

The Systems Requirements Review, 2 months after nominal program start was a review of the requirements that had been developed at the System, Functional, and Subsystem levels. Those requirements demonstrated a lack of software experience in flight programs of your author, as well as an understanding of the software needs that is typical of many spaceflight programs. In the entire requirements document, out of 40 subsystem level requirements, software requirements were directly addressed in only 4-5 — 10% of the requirements. At the Functional level, the number was only slightly better at 5/30, barely 17%.

At the Preliminary Design Review the schedule had shifted slightly (though not particularly significantly) and had added slightly more detail on the path to the Critical Design Review. That updated schedule showed:

| Action | Milestone | Due Date | Date Shift |
|---|---|---|---|
| 3 | Preliminary Design Review (PDR) | 08 June 2011 | +1 day |
| **SW 1** | **SPHERES Software Updates** | **12 Jul 2011** | **New** |
| 4 | Phase II Safety Review | 15 Aug 2011 | -2.5 months |
| **SW 2** | **VERTIGO Core Software Completion** | **19 Aug 2011** | **New** |
| **SW 3** | **Visual Navigation Algorithm Prototype** | **19 Aug 2011** | **New** |
| 5 | Critical Design Review | 25 Aug 2011 | -2 weeks |
| 8 | EMI/EMC Compliance Testing | 8 Feb 2012 | No change |
| 9 | Phase III Safety Review | 23 Mar 2012 | No change |
| 10 | Hardware Delivery | 09 May 2012 | No change |

Table 6.6: VERTIGO Post-PDR Delivery Schedule

The new software dates, as hindsight grants significant insight, were completely unrealistic, both technically and programmatically and the deadlines reflected only a very preliminary understanding of the program software requirements.

Many of the hardware requirements had been discussed, reviewed, and cleared at the Systems Requirement Review, but the same could not be said for two areas of software, the VERTIGO Core Software and the GUI for astronauts to operate the hardware on station. The latter software area, notably absent from the schedule, shows an acute underestimation of the software needs of the project. That shortcoming falls squarely on the program manager, particularly for having system requirements that were underdeveloped and hardware focused.

### 6.2.2 Design Completion

Around October 2011, the VERTIGO design reflected a 90% solution. By then the team had presented the Critical Design, an updated interface document was nearing completion, and the time was approaching for the hardware build to begin. What happened in the two and a half months following CDR, unfortunately, eliminated the significant schedule margin that existed at the beginning of the period. As shown in Figure ??, after the CDR (Item 2), the project was operating in a place that program managers love to be — ahead of schedule and under budget in terms of man-hours spent. On the path to the next two significant milestones, Crew Training (Usability testing), and Electromagnetic Interfer-

ence and Coupling testing (EMI/EMC), the schedule's retrograde drift placed the project approximately two months behind schedule, even when the 30-day contract margin was included. In order to minimize the schedule slip, it very quickly became apparent that significant investments of time resources (which serves as the proxy for financial resources in this analysis) were required. The problem was once again, multi-faceted.

The previous ability of the team to meet deadlines with virtually no slip meant that there was little concern about meeting future deadlines. The experience with the LIIVe hardware reinforced this view. Since schedule pressure did not seem to be a problem, VERTIGO was deemed low-risk which in turn meant that other pressing projects would come up and be addressed. Further, the lack of schedule pressure reduced the impetus to jump into hardware in favor of continual redesign and tweaking of the CDR-level designs. Without moving into more flight-like hardware, though, it wasn't possible to mature the design in a significant manner.

The second, and perhaps more important failure was that program management did not recognize the trajectory of the Schedule and Spending curve until the project had lost enough time that to bring it back on schedule required a large investment of manpower and energy in over the course of just a little over a month. That large investment is very visible in Figure ?? as the deliveries begin to tack closer to the predicted schedule just prior to the EMI/EMC testing delivery. The preceeding data point, Crew training was the peak of the schedule slip. Though the deadline was not a gating deliverable at that point in the schedule, the lack of hardware just a month and a half prior to that date, in combination with the state of the hardware on February 16th did indicate such a schedule slip. Particularly when the (optimistic but not unrealistic) plan for a November prototype hardware build is taken into account, a two-month slip squares well with reality (Table 6.7 vs. Action 7, Table 6.9).

Normally, a two-month slip on a flight program might be excused as minor; for VERTIGO however, such a delay had serious implications. Since the program relies on student scientists and staffing, a slip meant first, the burden for program management would be shifted either to a completely new manager or left for lab staff, of which time is already a tightly constrained resource. More importantly, even a short delay threatened to push the payload from its manifested vehicle, with an operational delay of at least three months until the next possible station increment. The delay means that student funding would

| Action | Milestone | Original Date | New Date |
|---|---|---|---|
| SW 1 | SPHERES Software Updates | 12 Jul 2011 | Oct |
| 4 | Phase II Safety Review | 15 Aug 2011 | Late Nov |
| SW 2 | VERTIGO Core Software Completion | 19 Aug 2011 | Nov |
| SW 3 | Visual Navigation Algorithm Prototype | 19 Aug 2011 | Nov (Successful Test) |
| 8 | EMI/EMC Compliance Testing | 8 Feb 2012 | 2-19 Mar 2012 |
| 8.1 | Hardware/Software Integration | — | 4 Apr 2012 |
| 9 | Phase III Safety Review | 23 Mar 2012 | No change |
| 10 | Hardware Delivery | 09 May 2012 | No change |

Table 6.7: VERTIGO Post-CDR Delivery Schedule

no longer be available to support the science objectives, requiring a search for additional resources. Lastly, a failure to meet the schedule and objectives laid out in the VERTIGO program would have been a blow to the credibility of the team and its ability to perform science successfully, and in a timely manner.

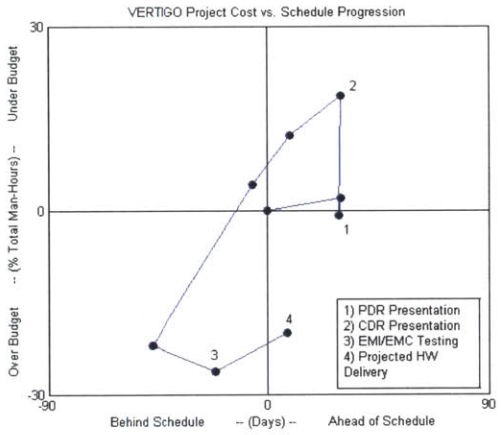


Figure 6-9: Schedule and Spending Progression

While the schedule did slip precipitously during this phase of development, hope was not lost. During the next phase, that of actual implementation of the project design into hardware and software packages for testing and demonstration purposes, an influx of resources and management attention began to turn the tide, and drawing the schedule closer to its original form, though at the cost of additional human resources.

### 6.2.3 Initial Build and Test

During the initial build and test phase, two general milestones were achieved: build of the first two revisions of hardware and the majority of testing to qualify the design for flight.

The tests which were run are identified in Table 6.8.

| Test | Start Date | Maturity |
|---|---|---|
| Vibration Test | 1 Feb 2012 | Prototype |
| Usability | 16 Feb 2012 | Prototype |
| EMI/EMC | 23 Mar 2012 | Protoflight |

Table 6.8: VERTIGO Testing Schedule (Spring 2012)

For each test, hardware needed to be delivered in either a prototype or protoflight form. The prototype, which did not require flight-like form for the avionics, but only the optics, consisted of first-cut boards mounted for use with a packaged optics mount. To prepare for a 1 February vibration test date, the team was assigned a member to work strictly on assembly and debugging. This influx of resources, combined with additional software support allowed the team to face the deadlines with a chance to meet them. Because most of the margin in the schedule had disappeared at this point, much more effort had to be focused in the "Build, Test, and Try" principles identified in subsection 6.1.1.

Ultimately, the team did make its deadlines, but doing so required many 18-hour+ days and weekends to make up the lost margin. This reinvestment of time and resources was realized as a course-correction in the project strategy. The adjusted "Iron Triangle" of Figure ?? demonstrates that realignment. Additional resources were brought to bear in order to reduce the schedule slip and get the design to a state where it performed to specification. Testing showed that the design was solid and resistant to vibrations larger than those expected to be seen during launch. Operationally, the ground work that had been done the previous fall did pay off, with the GUI requiring only minor tweaks in addition to the testing that it needed. EMI/EMC testing also proceeded with a few hiccups, but did complete with VERTIGO meeting NASA safety specifications.

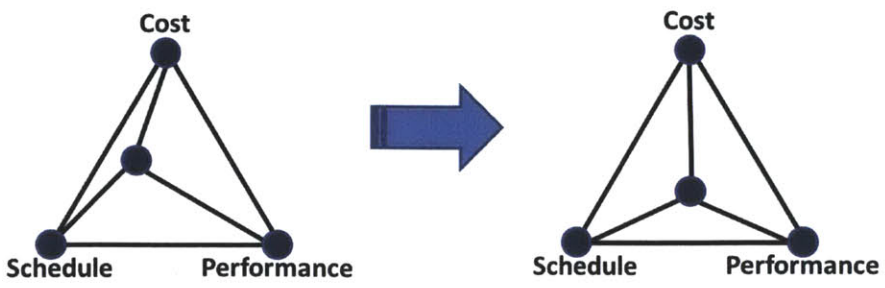


Figure 6-10: Cost/Schedule/Performance Weighting at During Hardware Build

The extra resources which had been given to the project allowed the schedule to closer to being on track, with a delay near 20 days rather than the almost 40 beyond contract margin that it had slipped to according to the crew training milestone, which was satisfied by usability. The shift by the EMI date also suggests that the flight hardware delivery date is back ahead of its margin.

### 6.2.4 Flight Hardware

Following the EMI/EMC test campaign, which came to a close with the month of March, the team transitioned into redesigning flight hardware. During April and May, the team finished testing the Flight GUI and sought to debug the remaining problems on the electronics. In doing so, the project came back in line with its original schedule in Table 6.5.

As the design and build is ongoing, it is not possible to fully comment on the work done since the end of the testing. Nevertheless, the final schedule as realized will closely mirror Table 6.9, with the potential for a few weeks slip of Action 10.

| Action | Milestone | Due Date | Delivery Date | Date Shift |
|---|---|---|---|---|
| 1 | Program Start | 15 Feb 2011 | 15 Feb 2011 | — |
| 2 | SRR | 12 April 2011 | 12 April 2011 | — |
| 3 | PDR | 07 June 2011 | 08 June 2011 | 1 Day |
| 4 | CDR | 08 Sept 2011 | 08 Sept 2011 | — |
| 5 | SPHERES ICD Updates | 26 Oct 2011 | 16 Nov 2011 | 21 Days |
| 6 | Phase II Safety Review | 01 Nov 2011 | 07 Dec 2011 | 36 Days |
| 7 | Crew Training (Usability) | 01 Dec 2011 | 16 Feb 2012 | 77 Days |
| 8 | EMI/EMC Compliance | 08 Feb 2012 | 30 Mar 2012 | 51 Days |
| SW 4 | Flight GUI Initial Delivery | — | 5 March 2012 | — |
| SW 5 | Flight GUI Final Delivery | — | 2 May 2012 | — |
| 9 | Phase III Safety Review | 23 Mar 2012 | 29 Jun 2012(est) | 93 Days (est) |
| 10 | Hardware Delivery | 09 May 2012 | 31 May 2012 (est) | 22 Days (est) |

Table 6.9: VERTIGO Realized Delivery Schedule

## 6.3 Lessons Learned

The experience of managing the VERTIGO program provides valuable lessons that future students and officers who are placed in the role of program manager should take to heart.

Over the course of the VERTIGO program the government managers took a very hands-off approach to the program as both contract terms and the history of performance from

MIT's Space Systems Laboratory and the subcontractor Aurora Flight Sciences had a strong history of performance. That history included flights and reflights of dynamics experiments on the Space Shuttle and International Space Station, as well as the original development of the SPHERES hardware upon which the VERTIGO hardware would build.

As a result of the flexibility granted by those overseeing the contract for the government, your author took two very different approaches to the management of the VERTIGO program and its staff. These two approaches were motivated by both previous experience and outside influences including additional projects and guidance from lab leadership. From it, a few last conclusions can be drawn:

First, for a military officer leading an engineering project in a non-military environment, leadership needs differ subtly yet substantially from those that training is designed for. Competence can be assumed for most players, but the resource-constrained environment makes project management difficult. Other projects also demand time and resources that are needed to accomplish the mission. In order to gain the needed resources, the manager must advocate for their project and remain vocal, lest it slip further and further behind. The flexibility from the higher-level government managers gave the team flexibility, but in the absence of that close oversight, there must be lower-level leadership to replace it as the driving force behind project success.

Second, a manager must know his or her shortcomings — and they will not be in the areas you know or expect them to be. The most difficult part of leading the VERTIGO team was never in those elements with which your author was familiar, like test and operations, but in electronics and software, where experience is less hands-on. This is where the schedule slip came for VERTIGO. Not because of a failure of the team to do their tasks, but rather in poor scheduling and time accounting by management. Underestimation is the result of unfamiliarity.

Finally, it is important to note the impact that additional resources have on forcing schedule and performance. From the beginning of the project, VERTIGO was considered a best-effort project by the funding agencies, but not developing sufficient capability was never an option for the development team. This fixed performance and left schedule and cost to trade off. The team was able to maintain the schedule by adding resources when needed. For any manager, there must be a recognition of the project goals, and where slips are allowable and/or increased investment may be necessary.

These three lessons, when combined with the eight themes discussed earlier, allow an inexperienced project manager to successfully navigate the pitfalls of engineering in an academic environment. A manager must be ready to *Understand*, to *Build*, to *Try and Test*, to *Grow*, to *Advocate*, to *Fail*, to develop *Depth*, and to maintain *Margin* to guide a program to a successful conclusion.

THIS PAGE INTENTIONALLY LEFT BLANK

# Chapter 7

# Conclusion

The thesis sought to prototype and demonstrate maneuvering and inspection algorithms for small satellite inspection missions. In particular, it aimed to implement these algorithms on the SPHERES satellite testbed on the ISS in preparation for the eventual launch of a specialized vision-navigation payload. By analyzing the results from station and comparing to simulation, a level of confidence was developed which allowed for more complex maneuvers to be evaluated.

Further, it sought to develop principles for the project management of small satellite projects. To do so, the VERTIGO vision-navigation system was used as a case study to examine what techniques were successful in meeting project goals. By taking stock of how VERTIGO progressed, these principles were derived from what did and did not work when applied by program leadership.

## 7.1 Conclusions

Results showed that the algorithm, when implemented with standard SPHERES controllers, was able to track the desired state within 10% error. Furthermore, the simulation and station results matched within a similar margin, with only a pair of exceptions. By modifying the mass of the target object, the rotational axes changed. Likewise, rotational rate noise in simulation was significantly larger than that from station tests. Both of these factors, however, do not adversely impact the achievement of the mission on station.

Simulation also implies that for a non-parallel inspector and target angular velocities, the most fuel- and time-efficient inspection paths are planar. For coverage better than a

95% threshold, however, it is more efficient to use an estimate of the rotational velocity of the target object to plan the inspection path.

On the program management side of the VERTIGO program, the principles discussed have allowed the project to begin to approach its original delivery schedule after a mid-course slip. With current predictions, it is expected that the maintenance of that management approach will result in a nearly-on-schedule delivery of flight hardware with enough margin to make the scheduled launch to station in Fall 2012.

In the course of the program management described within this thesis, the VERTIGO team was also able to successfully meet a number of software deadlines. Additionally, the team has now advanced the design beyond the protoflight stage and is in the midst of the build of flight hardware. Though time will tell if the team is ultimately successful in accomplishing its mission goals, signs point to that becoming the case.

## 7.2 Future Work

First and foremost, flight hardware for VERTIGO must be completed in time to test and deliver to the Space Test Program, which takes control of the hardware prior to launch. This will enable the science mission of the program to begin its work in earnest. In addition to the hardware delivery, there are a handful of other deliverables like a training session for crew members and safety reviews that are still pending before hardware turnover.

Besides the delivery of the hardware and the associated programmatic deliverables, the algorithms that were developed for the inspection mission as well as the serial communication code to interface with SPHERES must be integrated and tested on the satellites. As demonstrated by the changes that a small additional mass had during the prototype test session, integration must include adjustment of the controllers to account for changes in the physical characteristics brought on by attaching the VERTIGO payload.

Also left to be done is the implementation of the software on the station with the new code to ensure that it meets mission requirements. The code can be validated on the ground prior to launch, but prior to running the tests on station, those tests are only projections of what will happen in the microgravity environment, especially with new hardware in the loop.

The final element of the future work is the ongoing project to inculcate the next gener-

ation of MIT program managers with the lessons learned from the program management of VERTIGO. By passing this corporate knowledge onto future engineers, it is hoped that the next generation may lead their projects more efficiently and effectively. Eventually, these lessons should be applied to larger projects and teams to further refine and update the principles developed within this thesis.

# Appendices

# Appendix A

# VERTIGO Inspection Maneuver Codes

## A.1 Simple Maneuvers

```
/* Modified from:
 * gsp.c
 *
 * SPHERES Guest Scientist Program custom source code template.
 *
 * MIT Space Systems Laboratory
 * SPHERES Guest Scientist Program
 * http://ssl.mit.edu/spheres/
 *
 * Copyright 2005 Massachusetts Institute of Technology
 *
 * VERTIGO Inspection Maneuver
 * Last Update: 5 Oct 2011 by Michael O'Connor
 *
 *  ***9 Jul Update:***
 *  The code was modified to give the TGT object a path to follow during the maneuver
 *  ***:9 Jul Update***
 *
 *  ***5 Oct Update:***
 *  Code modified to have TGT maintain position in Test 1, L-maneuver in Test 2
 *  ***:5 Oct Update***
 *
 *
 *  *** SPH 1: INSPECTOR (INSP) ***
 *  *** SPH 2: TARGET    (TGT)  ***
 *
 *  ***30 Jun Description:***
 *  The purpose of this test is to demonstrate the 'Phase 1' VERTIGO inspection
     maneuver.
 *  As the Goggles are not yet on station, the relative position/velocity information
     is
 *  simulated using the global metrology system.
 *
 *  The relative information is essentially a transformation from the global frame to
     the
```

```
 *  body frame of the "Inspector" satellite. In this 2-Sat test, we use the second
     SPH
 *  as the "Target" to be inspected. It begins at a point in the center of the test
     volume
 *  (<0,0,0> on ISS, <0.85,0.55,0.3> on ground). From this initial position, it will
     either
 *  run in a pre-set position and attitude profile or maintain position in the center
      of the
 *  volume.
 *
 *  Each SPH will begin at a location roughly equidistant from the center of the test
      volume.
 *  After 10s of estimator convergence, the "Target" will move to the center of the
     test
 *  volume. The "Inspector" will move to a location ROT_RADIUS away from the
     satellite in -X
 *  with it's expansion port facing the Target. This initial positioning will take 30
     s.
 *  Afterward the Target sphere will spend 5s spinning up to a given rotation speed.
     For the
 *  following 150s, the Inspector will be commanded to rotate based on gyro
     information.
 *  While it rotates, it will translate to keep the Target in the same body-frame
     location.
 *  The Target will follow a proscribed path or maintain its location. The Inspector
     should
 *  still maintain pointing toward the Target throughout this phase.
 *
 *  Test 101: SPH2 (Target) holds position
 *  Test 102: SPH2 moves in L-shaped path
 *
 *  ***NOTE:***
 *  It is possible to change the rotation rate, the "center" of the test volume and
     the
 *  radius of the inspection circle by changing the values in the:
 *      "Change Rates, Center Points, etc here" section
 *  ***:NOTE***
 */


/*---------------------------------------------------------------------------*/
/*                          Do not modify this section.                      */
/*---------------------------------------------------------------------------*/

#include "comm.h"
#include "commands.h"
#include "control.h"
#include "gsp.h"
#include "gsp_task.h"
#include "pads.h"
#include "prop.h"
#include "spheres_constants.h"
#include "spheres_physical_parameters.h"
#include "spheres_types.h"
#include "std_includes.h"
#include "system.h"
#include "util_memory.h"

/*---------------------------------------------------------------------------*/
/*                      Modify as desired below this point.                  */
/*---------------------------------------------------------------------------*/
#include "ctrl_attitude.h"
#include "ctrl_position.h"
#include "find_state_error.h"
#include "ctrl_mix.h"
#include "math_matrix.h"
#include <math.h>
#include <string.h>
```

```
#include "gspVERTIGO2SatInspections.h"

void gspVERTIGO2SatInspections_InitTest(unsigned int test_number)
{
    extern state_vector initState;
    memset(&initState, 0, sizeof(initState));

    if (SPHERE_ID == SPHERE1) //INSP
    {
        initState[POS_X] = 0.0f;
        initState[POS_Y] = 0.4f;
        initState[POS_Z] = 0.0f;
    }

    if (SPHERE_ID == SPHERE2) //TGT
    {
        initState[POS_X] = 0.0f;
        initState[POS_Y] = -0.4f;
        initState[POS_Z] = 0.0f;
    }

    initState[QUAT_1] = 1.0f;//GROUND & ISS (Tank Down/DECK)

    if (sysIdentityGet() == SPHERE1)//                    205?Haven't changed
        padsEstimatorInitWaitAndSet(initState, 50, 200, 105,
            PADS_INIT_THRUST_INT_ENABLE,PADS_BEACONS_SET_1TO9); // ISS
    else
        padsEstimatorInitWaitAndSet(initState, 50, SYS_FOREVER, SYS_FOREVER,
            PADS_INIT_THRUST_INT_ENABLE,PADS_BEACONS_SET_1TO9); // ISS

    ctrlPeriodSet(1000);
}


void gspVERTIGO2SatInspections_Control(unsigned int test_number, unsigned int
    test_time, unsigned int maneuver_number, unsigned int maneuver_time)
{
    //dbg_short_packet DebugVecShort;
    //dbg_float_packet DebugVecFloat;
    state_vector ctrlState;
    state_vector ctrlStateTarget;
    state_vector ctrlStateError;
    state_vector ctrlStateTGT;//Inspection Target (SPH2) Control State
    float ctrlControl[6];
    prop_time firing_times;
    //*********************************Change Rates, Center Points, etc here
        :*********************************
    float CENTER_X = 0.0f;
    float CENTER_Y = 0.0f;
    float CENTER_Z = 0.0f;
    float ROT_RATE = -0.0436f; //(3 deg/s == 0.0524,2.5 deg/s == 0.0436, 2 deg/s ==
        0.0349)
    float ROT_RATE_TGT = 0.1047f; //0.1047 == 6 deg/s;
    float ROT_RADIUS = 0.36f;
    float L1 = 0.25f; //Size of L-shaped movement
    float L2 = 0.2f;
    //
        ***************************************************************************************

    const int min_pulse = 10;
    float R_temp[3];
    float V_temp[3];
    float cross[3];
    float mat[3][3];
    float RBody[3];

    extern const float KPattitudePD, KDattitudePD, KPpositionPD, KDpositionPD,
        VEHICLE_MASS;
```

```
//Clear all uninitialized vectors
memset(ctrlControl,0,sizeof(float)*6);
memset(ctrlStateTarget,0,sizeof(state_vector));
memset(ctrlStateError,0,sizeof(state_vector));
memset(ctrlStateTGT,0,sizeof(state_vector));
//memset(DebugVecShort, 0, sizeof(dbg_short_packet));
//memset(DebugVecFloat, 0, sizeof(dbg_float_packet));

padsStateGet(ctrlState);
if (maneuver_number > 1)
{
    unsigned int test_time_dummy = test_time;
    commBackgroundStateGet(SPHERE2, &test_time_dummy, (state_vector *)
        ctrlStateTGT);
}

switch(maneuver_number){
    case 1: //*********************************Estimator initialization
        ********************************
        if (test_time >= 10000){
            ctrlManeuverTerminate();
        }
        break;
    case 2: //*********************************Move to initial position
        ********************************
        if (sysIdentityGet()==SPHERE1)
            padsGlobalPeriodSet(SYS_FOREVER);
        switch(sysIdentityGet()){
            case SPHERE1://INSP
                ctrlStateTarget[POS_X] = CENTER_X - ROT_RADIUS;
                ctrlStateTarget[POS_Y] = CENTER_Y;
                ctrlStateTarget[POS_Z] = CENTER_Z;
            break;
            case SPHERE2://TGT
                ctrlStateTarget[POS_X] = CENTER_X;
                ctrlStateTarget[POS_Y] = CENTER_Y;
                ctrlStateTarget[POS_Z] = CENTER_Z;
            break;
        }

        ctrlStateTarget[QUAT_1] = 1.0f;

        //find error
        findStateError(ctrlStateError,ctrlState,ctrlStateTarget);

        //call controllers
        ctrlPositionPDgains(KPpositionPD, KDpositionPD, KPpositionPD,
            KDpositionPD, KPpositionPD, KDpositionPD, ctrlStateError, ctrlControl
            );
        ctrlAttitudeNLPDwie(KPattitudePD,KDattitudePD,KPattitudePD,KDattitudePD,
            KPattitudePD,KDattitudePD,ctrlStateError,ctrlControl);

        //mix forces/torques into thruster commands
        //FORCE_FRAME_BODY
        ctrlMixWLoc(&firing_times, ctrlControl, ctrlState, min_pulse, 20.0f,
            FORCE_FRAME_INERTIAL);
        //Set firing times
        propSetThrusterTimes(&firing_times);


        if (sysIdentityGet() == SPHERE1)
            padsGlobalPeriodSetAndWait(200,205);
        if (maneuver_time>=30000)
            ctrlManeuverTerminate();
        break;
    case 3://*********************************Rotate Center SPHERE(#2/TGT) if
        desired*********************************
```

```
        switch(sysIdentityGet()){
            case SPHERE1://INSP
                ctrlStateTarget[POS_X] = CENTER_X - ROT_RADIUS;
                ctrlStateTarget[POS_Y] = CENTER_Y;
                ctrlStateTarget[POS_Z] = CENTER_Z;
            break;
            case SPHERE2://TGT
                //Spin
                ctrlStateTarget[RATE_Z] = ROT_RATE_TGT;
                ctrlStateTarget[RATE_Y] = ROT_RATE_TGT;//Tumble
                ctrlStateTarget[POS_X] = CENTER_X;
                ctrlStateTarget[POS_Y] = CENTER_Y;
                ctrlStateTarget[POS_Z] = CENTER_Z;
            break;
        }

            ctrlStateTarget[QUAT_1] = 1.0f;

        //Estimate, Calculate Control, and Fire Thrusters
                findStateError(ctrlStateError,ctrlState,ctrlStateTarget);
                ctrlPositionPDgains(KPpositionPD, KDpositionPD, KPpositionPD,
                    KDpositionPD, KPpositionPD, KDpositionPD, ctrlStateError,
                    ctrlControl);
                if (sysIdentityGet() == SPHERE1)
                    ctrlAttitudeNLPDwie(KPattitudePD,KDattitudePD,KPattitudePD,
                        KDattitudePD,KPattitudePD,KDattitudePD,ctrlStateError,
                        ctrlControl);
                else
                    ctrlAttitudeNLPDwie(0,KDattitudePD,0,KDattitudePD,0,
                        KDattitudePD,ctrlStateError,ctrlControl);//Use this to
                        ignore quaternion error from global met
                ctrlMixWLoc(&firing_times, ctrlControl, ctrlState, min_pulse,
                    20.0f, FORCE_FRAME_INERTIAL);//Changed from 40.0f to 20.0f
                propSetThrusterTimes(&firing_times);

        if (sysIdentityGet() == SPHERE1)
            padsGlobalPeriodSetAndWait(200,205);
        //if (sysIdentityGet() == SPHERE2)
        //  padsGlobalPeriodSetAndWait(200,205);
        if (maneuver_time>=5000)
            ctrlManeuverTerminate();
        break;

    case 4: //*********************************Begin Inspector Rotation and
        Inspection Maneuver**********************************
        if (sysIdentityGet()==SPHERE1)
        {
            padsGlobalPeriodSet(SYS_FOREVER);

            //Gather Simulated Vision Data
            /*  ctrlState (current sph state) begins in global frame
             *  ...convert to body frame:
             *  POS are in global
             *  VEL are in global
             *  QUAT are from global frame to body frame
             *  RATE are in body
             * We will use the quaternions to take the postion and velocity
                 vectors
             * from the global frame to the body frame
             */
            //Make measurements relative:
            //Moves about point at center of volume (0,0,0)
                R_temp[0] = ctrlStateTGT[POS_X] - ctrlState[POS_X];
                R_temp[1] = ctrlStateTGT[POS_Y] - ctrlState[POS_Y];
                R_temp[2] = ctrlStateTGT[POS_Z] - ctrlState[POS_Z];
            //Move to Body Frame
                quat2matrixIn(mat, &ctrlState[QUAT_1]);//MAT <= rotation matrix
                    from global to body
```

```
            mathMatVecMult(RBody, (float**)mat, R_temp, 3, 3);
            ctrlState[POS_X] = RBody[0];
            ctrlState[POS_Y] = RBody[1];
            ctrlState[POS_Z] = RBody[2];

        //V = Rot*(r') - wx(Rot(r)))
            ctrlState[VEL_X]  = ctrlStateTGT[VEL_X] - ctrlState[VEL_X];
            ctrlState[VEL_Y]  = ctrlStateTGT[VEL_Y] - ctrlState[VEL_Y];
            ctrlState[VEL_Z]  = ctrlStateTGT[VEL_Z] - ctrlState[VEL_Z];
            mathMatVecMult(V_temp, (float**)mat, &ctrlState[VEL_X], 3, 3);
            mathVecCross(cross, &ctrlState[RATE_X], &ctrlState[POS_X]);
            ctrlState[VEL_X] = V_temp[0] - cross[0];
            ctrlState[VEL_Y] = V_temp[1] - cross[1];
            ctrlState[VEL_Z] = V_temp[2] - cross[2];
        //End Gathering Simulated Vision Data

        ctrlStateTarget[POS_X] = ROT_RADIUS;

            ctrlStateTarget[RATE_Z] = -ROT_RATE;
        //May need to reverse of other maneuvers because of global to body
            frame transformation, though QUAT is uncontrolled-for


            ctrlStateTarget[QUAT_1] = 1.0f;

        //find error
            findStateError(ctrlStateError,ctrlState,ctrlStateTarget);
        //call controllers
            ctrlPositionPDgains(KPpositionPD, KDpositionPD, KPpositionPD,
                KDpositionPD, KPpositionPD, KDpositionPD, ctrlStateError,
                ctrlControl);
            ctrlAttitudeNLPDwie(0,KDattitudePD,0,KDattitudePD,0,KDattitudePD,
                ctrlStateError,ctrlControl);//Use this to ignore quaternion
                error from global met
        //Adjust for frame change
            ctrlControl[0] *= -1;
            ctrlControl[1] *= -1;
            ctrlControl[2] *= -1;
        //Feedforward Term
            ctrlControl[0] += (VEHICLE_MASS*ctrlStateTarget[POS_X]*
                ctrlStateTarget[RATE_Z]*ctrlStateTarget[RATE_Z]);
        //Set firing times, schedule firing
            ctrlMixWLoc(&firing_times, ctrlControl, ctrlState, min_pulse,
                20.0f, FORCE_FRAME_BODY);//Changed from 40.0f to 20.0f
            propSetThrusterTimes(&firing_times);
    }

    //If SPH_2 is to follow some path or movement, insert it here:
    if (sysIdentityGet() == SPHERE2)
    {
        if ((maneuver_time > 60000) && (test_number == 2))
            ctrlStateTarget[POS_X] = CENTER_X - L2;
        else
            ctrlStateTarget[POS_X] = CENTER_X;

        if ((maneuver_time > 30000) && (test_number == 2))
            ctrlStateTarget[POS_Y] = CENTER_Y - L1;
        else
            ctrlStateTarget[POS_Y] = CENTER_Y;


        ctrlStateTarget[QUAT_1] = 1.0f;
        ctrlStateTarget[POS_Z] = CENTER_Z;

        //find error
            findStateError(ctrlStateError,ctrlState,ctrlStateTarget);
        //call controllers (no attitude control)
```

```
                ctrlPositionPDgains(KPpositionPD, KDpositionPD, KPpositionPD,
                    KDpositionPD, KPpositionPD, KDpositionPD, ctrlStateError,
                    ctrlControl);
            //Set firing times, schedule firing
                ctrlMixWLoc(&firing_times, ctrlControl, ctrlState, min_pulse,
                    20.0f, FORCE_FRAME_INERTIAL);//Changed from 40.0f to 20.0f
                propSetThrusterTimes(&firing_times);
        }

        if (sysIdentityGet() == SPHERE1)
            padsGlobalPeriodSetAndWait(200,205);
        if (maneuver_time>=150000)
            ctrlTestTerminate(TEST_RESULT_NORMAL);
        break;
    default:
        ctrlTestTerminate(TEST_RESULT_ERROR);
        break;
}

//DebugPackets
    /*
    * We want to know:
    *   1) Test Time
    *   2) Actual Position (Relative)
    *   3) Desired Position (Relative)
    *   4) Actual Angular Rate
    *   5) Desired Angular Rate
    *   4) Forces (Body Frame)
    *   5) Torques (Body Frame)
    */
    /*
    //To Debug, in the data file in Matlab, divide by the constant
        //in order to get the values in ms, m, and rad/s, respectively
    //Time (in tenths of a seconds)
    DebugVecShort[0] = (short) (test_time*0.01f);
    DebugVecFloat[0] = (float) (test_time*0.01f);
    //Actual Relative Position (in 1/10ths of a mm)
    DebugVecShort[1] = (short) (ctrlState[POS_X]*10000.0f);
    DebugVecShort[2] = (short) (ctrlState[POS_Y]*10000.0f);
    DebugVecShort[3] = (short) (ctrlState[POS_Z]*10000.0f);
    //Desired Relative Position (in 1/10ths of a mm)
    DebugVecShort[5] = (short) (ctrlStateTarget[POS_X]*10000.0f);
    DebugVecShort[6] = (short) (ctrlStateTarget[POS_Y]*10000.0f);
    DebugVecShort[7] = (short) (ctrlStateTarget[POS_Z]*10000.0f);//(
        ctrlStateTarget[QUAT_1]*100.0f);
    //Actual Angular Velocity (in 1/10000ths of a rad/s)
    DebugVecShort[8] = (short) (ctrlState[RATE_X]*10000.0f);//(ctrlStateTarget[
        QUAT_2]*100.0f);
    DebugVecShort[9] = (short) (ctrlState[RATE_Y]*10000.0f);//(ctrlStateTarget[
        QUAT_3]*100.0f);
    DebugVecShort[10] = (short) (ctrlState[RATE_Z]*10000.0f);//(ctrlStateTarget[
        QUAT_4]*100.0f);
    //Desired Angular Velocity (in 1/10000ths of a rad/s)
    DebugVecShort[11] = (short) (ctrlStateTarget[RATE_X]*10000.0f);
    DebugVecShort[12] = (short) (ctrlStateTarget[RATE_Y]*10000.0f);
    DebugVecShort[13] = (short) (ctrlStateTarget[RATE_Z]*10000.0f);
    //Maneuver Number
    DebugVecShort[14] = (short) (maneuver_number);
    //Commanded Force
    DebugVecFloat[1] = ctrlControl[FORCE_X];
    DebugVecFloat[2] = ctrlControl[FORCE_Y];
    DebugVecFloat[3] = ctrlControl[FORCE_Z];
    //Commanded Torque
    DebugVecFloat[5] = ctrlControl[TORQUE_X];
    DebugVecFloat[6] = ctrlControl[TORQUE_Y];
    DebugVecFloat[7] = ctrlControl[TORQUE_Z];
// Send DBG Packets
```

```
    commSendPacket(COMM_CHANNEL_STL,GROUND,sysIdentityGet(),
        COMM_CMD_DBG_SHORT_SIGNED, (unsigned char *) DebugVecShort, 0);//May end in
        COMM_MODE_NO_ACK instead of 0
    commSendPacket(COMM_CHANNEL_STL,GROUND,sysIdentityGet(), COMM_CMD_DBG_FLOAT, (
        unsigned char *) DebugVecFloat, 0);
    */

}
```

## A.2 Advanced Maneuvers

```
/* Modified from:
 * gsp.c
 *
 * SPHERES Guest Scientist Program custom source code template.
 *
 * MIT Space Systems Laboratory
 * SPHERES Guest Scientist Program
 * http://ssl.mit.edu/spheres/
 *
 * Copyright 2005 Massachusetts Institute of Technology
 *
 * VERTIGO 2Sat Paths Experiment
 * Last Update: 09 Mar 2012 by Michael O'Connor
 * Based off of VERTIGO Inspection Maneuver Code
 *  Modification from 27 Feb to 09 Mar includes:
 *  -Addition of "Closest Point" algorithm
 *  -Includes Changing of algorithm from rotating and controlling translation to
     translating
 *  and controlling rotation
 *
 *  *** SPH 1: INSPECTOR (INSP) ***
 *  *** SPH 2: TARGET    (TGT)  ***
 *
 *
 *  ***27 Feb 2012 Description:***
 *
 *  Test 301: SPH2 (Target) moves toward INSP, then moves in Z-direction
 *  Test 302: SPH1 (Inspector) moves in 3-D path
 *  Test 303: SPH1 performs 10-min inspection
 *  Test 304: SPH1 inspects using SPH2 rotation information
 *
 *  Test 301: SPH2 (Target) moves toward INSP, then moves in Z-direction
 *      This motion finds the TGT satellite rotating in the center of the volume. INSP
     circumnavigates TGT at
 *  a constant range. TGT will move toward INSP and INSP will compensate to maintain
     pointing and range. After
 *  more time, the TGT will move out of the inspection plane. INSP should compensate by
     matching upward motion.
 *
 *  Test 302: SPH1 (Inspector) moves in 3-D path
 *      TGT rotates in center of volume. INSP moves 90 degrees around TGT by rotating
     about its Z axis. It then
 *  rotates 270 degrees about the Y axis until it is between the rotating TGT and the DECK
     . It then completes
 *  coverage by rotating 90 degrees about Z once more.
 *
 *  Test 303: SPH1 performs 10-min inspection
 *      TGT rotates in center of volume. INSP circumnavigates TGT for a period of
     approximately 10 minutes. It
 *  should complete about 2.5 "orbits".
 *
 *  Test 304: SPH1 inspects using SPH2 rotation information:
 *      The TGT satellite will rotate in the center of the volume. Since vision can give
     rotation information,
 *  we will get rate state information from the TGT. After INSP determines direction of
     spin, INSP will move
 *  to location perpindicular to spin axis. It will start moving in direction of TGT spin
     axis while also
 *  moving around the TGT in a direction opposite the spin. The motion in the spin axis
     direction will complete
 *  as soon as possible. The motion opposite the spin direction should continue until the
     sum of the TGT and
 *  INSP motion sums to 2pi.
 *      The INSP should then move antiparallel to the spin axis direction and repeat its
     observations of the
```

```
 *  "southern hemisphere" of the TGT. It will repeat this and then inspect the "equator"
     of the TGT.
 *
 *
 *  ***NOTE:***
 *  It is possible to change the rotation rate, the "center" of the test volume and the
 *  radius of the inspection circle by changing the values in the:
 *      "Change Rates, Center Points, etc here" section
 *  ***:NOTE***
 */


/*-------------------------------------------------------------------------*/
/*                          Do not modify this section.                    */
/*-------------------------------------------------------------------------*/

#include "comm.h"
#include "commands.h"
#include "control.h"
#include "gsp.h"
#include "gsp_task.h"
#include "pads.h"
#include "prop.h"
#include "spheres_constants.h"
#include "spheres_physical_parameters.h"
#include "spheres_types.h"
#include "std_includes.h"
#include "system.h"
#include "util_memory.h"

/*-------------------------------------------------------------------------*/
/*                      Modify as desired below this point.                */
/*-------------------------------------------------------------------------*/
#include "ctrl_attitude.h"
#include "ctrl_position.h"
#include "find_state_error.h"
#include "housekeeping_internal.h"
#include "housekeeping.h"
#include "ctrl_mix.h"
#include "math_matrix.h"
#include <math.h>
#include <string.h>
#include "gspVERTIGO_2SatPaths.h"

float throughAngle;
float maneuverCounter;
int rotFlag;

void gspVERTIGO_2SatPaths_InitTest(unsigned int test_number)
{
    extern state_vector initState;
    memset(&initState, 0, sizeof(initState));

    if (SPHERE_ID == SPHERE1) //INSP
    {
        initState[POS_X] = 0.0f;
        initState[POS_Y] = 0.4f;
        initState[POS_Z] = 0.0f;
    }

    if (SPHERE_ID == SPHERE2) //TGT
    {
        initState[POS_X] = 0.0f;
        initState[POS_Y] = -0.4f;
        initState[POS_Z] = 0.0f;
    }

    initState[QUAT_1] = 1.0f;//GROUND & ISS (Tank Down/DECK)
```

```
    if (sysIdentityGet() == SPHERE1)//                    205?Haven't changed
        padsEstimatorInitWaitAndSet(initState, 50, 200, 105, PADS_INIT_THRUST_INT_ENABLE,
            PADS_BEACONS_SET_1TO9); // ISS
    else
        padsEstimatorInitWaitAndSet(initState, 50, SYS_FOREVER, SYS_FOREVER,
            PADS_INIT_THRUST_INT_ENABLE,PADS_BEACONS_SET_1TO9); // ISS

    ctrlPeriodSet(1000);
    throughAngle = 0.0f;
    maneuverCounter = 0.0f;
}


void gspVERTIGO_2SatPaths_Control(unsigned int test_number, unsigned int test_time,
    unsigned int maneuver_number, unsigned int maneuver_time)
{
    //dbg_short_packet DebugVecShort;
    //dbg_float_packet DebugVecFloat;
    state_vector ctrlState;
    state_vector ctrlStateTarget;
    state_vector ctrlStateError;
    state_vector ctrlStateTGT;//Inspection Target (SPH2) Control State
    float ctrlControl[6];
    float RATE;
    float ROT_RATE_DIR[4];
    float vecOut[4];
    float TGT_RATE;
    prop_time firing_times;
    //*******************************Change Rates, Center Points, etc here
        :*********************************
    float CENTER_X = 0.0f;
    float CENTER_Y = 0.0f;
    float CENTER_Z = 0.0f;
    float ROT_RATE = 0.0262f; //(3 deg/s == 0.0524, 2.5 deg/s == 0.0436, 2 deg/s ==
        0.0349,  1.5 deg/s == 0.0262)
    float ROT_RATE_TGT = -0.1047f; //0.1047 == 6 deg/s;
    float ROT_RADIUS = 0.70f;
    float L1 = 0.25f; //Size of L-shaped movement
    float L2 = 0.20f;
        //
            ***************************************************************************************************

    const int min_pulse = 10;
    float MAN4_TIME_LIMIT = 150000.0f;

    dbg_float_packet DebugVecFloat;
    dbg_short_packet DebugVecShort;

    extern const float KPattitudePD, KDattitudePD, KPpositionPD, KDpositionPD,
        VEHICLE_MASS;

    memset(DebugVecFloat, 0, sizeof(DebugVecFloat));
    memset(DebugVecShort, 0, sizeof(DebugVecShort));

    //Account for movement of target during this test - try to remain in volume
    if (test_number <= 1)
    {
        CENTER_Y = -1.0f*L1;
        CENTER_Z = L2;
    }

    //Clear all uninitialized vectors
    memset(ctrlControl,0,sizeof(float)*6);
    memset(ctrlStateTarget,0,sizeof(state_vector));
    memset(ctrlStateError,0,sizeof(state_vector));
    memset(ctrlStateTGT,0,sizeof(state_vector));
    //memset(DebugVecShort, 0, sizeof(dbg_short_packet));
```

```
//memset(DebugVecFloat, 0, sizeof(dbg_float_packet));

padsStateGet(ctrlState);
commBackgroundStateGet(SPHERE2, &test_time, (state_vector *)ctrlStateTGT);

switch(maneuver_number){
    case 1: //*********************************************************************
        Maneuver 1: Estimator initialization
        ********************************************************************
        //Termination after 10s
        if (maneuver_time >= 10000){
            ctrlManeuverTerminate();
        }
        break;
    case 2: //*********************************************************************
        Maneuver 2: Move to initial position
        ********************************************************************
        //Termination after 30s
        if (sysIdentityGet()==SPHERE1)
            padsGlobalPeriodSet(SYS_FOREVER);
        switch(sysIdentityGet()){
            case SPHERE1://INSP
                ctrlStateTarget[POS_X] = CENTER_X - ROT_RADIUS;
                ctrlStateTarget[POS_Y] = CENTER_Y;
                ctrlStateTarget[POS_Z] = CENTER_Z;
            break;
            case SPHERE2://TGT
                ctrlStateTarget[POS_X] = CENTER_X;
                ctrlStateTarget[POS_Y] = CENTER_Y;
                ctrlStateTarget[POS_Z] = CENTER_Z;
            break;
        }

        //Rotate Inspector Satellite to show Initial Positioning has begun and to
            distinguish INSP from TGT

        ctrlStateTarget[QUAT_1] = 1.0f;

        //find error
        findStateError(ctrlStateError,ctrlState,ctrlStateTarget);

        //call controllers
        ctrlPositionPDgains(KPpositionPD, KDpositionPD, KPpositionPD, KDpositionPD,
            KPpositionPD, KDpositionPD, ctrlStateError, ctrlControl);
        ctrlAttitudeNLPDwie(KPattitudePD,KDattitudePD,KPattitudePD,KDattitudePD,
            KPattitudePD,KDattitudePD,ctrlStateError,ctrlControl);

        //mix forces/torques into thruster commands
        //FORCE_FRAME_BODY
        ctrlMixWLoc(&firing_times, ctrlControl, ctrlState, min_pulse, 20.0f,
            FORCE_FRAME_INERTIAL);
        //Set firing times
        propSetThrusterTimes(&firing_times);


        if (sysIdentityGet() == SPHERE1)
            padsGlobalPeriodSetAndWait(200,205);
        if (maneuver_time>=30000)
            ctrlManeuverTerminate();
        break;
    case 3://*********************************************************************
        Maneuver 3: Rotate Center SPHERE(#2/TGT) if desired
        ********************************************************************
        //Termination after 05s
        switch(sysIdentityGet()){
            case SPHERE1://INSP
                ctrlStateTarget[POS_X] = CENTER_X - ROT_RADIUS;
                ctrlStateTarget[POS_Y] = CENTER_Y;
```

```
            ctrlStateTarget[POS_Z] = CENTER_Z;
        break;
        case SPHERE2://TGT
            ctrlStateTarget[RATE_Z] = ROT_RATE_TGT;//Spin
            ctrlStateTarget[RATE_Y] = ROT_RATE_TGT;//Tumble
            if (test_number == 4)
            {
                //ctrlStateTarget[RATE_Y] = ctrlStateTarget[RATE_Y]/(4.0f);
                ctrlStateTarget[RATE_Z] = ctrlStateTarget[RATE_Z]/(4.0f);// 0.0f;
            }
            ctrlStateTarget[POS_X] = CENTER_X;
            ctrlStateTarget[POS_Y] = CENTER_Y;
            ctrlStateTarget[POS_Z] = CENTER_Z;
        break;
    }

    ctrlStateTarget[QUAT_1] = 1.0f;

    //Estimate, Calculate Control, and Fire Thrusters
            findStateError(ctrlStateError,ctrlState,ctrlStateTarget);
            ctrlPositionPDgains(KPpositionPD, KDpositionPD, KPpositionPD,
                KDpositionPD, KPpositionPD, KDpositionPD, ctrlStateError,
                ctrlControl);
            if (sysIdentityGet() == SPHERE1)
                ctrlAttitudeNLPDwie(KPattitudePD,KDattitudePD,KPattitudePD,
                    KDattitudePD,KPattitudePD,KDattitudePD,ctrlStateError,
                    ctrlControl);
            else
                ctrlAttitudeNLPDwie(0,KDattitudePD,0,KDattitudePD,0,KDattitudePD,
                    ctrlStateError,ctrlControl);//Use this to ignore quaternion
                    error from global met
            ctrlMixWLoc(&firing_times, ctrlControl, ctrlState, min_pulse, 20.0f,
                FORCE_FRAME_INERTIAL);//Changed from 40.0f to 20.0f
            propSetThrusterTimes(&firing_times);

    if (sysIdentityGet() == SPHERE1)
        padsGlobalPeriodSetAndWait(200,205);
    //if (sysIdentityGet() == SPHERE2)
    //  padsGlobalPeriodSetAndWait(200,205);
    if (maneuver_time>=5000)
        ctrlManeuverTerminate();
    break;

case 4: //*****************************************************************
    Maneuver 4: Begin Inspector Rotation and Inspection Maneuver
    ****************************************************************
    //*****************************************************************SPHERE 1:
        INSPECTOR
        ****************************************************************
    if (sysIdentityGet() == SPHERE1)
    {
        padsGlobalPeriodSet(SYS_FOREVER);

        //*****************************************************Gather Simulated
            Vision Data*************************************************
        changetoBodyFrame(&ctrlStateTGT[POS_X], &ctrlState[POS_X], vecOut,
            POSITION_VECTOR);
        ctrlState[POS_X] = vecOut[0];
        ctrlState[POS_Y] = vecOut[1];
        ctrlState[POS_Z] = vecOut[2];
        changetoBodyFrame(&ctrlStateTGT[POS_X], &ctrlState[POS_X], vecOut,
            VELOCITY_VECTOR);
        ctrlState[VEL_X] = vecOut[0];
        ctrlState[VEL_Y] = vecOut[1];
        ctrlState[VEL_Z] = vecOut[2];
        changetoBodyFrame(&ctrlStateTGT[POS_X], &ctrlState[POS_X], vecOut,
            ROTATION_VECTOR);
        ROT_RATE_DIR[0] = vecOut[0];
```

```
ROT_RATE_DIR[1] = vecOut[1];
ROT_RATE_DIR[2] = vecOut[2];
ROT_RATE_TGT = vecOut[3];
//*******************************************************End Gathering
    Simulated Vision Data
    ******************************************************

//Inspection Motion/Path Parameters
switch(test_number){
case 2://Test 2: SPH1 (Inspector) moves in 3-D path
    ctrlStateTarget[POS_X] = ROT_RADIUS;
    // Use an integrator to estimate the points at which the rotations
        should change from Z to Y and back to Z
    if ((throughAngle >= 2*PI) || (throughAngle <= -2*PI))
    {
        ctrlStateTarget[RATE_Z] = ROT_RATE;
        throughAngle = throughAngle + (ctrlState[RATE_Z]*((float)
            maneuver_time - maneuverCounter)/1000.0f);
    }
    else if((throughAngle >= PI/2) || (throughAngle <= -PI/2))
    {
        ctrlStateTarget[RATE_Y] = ROT_RATE;
        throughAngle = throughAngle + (ctrlState[RATE_Y]*((float)
            maneuver_time - maneuverCounter)/1000.0f);
    }
    else
    {
        ctrlStateTarget[RATE_Z] = ROT_RATE;
        throughAngle = throughAngle + (ctrlState[RATE_Z]*((float)
            maneuver_time - maneuverCounter)/1000.0f);
    }
    maneuverCounter = (float)maneuver_time;
break;
case 4://Test 4: SPH1 inspects using SPH2 rotation information
    ctrlStateTarget[POS_X] = ROT_RADIUS;
    //Time/Coverage-based movement procedures:
    if (rotFlag == 0) //Align so TGT spin axis is roughly in INSP's Z-Body
         Direction
        {
            if (ROT_RATE_DIR[0] >= .01f) //Align if errors in X
                ctrlStateTarget[RATE_Y] = ROT_RATE;
            else if (ROT_RATE_DIR[0] <= -.01f)
                ctrlStateTarget[RATE_Y] = -ROT_RATE;
            else
                rotFlag = 1;

            if (ROT_RATE_DIR[1] >= .01) //Align if errors in Y
                ctrlStateTarget[RATE_X] = ROT_RATE;
            else if (ROT_RATE_DIR[1] <= -.01f)
                ctrlStateTarget[RATE_X] = -ROT_RATE;
            else
                rotFlag = rotFlag + 1;

            if (rotFlag != 2) //If TGT rotation is aligned with Z axis of
                INSP, proceed
                rotFlag = 0;
        }
    else if (rotFlag == 2) //Begin inspection motion moving to "Northern
        Hemisphere"
        {
            ctrlStateTarget[RATE_Z] = 0.0f;
            ctrlStateTarget[RATE_Y] = ROT_RATE; //For Moving to "North
                Pole" of TGT
            ctrlStateTarget[RATE_X] = 0.0f;
            throughAngle = throughAngle + (((float)fabs(ctrlState[RATE_Y])
                )*((float)maneuver_time - maneuverCounter)/1000);
            if(throughAngle >= PI/4)
            {
```

```
            rotFlag++;
            throughAngle = 0.0f;
        }
    }
else if (rotFlag == 3) //Hold in "Northern Hemisphere" until entire
    hemisphere has been seen.
    {
        ctrlStateTarget[RATE_Z] = ROT_RATE; //For Coverage
        ctrlStateTarget[RATE_X] = -ROT_RATE; //Maintaining Pointing
        ctrlStateTarget[RATE_Y] = 0.0f;
        TGT_RATE = sqrtf(ctrlStateTGT[RATE_X]*ctrlStateTGT[RATE_X] +
            ctrlStateTGT[RATE_Y]*ctrlStateTGT[RATE_Y] + ctrlStateTGT[
            RATE_Z]*ctrlStateTGT[RATE_Z]);
        throughAngle = throughAngle + ((((float)fabs(ctrlState[RATE_Z
            ])) + ((float)fabs(TGT_RATE)))*((float)maneuver_time -
            maneuverCounter)/1000);
        if (throughAngle >= 2*PI)
        {
            rotFlag++;
            throughAngle = 0.0f;
        }
    }
else if (rotFlag == 4) //Move to "Southern Hemisphere"
    {
        ctrlStateTarget[RATE_Z] = 0.0f;
        ctrlStateTarget[RATE_Y] = -ROT_RATE; //For Moving to "South
            Pole" of TGT
        ctrlStateTarget[RATE_X] = 0.0f;
        throughAngle = throughAngle + (((float)fabs(ctrlState[RATE_Y])
            )*((float)maneuver_time - maneuverCounter)/1000);
        if(throughAngle >= PI/2)
        {
            rotFlag++;
            throughAngle = 0.0f;
        }
    }
else if (rotFlag == 5) //Hold in "Southern Hemisphere" until entire
    hemisphere has been seen.
    {
        ctrlStateTarget[RATE_Z] = ROT_RATE; //For Coverage
        ctrlStateTarget[RATE_X] = ROT_RATE; //Maintaining Pointing
        ctrlStateTarget[RATE_Y] = 0.0f;
        TGT_RATE = sqrtf(ctrlStateTGT[RATE_X]*ctrlStateTGT[RATE_X] +
            ctrlStateTGT[RATE_Y]*ctrlStateTGT[RATE_Y] + ctrlStateTGT[
            RATE_Z]*ctrlStateTGT[RATE_Z]);
        throughAngle = throughAngle + ((((float)fabs(ctrlState[RATE_Z
            ])) + ((float)fabs(TGT_RATE)))*((float)maneuver_time -
            maneuverCounter)/1000);
        if (throughAngle >= 2*PI)
        {
            rotFlag++;
            throughAngle = 0.0f;
        }
    }
else if (rotFlag == 6) //Begin inspection motion moving to "Equator"
    {
        ctrlStateTarget[RATE_Z] = 0.0f;
        ctrlStateTarget[RATE_Y] = ROT_RATE; //For Moving to "Equator"
            of TGT
        ctrlStateTarget[RATE_X] = 0.0f;
        throughAngle = throughAngle + (((float)fabs(ctrlState[RATE_Y])
            )*((float)maneuver_time - maneuverCounter)/1000);
        if(throughAngle >= PI/4)
        {
            rotFlag++;
            throughAngle = 0.0f;
        }
    }
```

```
            else //Hold at equator until full orbit is complete.
                {
                    ctrlStateTarget[RATE_Z] = ROT_RATE; //For Coverage
                    ctrlStateTarget[RATE_Y] = 0.0f;
                    ctrlStateTarget[RATE_X] = 0.0f;
                    TGT_RATE = sqrtf(ctrlStateTGT[RATE_X]*ctrlStateTGT[RATE_X] +
                        ctrlStateTGT[RATE_Y]*ctrlStateTGT[RATE_Y] + ctrlStateTGT[
                        RATE_Z]*ctrlStateTGT[RATE_Z]);
                    throughAngle = throughAngle + ((((float)fabs(ctrlState[RATE_Z
                        ])) + ((float)fabs(ctrlState[RATE_X]))+ ((float)fabs(
                        TGT_RATE)))*((float)maneuver_time - maneuverCounter)/1000)
                        ;
                    if ((throughAngle >= 2*PI))
                    {
                        ctrlStateTarget[RATE_Z] = 0.0f;
                        ctrlStateTarget[RATE_Y] = 0.0f;
                        ctrlStateTarget[POS_X] = ROT_RADIUS;
                        ctrlStateTarget[RATE_X] = 3*ROT_RATE;
                    }
                }
            maneuverCounter = (float)maneuver_time;
            break;
        default://  Test 1: SPH2 (Target) moves toward INSP, then moves in Z-
            direction & Test 3: SPH1 performs 10-min inspection
            ctrlStateTarget[POS_X] = ROT_RADIUS;
            ctrlStateTarget[RATE_Z] = ROT_RATE;
        break;
        }

        //May need to reverse of other maneuvers because of global to body frame
            transformation, though QUAT is uncontrolled-for
        ctrlStateTarget[QUAT_1] = 1.0f;

        //find error
            findStateError(ctrlStateError,ctrlState,ctrlStateTarget);
        //call controllers
            ctrlPositionPDgains(KPpositionPD, KDpositionPD, KPpositionPD,
                KDpositionPD, KPpositionPD, KDpositionPD, ctrlStateError,
                ctrlControl);
            ctrlAttitudeNLPDwie(0,KDattitudePD,0,KDattitudePD,0,KDattitudePD,
                ctrlStateError,ctrlControl);//Use this to ignore quaternion error
                from global met
        //Adjust for frame change
            ctrlControl[0] *= -1;
            ctrlControl[1] *= -1;
            ctrlControl[2] *= -1;
        //Feedforward Term
            RATE = (ctrlStateTarget[RATE_X]*ctrlStateTarget[RATE_X] +
                ctrlStateTarget[RATE_Y]*ctrlStateTarget[RATE_Y] + ctrlStateTarget[
                RATE_Z]*ctrlStateTarget[RATE_Z]);
            if (rotFlag <= 6)
                ctrlControl[0] += (VEHICLE_MASS*ctrlStateTarget[POS_X]*RATE);//
                    RATE actually RATE^2
        //Set firing times, schedule firing
            ctrlMixWLoc(&firing_times, ctrlControl, ctrlState, min_pulse, 20.0f,
                FORCE_FRAME_BODY);
            propSetThrusterTimes(&firing_times);
    }
    //*************************************************************************SPHERE 2:
        TARGET
        *************************************************************************
    //If SPH_2 is to follow some path or movement, insert it here:
    if (sysIdentityGet() == SPHERE2)
    {
        switch(test_number){
        case 1://  Test 1: SPH2 (Target) moves toward INSP, then moves in Z-
            direction
            if (maneuver_time > 120000)
```

```
            ctrlStateTarget[POS_Z] = CENTER_Z - L2;
        else
            ctrlStateTarget[POS_Z] = CENTER_Z;
        if (maneuver_time > 60000)
            ctrlStateTarget[POS_Y] = CENTER_Y + L1;
        else
            ctrlStateTarget[POS_Y] = CENTER_Y;
    break;
    case 2:
        if (maneuver_time >= 180000.0f) {
            ctrlStateTarget[POS_Z] = CENTER_Z - L1;
        }
        else if (maneuver_time >= 60000.0f) {
            ctrlStateTarget[POS_Z] = CENTER_Z + L1;
        }
        else
        {
            ctrlStateTarget[POS_X] = CENTER_X;
            ctrlStateTarget[POS_Y] = CENTER_Y;
            ctrlStateTarget[POS_Z] = CENTER_Z;
        }
    break;
    default://  Test 2: SPH1 (Inspector) moves in 3-D path, Test 3: SPH1
        performs 10-min inspection, & Test 4: SPH1 inspects using SPH2
        rotation information
        ctrlStateTarget[POS_X] = CENTER_X;
        ctrlStateTarget[POS_Y] = CENTER_Y;
        ctrlStateTarget[POS_Z] = CENTER_Z;
    break;
    }
    ctrlStateTarget[QUAT_1] = 1.0f;

    //find error
        findStateError(ctrlStateError,ctrlState,ctrlStateTarget);
    //call controllers (no attitude control)
        ctrlPositionPDgains(KPpositionPD, KDpositionPD, KPpositionPD,
            KDpositionPD, KPpositionPD, KDpositionPD, ctrlStateError,
            ctrlControl);
    //Set firing times, schedule firing
        ctrlMixWLoc(&firing_times, ctrlControl, ctrlState, min_pulse, 20.0f,
            FORCE_FRAME_INERTIAL);//Changed from 40.0f to 20.0f
        propSetThrusterTimes(&firing_times);
}

//*********************************Termination Conditions
    *********************************
//Determine length of this maneuver
switch(test_number){
    case 1://  Test 1: SPH2 (Target) moves toward INSP, then moves in Z-
        direction
        MAN4_TIME_LIMIT = 240000.0f;
    break;
    case 2://  Test 2: SPH1 (Inspector) moves in 3-D path
        MAN4_TIME_LIMIT = 300000.0f;
    break;
    case 3://  Test 3: SPH1 performs 10-min inspection
        MAN4_TIME_LIMIT = 600000.0f;
    break;
    default://  Test 4: SPH1 inspects using SPH2 rotation information
        MAN4_TIME_LIMIT = 360000.0f;
    break;
}

if (sysIdentityGet() == SPHERE1)
    padsGlobalPeriodSetAndWait(200,205);
if (MAN4_TIME_LIMIT <= (float)maneuver_time)
    ctrlTestTerminate(TEST_RESULT_NORMAL);
break;
```

```
        default:
            ctrlTestTerminate(TEST_RESULT_ERROR);
        break;
    }

    //%%%%%%%%%%%%%%%%%% DEBUG %%%%%%%%%%%%%%%%%%

        DebugVecFloat[0] = ctrlState[POS_X];
        DebugVecFloat[1] = ctrlState[POS_Y];
        DebugVecFloat[2] = ctrlState[POS_Z];
        DebugVecFloat[3] = ctrlState[VEL_X];
        DebugVecFloat[4] = ctrlState[VEL_Y];
        DebugVecFloat[5] = ctrlState[VEL_Z];
        DebugVecFloat[6] = (float)test_time/1000;
        DebugVecFloat[7] = (float)maneuver_time/1000;
        commSendPacket(COMM_CHANNEL_STL, GROUND, 0, COMM_CMD_DBG_FLOAT, (unsigned char *)
            DebugVecFloat, 0);

        DebugVecShort[0] = (short) maneuver_number;
        DebugVecShort[1] = (short) (ctrlStateError[POS_X]*10000);
        DebugVecShort[2] = (short) (ctrlStateError[POS_Y]*10000);
        DebugVecShort[3] = (short) (ctrlStateError[POS_Z]*10000);
        DebugVecShort[4] = (short) (ctrlStateError[RATE_X]*10000);
        DebugVecShort[5] = (short) (ctrlStateError[RATE_Y]*10000);
        DebugVecShort[6] = (short) (ctrlStateError[RATE_Z]*10000);
        commSendPacket(COMM_CHANNEL_STL,GROUND,0, COMM_CMD_DBG_SHORT_SIGNED, (unsigned
            char *) DebugVecShort, 0);

}

void changetoBodyFrame(state_vector TargetState, state_vector InspectorState, float *
    vectorOut, unsigned int vectorType)
{
    /*  TargetState and InspectorState begins in global frame
    *   ...convert to body frame:
    *  POS are in global
    *  VEL are in global
    *  QUAT are from global frame to body frame
    *  RATE are in body
    * We will use the quaternions to take the postion and velocity vectors
    * from the global frame to the body frame
    */
    float R_temp[3];
    float RBody[3];
    float cross[3];
    float V_temp[3];
    float mat[3][3];

    switch (vectorType){
    case POSITION_VECTOR:
        //Make measurements relative:
        //Moves about point at center of volume (0,0,0)
        R_temp[0] = TargetState[POS_X] - InspectorState[POS_X];
        R_temp[1] = TargetState[POS_Y] - InspectorState[POS_Y];
        R_temp[2] = TargetState[POS_Z] - InspectorState[POS_Z];
        //Move to INSP Body Frame
        quat2matrixIn(mat, &InspectorState[QUAT_1]);//MAT <= rotation matrix from global
            to INSP body
        mathMatVecMult(RBody, (float**)mat, R_temp, 3, 3);
        vectorOut[0] = RBody[0];//POS_X
        vectorOut[1] = RBody[1];//POS_Y
        vectorOut[2] = RBody[2];//POS_Z
        break;
    case VELOCITY_VECTOR:
        //V = Rot*(r') - wx(Rot(r)))
        InspectorState[VEL_X]  = TargetState[VEL_X] - InspectorState[VEL_X];
        InspectorState[VEL_Y]  = TargetState[VEL_Y] - InspectorState[VEL_Y];
        InspectorState[VEL_Z]  = TargetState[VEL_Z] - InspectorState[VEL_Z];
```

```
        mathMatVecMult(V_temp, (float**)mat, &InspectorState[VEL_X], 3, 3);
        mathVecCross(cross, &InspectorState[RATE_X], &InspectorState[POS_X]);
        vectorOut[0] = V_temp[0] - cross[0];//VEL_X
        vectorOut[1] = V_temp[1] - cross[1];//VEL_Y
        vectorOut[2] = V_temp[2] - cross[2];//VEL_Z
        break;
    case ACCEL_VECTOR:
        vectorOut[0] = 0.0f;
        vectorOut[1] = 0.0f;
        vectorOut[2] = 0.0f;
        break;
    case ROTATION_VECTOR:
        //Move TGT Rot in TGT Body to INSP Body
        R_temp[0] = TargetState[RATE_X];//Get TGT Rotation Rates in TGT Body Frame
        R_temp[1] = TargetState[RATE_Y];
        R_temp[2] = TargetState[RATE_Z];
        quat2matrixOut(mat, &TargetState[QUAT_1]);//MAT <= rotation matrix from TGT Body
            to Global
        mathMatVecMult(RBody, (float**)mat, R_temp, 3, 3); //TGT Body to Global
        R_temp[0] = RBody[0];
        R_temp[1] = RBody[1];
        R_temp[2] = RBody[2];
        memset(RBody,0,sizeof(float)*3);
        quat2matrixIn(mat, &InspectorState[QUAT_1]);//MAT <= rotation matrix from global
            to INSP body
        mathMatVecMult(RBody, (float**)mat, R_temp, 3, 3); //Global to INSP Body
        //vectorOut = ROT_RATE_DIR[0-2]
        vectorOut[0] = RBody[0];//X
        vectorOut[1] = RBody[1];//Y
        vectorOut[2] = RBody[2];//Z
        //Find Magnitude
        //ROT_RATE_TGT
        vectorOut[3] = (float)sqrt(vectorOut[0]*vectorOut[0] + vectorOut[1]*vectorOut[1] +
            vectorOut[2]*vectorOut[2]);
        break;
    default:
        ctrlTestTerminate(13);//ERROR: Incorrect call to changetoBodyFrame
        break;
    }
}
```

## A.3 Example Code using Video Data

```
/* Modified from:
 * gsp.c
 *
 * SPHERES Guest Scientist Program custom source code template.
 *
 * MIT Space Systems Laboratory
 * SPHERES Guest Scientist Program
 * http://ssl.mit.edu/spheres/
 *
 * Copyright 2005 Massachusetts Institute of Technology
 *
 * VERTIGO 2Sat Paths Experiment
 *  Last Update: 09 April 2012 by Michael O'Connor:
 *  -Integration of Serial Comm & real video information into code
 *  Update: 09 Mar 2012 by Michael O'Connor:
 *  -Addition of "Closest Point" algorithm
 *  -Includes Changing of algorithm from rotating and controlling translation to
    translating
 *  and controlling rotation
 *  Update: 27 Feb 2012 by Michael O'Connor
 *
 *  *** SPH 1: INSPECTOR (INSP) ***
 *  *** SPH 2: TARGET    (TGT)  ***
 *
 *  ***Test Descriptions:***
 *
 *  Test 201: SPH2 (Target) moves toward INSP, then moves in Z-direction
 *  Test 202: SPH1 (Inspector) moves in 3-D path
 *  Test 203: SPH1 performs 10-min inspection
 *  Test 204: SPH1 inspects using SPH2 rotation information
 *
 * Longer descriptions available in previous versions of code (pre-09 April updates).
 *
 *  ***NOTE:***
 *  It is possible to change the rotation rate, the "center" of the test volume and the
 *  radius of the inspection circle by changing the values in the:
 *      "Change Rates, Center Points, etc here" section
 */


/*------------------------------------------------------------------------------*/
/*                          Do not modify this section.                         */
/*------------------------------------------------------------------------------*/

#include "comm.h"
#include "commands.h"
#include "control.h"
#include "gsp.h"
#include "gsp_task.h"
#include "pads.h"
#include "prop.h"
#include "spheres_constants.h"
#include "spheres_physical_parameters.h"
#include "spheres_types.h"
#include "std_includes.h"
#include "system.h"
#include "util_memory.h"
#include "exp_v2.h"

/*------------------------------------------------------------------------------*/
/*                       Modify as desired below this point.                    */
/*------------------------------------------------------------------------------*/
#include "ctrl_attitude.h"
#include "ctrl_position.h"
#include "find_state_error.h"
```

```
#include "housekeeping_internal.h"
#include "housekeeping.h"
#include "ctrl_mix.h"
#include "math_matrix.h"
#include "smt335async.h"
#include "comm_internal.h"
#include "gsutil_thr_times.h"
#include "gspVERTIGO_2SatPaths.h"
#include <math.h>
#include <string.h>

//***********BEGINNING OF COMM DEFINITIONS***********
//# = Sphere Comm...A = Test Start/Stop...B = Watchdog...
//C = Terminate...D = FORCE/TORQUE...E = Target Info...
//F = Misc
#define START_BYTE          0xA7
#define FROM_SPHERES        0x01
#define FROM_GOGGLES        0x02
#define WATCHDOG_REQUEST    0xB1
#define WATCHDOG_REPLY      0xB2
#define TERMINATE_TEST      0xC1
#define SYNC_TEST           0x91
#define START_TEST          0xA3
#define FORCES_TORQUES      0xD1
#define TGT_POSITION        0xE1
#define WATCHDOG_LIMIT      3
#define ANY_GOGGLES         0x40
#define SPHERE_ID_REQUEST   0xA2
#define max_length          255

int watchdog_flag;
float forces[3];
float torques[3];
float position[3];
float velocity[3];
unsigned char packet_buffer[max_length];
int packet_buffer_length = 0;
int initTest = 0;
int GogglesAttached = 0;
//***********END OF COMM DEFINITIONS***********
//***********BEGINNING OF MANEUVER DEFINITIONS***********
float throughAngle;
float maneuverCounter;
int rotFlag;
//***********END OF MANEUVER DEFINITIONS***********
//***********BEGINNING OF COMM STRUCT DEFINITIONS***********
typedef struct {
    unsigned char return_code;
} msg_terminate_test;

typedef struct {
    unsigned char to;
    unsigned char from;
    unsigned char ID;
    unsigned char test_number;
} msg_start_test;

typedef struct {
    float forces[3];
    float torques[3];
} msg_body_forces_torques;

typedef struct {
    float xyzPos[3];
    float xyzVel[3];
} msg_body_tgt_location;

typedef struct {
```

```
    unsigned char to;
    unsigned char from;
    unsigned char ID;
    unsigned char spheresLogicID;
    unsigned int programID;
} msg_spheres_id;

typedef struct {
    unsigned char startByte;
    unsigned char length;
    unsigned char from;
    unsigned char ID;
} msg_header;
//***********END OF COMM STRUCT DEFINITIONS**********


void gspVERTIGO_2SatPaths_InitTest(unsigned int test_number)
{
    extern state_vector initState;
    //***********BEGINNING OF COMM DEFINITIONS**********
    msg_start_test msgStart;
    msgStart.to = ANY_GOGGLES;
    msgStart.from = commHWAddrGet();
    msgStart.ID = START_TEST;
    msgStart.test_number = (unsigned char) test_number;
    expv2_uart_send(SERIALPORT_DAEMON,sizeof(msgStart),(unsigned char*) &msgStart);

    initTest = 1;


    memset(forces,0,sizeof(float)*3);
    memset(torques,0,sizeof(float)*3);
    watchdog_flag = 0;
    //***********END OF COMM DECLARATIONS**********
    memset(&initState, 0, sizeof(initState));

    if (SPHERE_ID == SPHERE1) //INSP
    {
        initState[POS_X] = 0.0f;
        initState[POS_Y] = 0.4f;
        initState[POS_Z] = 0.0f;
    }

    if (SPHERE_ID == SPHERE2) //TGT
    {
        initState[POS_X] = 0.0f;
        initState[POS_Y] = -0.4f;
        initState[POS_Z] = 0.0f;
    }

    initState[QUAT_1] = 1.0f;//GROUND & ISS (Tank Down/DECK)

    if (sysIdentityGet() == SPHERE1)//                    205?Haven't changed
        padsEstimatorInitWaitAndSet(initState, 50, 200, 105, PADS_INIT_THRUST_INT_ENABLE,
            PADS_BEACONS_SET_1TO9); // ISS
    else
        padsEstimatorInitWaitAndSet(initState, 50, SYS_FOREVER, SYS_FOREVER,
            PADS_INIT_THRUST_INT_ENABLE,PADS_BEACONS_SET_1TO9); // ISS

    ctrlPeriodSet(1000);
    throughAngle = 0.0f;
    maneuverCounter = 0.0f;
}


void gspVERTIGO_2SatPaths_Control(unsigned int test_number, unsigned int test_time,
    unsigned int maneuver_number, unsigned int maneuver_time)
{
```

```
extern const float KPattitudePD, KDattitudePD, KPpositionPD, KDpositionPD,
    VEHICLE_MASS;
//dbg_short_packet DebugVecShort;
//dbg_float_packet DebugVecFloat;
state_vector ctrlState;//Actual State
state_vector ctrlStateTarget;//Desired State
state_vector ctrlStateError;
state_vector ctrlStateTGT;//Inspection Target (SPH2) Control State
float ctrlControl[6];
float RATE;
float ROT_RATE_DIR[4];
float vecOut[4];
float TGT_RATE;
dbg_float_packet DebugVecFloat;
dbg_short_packet DebugVecShort;
dbg_ushort_packet DebugVecUShort;
prop_time firing_times;
//*********************************Change Rates, Center Points, etc here
    :*********************************
float CENTER_X = 0.0f;
float CENTER_Y = 0.0f;
float CENTER_Z = 0.0f;
float ROT_RATE = 0.0262f; //(3 deg/s == 0.0524, 2.5 deg/s == 0.0436, 2 deg/s ==
    0.0349,  1.5 deg/s == 0.0262)
float ROT_RATE_TGT = -0.1047f; //0.1047 == 6 deg/s;
float ROT_RADIUS = 0.70f;
float L1 = 0.25f; //Size of L-shaped movement
float L2 = 0.20f;
    //
        ***************************************************************************************************

const int min_pulse = 10;
float MAN4_TIME_LIMIT = 150000.0f;
//***********MESSAGE TYPE DECLARATIONS***********
msg_header msgTP;
msg_header msg;
msgTP.startByte = START_BYTE;
msgTP.from = FROM_SPHERES;
msgTP.length = 0;
msgTP.ID = WATCHDOG_REQUEST;
//***********END MESSAGE TYPE DECLARATIONS***********


memset(DebugVecFloat, 0, sizeof(DebugVecFloat));
memset(DebugVecShort, 0, sizeof(DebugVecShort));
memset(DebugVecUShort, 0, sizeof(DebugVecUShort));

//Account for movement of target during this test - try to remain in volume
if (test_number <= 1)
{
    CENTER_Y = -1.0f*L1;
    CENTER_Z = L2;
}

//Clear all uninitialized vectors
memset(ctrlControl,0,sizeof(float)*6);
memset(ctrlStateTarget,0,sizeof(state_vector));
memset(ctrlStateError,0,sizeof(state_vector));
memset(ctrlStateTGT,0,sizeof(state_vector));
//memset(DebugVecShort, 0, sizeof(dbg_short_packet));
//memset(DebugVecFloat, 0, sizeof(dbg_float_packet));

padsStateGet(ctrlState);
//commBackgroundStateGet(SPHERE2, &test_time, (state_vector *)ctrlStateTGT);
ctrlStateTGT[QUAT_1] = 1;
ctrlStateTGT[RATE_Z] = ROT_RATE_TGT;
```

```
//Check to see if WD flag was set (to 0); if it = 1, end test
if (watchdog_flag >= WATCHDOG_LIMIT)
{
    initTest = 0;
    ctrlTestTerminate(RESULT_PAYLOAD_ERROR);
}
else if ((test_time % 5000) < 1000)
{
    watchdog_flag++;
}


switch(maneuver_number){
    case 1: //*********************************Maneuver 1: Estimator initialization
        *********************************
        //Termination after 10s
        if (maneuver_time >= 10000){
            ctrlManeuverTerminate();
        }
        else if ((maneuver_time >= 5000) && (maneuver_time <= 7000))//initialize
            Goggles
        {
            //(initTest <= 2)
            msg.startByte = START_BYTE;
            msg.from = FROM_SPHERES;
            msg.length = 0;
            msg.ID = SYNC_TEST;
            expv2_uart_send(SERIALPORT_TESTPROG,sizeof(msg),(unsigned char*) &msg);

            initTest++;
        }
        //Check watchdog
        if ((test_time % 5000) < 1000)
        {
            expv2_uart_send(SERIALPORT_TESTPROG,sizeof(msgTP),(unsigned char*) &msgTP)
                ;
        }
        break;
    case 2: //*********************************Maneuver 2: Move to initial position
        *********************************
        //Termination after 30s
        if (sysIdentityGet()==SPHERE1)
            padsGlobalPeriodSet(SYS_FOREVER);
        switch(sysIdentityGet()){
            case SPHERE1://INSP
                ctrlStateTarget[POS_X] = CENTER_X - ROT_RADIUS;
                ctrlStateTarget[POS_Y] = CENTER_Y;
                ctrlStateTarget[POS_Z] = CENTER_Z;
            break;
            case SPHERE2://TGT
                ctrlStateTarget[POS_X] = CENTER_X;
                ctrlStateTarget[POS_Y] = CENTER_Y;
                ctrlStateTarget[POS_Z] = CENTER_Z;
            break;
        }

        //Rotate Inspector Satellite to show Initial Positioning has begun and to
            distinguish INSP from TGT

        ctrlStateTarget[QUAT_1] = 1.0f;

        //find error
        findStateError(ctrlStateError,ctrlState,ctrlStateTarget);

        //call controllers
        ctrlPositionPDgains(KPpositionPD, KDpositionPD, KPpositionPD, KDpositionPD,
            KPpositionPD, KDpositionPD, ctrlStateError, ctrlControl);
```

```
        ctrlAttitudeNLPDwie(KPattitudePD,KDattitudePD,KPattitudePD,KDattitudePD,
            KPattitudePD,KDattitudePD,ctrlStateError,ctrlControl);
        if ((test_number == 5) && (sysIdentityGet() == SPHERE1))
        {
            ctrlControl[FORCE_X] = forces[0];
            ctrlControl[FORCE_Y] = forces[1];
            ctrlControl[FORCE_Z] = forces[2];
            ctrlControl[TORQUE_X] = torques[0];
            ctrlControl[TORQUE_Y] = torques[1];
            ctrlControl[TORQUE_Z] = torques[2];
            ctrlMixWLoc(&firing_times, ctrlControl, ctrlState, min_pulse, 20.0f,
                FORCE_FRAME_BODY);
        }
        else
        {
        //mix forces/torques into thruster commands
        //FORCE_FRAME_BODY
        ctrlMixWLoc(&firing_times, ctrlControl, ctrlState, min_pulse, 20.0f,
            FORCE_FRAME_INERTIAL);
        }
        //Set firing times
        propSetThrusterTimes(&firing_times);
        memset(forces,0,3*sizeof(float));
        memset(torques,0,3*sizeof(float));
        //Check watchdog
        if ((test_time % 5000) < 1000)
        {
            expv2_uart_send(SERIALPORT_TESTPROG,sizeof(msgTP),(unsigned char*) &msgTP)
                ;
        }
        if (sysIdentityGet() == SPHERE1)
            padsGlobalPeriodSetAndWait(200,205);
        if (maneuver_time>=30000)
            ctrlManeuverTerminate();
        break;
    case 3://*********************************Maneuver 3: Rotate Center SPHERE(#2/TGT
        ) if desired*********************************
        //Termination after 05s
        switch(sysIdentityGet()){
            case SPHERE1://INSP
                ctrlStateTarget[POS_X] = CENTER_X - ROT_RADIUS;
                ctrlStateTarget[POS_Y] = CENTER_Y;
                ctrlStateTarget[POS_Z] = CENTER_Z;
            break;
            case SPHERE2://TGT
                ctrlStateTarget[RATE_Z] = ROT_RATE_TGT;//Spin
                ctrlStateTarget[RATE_Y] = ROT_RATE_TGT;//Tumble
                if (test_number == 4)
                {
                    //ctrlStateTarget[RATE_Y] = ctrlStateTarget[RATE_Y]/(4.0f);
                    ctrlStateTarget[RATE_Z] = ctrlStateTarget[RATE_Z]/(4.0f);// 0.0f;
                }
                ctrlStateTarget[POS_X] = CENTER_X;
                ctrlStateTarget[POS_Y] = CENTER_Y;
                ctrlStateTarget[POS_Z] = CENTER_Z;
            break;
        }

        ctrlStateTarget[QUAT_1] = 1.0f;

        //Estimate, Calculate Control, and Fire Thrusters
                findStateError(ctrlStateError,ctrlState,ctrlStateTarget);
                ctrlPositionPDgains(KPpositionPD, KDpositionPD, KPpositionPD,
                    KDpositionPD, KPpositionPD, KDpositionPD, ctrlStateError,
                    ctrlControl);
                if (sysIdentityGet() == SPHERE1)
                    ctrlAttitudeNLPDwie(KPattitudePD,KDattitudePD,KPattitudePD,
                        KDattitudePD,KPattitudePD,KDattitudePD,ctrlStateError,
```

```
                    ctrlControl);
            else
                ctrlAttitudeNLPDwie(0,KDattitudePD,0,KDattitudePD,0,KDattitudePD,
                    ctrlStateError,ctrlControl);//Use this to ignore quaternion
                    error from global met

            if (test_number == 5)
            {
                ctrlControl[FORCE_X] = forces[0];
                ctrlControl[FORCE_Y] = forces[1];
                ctrlControl[FORCE_Z] = forces[2];
                ctrlControl[TORQUE_X] = torques[0];
                ctrlControl[TORQUE_Y] = torques[1];
                ctrlControl[TORQUE_Z] = torques[2];
                ctrlMixWLoc(&firing_times, ctrlControl, ctrlState, min_pulse, 20.0
                    f, FORCE_FRAME_BODY);
            }
            else
            {
                ctrlMixWLoc(&firing_times, ctrlControl, ctrlState, min_pulse, 20.0
                    f, FORCE_FRAME_INERTIAL);//Changed from 40.0f to 20.0f
            }
            propSetThrusterTimes(&firing_times);
            memset(forces,0,3*sizeof(float));
            memset(torques,0,3*sizeof(float));
        //Check watchdog
        if ((test_time % 5000) < 1000)
        {
            expv2_uart_send(SERIALPORT_TESTPROG,sizeof(msgTP),(unsigned char*) &msgTP)
                ;
        }
        if (sysIdentityGet() == SPHERE1)
            padsGlobalPeriodSetAndWait(200,205);
        //if (sysIdentityGet() == SPHERE2)
        //  padsGlobalPeriodSetAndWait(200,205);
        if (maneuver_time>=5000)
            ctrlManeuverTerminate();
        break;

    case 4: //**********************************Maneuver 4: Begin Inspector Rotation
        and Inspection Maneuver**********************************
        //**********************************SPHERE 1: INSPECTOR
            **********************************
        if (sysIdentityGet() == SPHERE1)
        {
            padsGlobalPeriodSet(SYS_FOREVER);

            if (GogglesAttached == 0)
            {
            //**********************************Gather Simulated Vision Data
                **********************************
            changetoBodyFrame(&ctrlStateTGT[POS_X], &ctrlState[POS_X], vecOut,
                POSITION_VECTOR);
            ctrlState[POS_X] = vecOut[0];
            ctrlState[POS_Y] = vecOut[1];
            ctrlState[POS_Z] = vecOut[2];
            changetoBodyFrame(&ctrlStateTGT[POS_X], &ctrlState[POS_X], vecOut,
                VELOCITY_VECTOR);
            ctrlState[VEL_X] = vecOut[0];
            ctrlState[VEL_Y] = vecOut[1];
            ctrlState[VEL_Z] = vecOut[2];
            changetoBodyFrame(&ctrlStateTGT[POS_X], &ctrlState[POS_X], vecOut,
                ROTATION_VECTOR);
            ROT_RATE_DIR[0] = vecOut[0];
            ROT_RATE_DIR[1] = vecOut[1];
            ROT_RATE_DIR[2] = vecOut[2];
            ROT_RATE_TGT = vecOut[3];
```

```
//*********************************End Gathering Simulated Vision Data
    *********************************
}
else
{
//*********************************Gather Actual Vision Data
    *********************************
ctrlState[POS_X] = position[POS_Z] + 0.234;//Move from camera frame to SPH
     body frame
ctrlState[POS_Y] = -position[POS_X] + 0.045;
ctrlState[POS_Z] = -position[POS_Y] + 0.030;
ctrlState[VEL_X] = velocity[2];
ctrlState[VEL_Y] = velocity[0];
ctrlState[VEL_Z] = velocity[1];
changetoBodyFrame(&ctrlStateTGT[POS_X], &ctrlState[POS_X], vecOut,
    ROTATION_VECTOR);
ROT_RATE_DIR[0] = vecOut[0];
ROT_RATE_DIR[1] = vecOut[1];
ROT_RATE_DIR[2] = vecOut[2];
ROT_RATE_TGT = vecOut[3];
//*********************************End Gathering Actual Vision Data
    *********************************
}

//Inspection Motion/Path Parameters
switch(test_number){
case 2://Test 2: SPH1 (Inspector) moves in 3-D path
    ctrlStateTarget[POS_X] = ROT_RADIUS;
    // Use an integrator to estimate the points at which the rotations
        should change from Z to Y and back to Z
    if ((throughAngle >= 2*PI) || (throughAngle <= -2*PI))
    {
        ctrlStateTarget[RATE_Z] = ROT_RATE;
        throughAngle = throughAngle + (ctrlState[RATE_Z]*((float)
            maneuver_time - maneuverCounter)/1000.0f);
    }
    else if((throughAngle >= PI/2) || (throughAngle <= -PI/2))
    {
        ctrlStateTarget[RATE_Y] = ROT_RATE;
        throughAngle = throughAngle + (ctrlState[RATE_Y]*((float)
            maneuver_time - maneuverCounter)/1000.0f);
    }
    else
    {
        ctrlStateTarget[RATE_Z] = ROT_RATE;
        throughAngle = throughAngle + (ctrlState[RATE_Z]*((float)
            maneuver_time - maneuverCounter)/1000.0f);
    }
    maneuverCounter = (float)maneuver_time;
break;
case 4://Test 4: SPH1 inspects using SPH2 rotation information
    ctrlStateTarget[POS_X] = ROT_RADIUS;
    //Time/Coverage-based movement procedures:
    if (rotFlag == 0) //Align so TGT spin axis is roughly in INSP's Z-Body
         Direction
        {
            if (ROT_RATE_DIR[0] >= .01f) //Align if errors in X
                ctrlStateTarget[RATE_Y] = ROT_RATE;
            else if (ROT_RATE_DIR[0] <= -.01f)
                ctrlStateTarget[RATE_Y] = -ROT_RATE;
            else
                rotFlag = 1;

            if (ROT_RATE_DIR[1] >= .01) //Align if errors in Y
                ctrlStateTarget[RATE_X] = ROT_RATE;
            else if (ROT_RATE_DIR[1] <= -.01f)
                ctrlStateTarget[RATE_X] = -ROT_RATE;
            else
```

```
            rotFlag = rotFlag + 1;

        if (rotFlag != 2) //If TGT rotation is aligned with Z axis of
            INSP, proceed
            rotFlag = 0;
    }
else if (rotFlag == 2) //Begin inspection motion moving to "Northern
    Hemisphere"
    {
        ctrlStateTarget[RATE_Z] = 0.0f;
        ctrlStateTarget[RATE_Y] = ROT_RATE; //For Moving to "North
            Pole" of TGT
        ctrlStateTarget[RATE_X] = 0.0f;
        throughAngle = throughAngle + (((float)fabs(ctrlState[RATE_Y])
            )*((float)maneuver_time - maneuverCounter)/1000);
        if(throughAngle >= PI/4)
        {
            rotFlag++;
            throughAngle = 0.0f;
        }
    }
else if (rotFlag == 3) //Hold in "Northern Hemisphere" until entire
    hemisphere has been seen.
    {
        ctrlStateTarget[RATE_Z] = ROT_RATE; //For Coverage
        ctrlStateTarget[RATE_X] = -ROT_RATE; //Maintaining Pointing
        ctrlStateTarget[RATE_Y] = 0.0f;
        TGT_RATE = sqrtf(ctrlStateTGT[RATE_X]*ctrlStateTGT[RATE_X] +
            ctrlStateTGT[RATE_Y]*ctrlStateTGT[RATE_Y] + ctrlStateTGT[
            RATE_Z]*ctrlStateTGT[RATE_Z]);
        throughAngle = throughAngle + ((((float)fabs(ctrlState[RATE_Z
            ])) + ((float)fabs(TGT_RATE)))*((float)maneuver_time -
            maneuverCounter)/1000);
        if (throughAngle >= 2*PI)
        {
            rotFlag++;
            throughAngle = 0.0f;
        }
    }
else if (rotFlag == 4) //Move to "Southern Hemisphere"
    {
        ctrlStateTarget[RATE_Z] = 0.0f;
        ctrlStateTarget[RATE_Y] = -ROT_RATE; //For Moving to "South
            Pole" of TGT
        ctrlStateTarget[RATE_X] = 0.0f;
        throughAngle = throughAngle + (((float)fabs(ctrlState[RATE_Y])
            )*((float)maneuver_time - maneuverCounter)/1000);
        if(throughAngle >= PI/2)
        {
            rotFlag++;
            throughAngle = 0.0f;
        }
    }
else if (rotFlag == 5) //Hold in "Southern Hemisphere" until entire
    hemisphere has been seen.
    {
        ctrlStateTarget[RATE_Z] = ROT_RATE; //For Coverage
        ctrlStateTarget[RATE_X] = ROT_RATE; //Maintaining Pointing
        ctrlStateTarget[RATE_Y] = 0.0f;
        TGT_RATE = sqrtf(ctrlStateTGT[RATE_X]*ctrlStateTGT[RATE_X] +
            ctrlStateTGT[RATE_Y]*ctrlStateTGT[RATE_Y] + ctrlStateTGT[
            RATE_Z]*ctrlStateTGT[RATE_Z]);
        throughAngle = throughAngle + ((((float)fabs(ctrlState[RATE_Z
            ])) + ((float)fabs(TGT_RATE)))*((float)maneuver_time -
            maneuverCounter)/1000);
        if (throughAngle >= 2*PI)
        {
            rotFlag++;
```

```
                throughAngle = 0.0f;
            }
        }
    else if (rotFlag == 6) //Begin inspection motion moving to "Equator"
        {
            ctrlStateTarget[RATE_Z] = 0.0f;
            ctrlStateTarget[RATE_Y] = ROT_RATE; //For Moving to "Equator"
                of TGT
            ctrlStateTarget[RATE_X] = 0.0f;
            throughAngle = throughAngle + (((float)fabs(ctrlState[RATE_Y])
                )*((float)maneuver_time - maneuverCounter)/1000);
            if(throughAngle >= PI/4)
            {
                rotFlag++;
                throughAngle = 0.0f;
            }
        }
    else //Hold at equator until full orbit is complete.
        {
            ctrlStateTarget[RATE_Z] = ROT_RATE; //For Coverage
            ctrlStateTarget[RATE_Y] = 0.0f;
            ctrlStateTarget[RATE_X] = 0.0f;
            TGT_RATE = sqrtf(ctrlStateTGT[RATE_X]*ctrlStateTGT[RATE_X] +
                ctrlStateTGT[RATE_Y]*ctrlStateTGT[RATE_Y] + ctrlStateTGT[
                RATE_Z]*ctrlStateTGT[RATE_Z]);
            throughAngle = throughAngle + ((((float)fabs(ctrlState[RATE_Z
                ])) + ((float)fabs(ctrlState[RATE_X]))+ ((float)fabs(
                TGT_RATE)))*((float)maneuver_time - maneuverCounter)/1000)
                ;
            if ((throughAngle >= 2*PI))
            {
                ctrlStateTarget[RATE_Z] = 0.0f;
                ctrlStateTarget[RATE_Y] = 0.0f;
                ctrlStateTarget[POS_X] = ROT_RADIUS;
                ctrlStateTarget[RATE_X] = 3*ROT_RATE;
            }
        }
    maneuverCounter = (float)maneuver_time;
    break;
default://  Test 1: SPH2 (Target) moves toward INSP, then moves in Z-
    direction & Test 3: SPH1 performs 10-min inspection
    ctrlStateTarget[POS_X] = ROT_RADIUS;
    ctrlStateTarget[RATE_Z] = ROT_RATE;
break;
}

//May need to reverse of other maneuvers because of global to body frame
    transformation, though QUAT is uncontrolled-for
ctrlStateTarget[QUAT_1] = 1.0f;

//find error
    findStateError(ctrlStateError,ctrlState,ctrlStateTarget);
//call controllers
    ctrlPositionPDgains(KPpositionPD, KDpositionPD, KPpositionPD,
        KDpositionPD, KPpositionPD, KDpositionPD, ctrlStateError,
        ctrlControl);
    ctrlAttitudeNLPDwie(0,KDattitudePD,0,KDattitudePD,0,KDattitudePD,
        ctrlStateError,ctrlControl);//Use this to ignore quaternion error
        from global met
//Adjust for frame change
    ctrlControl[0] *= -1;
    ctrlControl[1] *= -1;
    ctrlControl[2] *= -1;
//Feedforward Term
    RATE = (ctrlStateTarget[RATE_X]*ctrlStateTarget[RATE_X] +
        ctrlStateTarget[RATE_Y]*ctrlStateTarget[RATE_Y] + ctrlStateTarget[
        RATE_Z]*ctrlStateTarget[RATE_Z]);
    if (rotFlag <= 6)
```

```
            ctrlControl[0] += (VEHICLE_MASS*ctrlStateTarget[POS_X]*RATE);//
                RATE actually RATE^2: changed to eliminate redundant math
                steps
        if (test_number == 5)
        {
            ctrlControl[FORCE_X] = forces[0];
            ctrlControl[FORCE_Y] = forces[1];
            ctrlControl[FORCE_Z] = forces[2];
            ctrlControl[TORQUE_X] = torques[0];
            ctrlControl[TORQUE_Y] = torques[1];
            ctrlControl[TORQUE_Z] = torques[2];
            ctrlMixWLoc(&firing_times, ctrlControl, ctrlState, min_pulse, 20.0
                f, FORCE_FRAME_BODY);
        }
        else
        {
        //Set firing times, schedule firing
        ctrlMixWLoc(&firing_times, ctrlControl, ctrlState, min_pulse, 20.0f,
            FORCE_FRAME_BODY);
        }
        propSetThrusterTimes(&firing_times);
        memset(forces,0,3*sizeof(float));
        memset(torques,0,3*sizeof(float));
}
//*****************************************************************SPHERE 2:
    TARGET
    ********************************************************************
//If SPH_2 is to follow some path or movement, insert it here:
if (sysIdentityGet() == SPHERE2)
{
    switch(test_number){
    case 1://  Test 1: SPH2 (Target) moves toward INSP, then moves in Z-
        direction
        if (maneuver_time > 120000)
            ctrlStateTarget[POS_Z] = CENTER_Z - L2;
        else
            ctrlStateTarget[POS_Z] = CENTER_Z;
        if (maneuver_time > 60000)
            ctrlStateTarget[POS_Y] = CENTER_Y + L1;
        else
            ctrlStateTarget[POS_Y] = CENTER_Y;
    break;
    case 2:
        if (maneuver_time >= 180000.0f) {
            ctrlStateTarget[POS_Z] = CENTER_Z - L1;
        }
        else if (maneuver_time >= 60000.0f) {
            ctrlStateTarget[POS_Z] = CENTER_Z + L1;
        }
        else
        {
            ctrlStateTarget[POS_X] = CENTER_X;
            ctrlStateTarget[POS_Y] = CENTER_Y;
            ctrlStateTarget[POS_Z] = CENTER_Z;
        }
    break;
    default://  Test 2: SPH1 (Inspector) moves in 3-D path, Test 3: SPH1
        performs 10-min inspection, & Test 4: SPH1 inspects using SPH2
        rotation information
        ctrlStateTarget[POS_X] = CENTER_X;
        ctrlStateTarget[POS_Y] = CENTER_Y;
        ctrlStateTarget[POS_Z] = CENTER_Z;
    break;
    }
    ctrlStateTarget[QUAT_1] = 1.0f;

    //find error
        findStateError(ctrlStateError,ctrlState,ctrlStateTarget);
```

```
            //call controllers (no attitude control)
                ctrlPositionPDgains(KPpositionPD, KDpositionPD, KPpositionPD,
                    KDpositionPD, KPpositionPD, KDpositionPD, ctrlStateError,
                    ctrlControl);
            //Set firing times, schedule firing
                if (test_number == 5)
                {
                    ctrlControl[FORCE_X] = forces[0];
                    ctrlControl[FORCE_Y] = forces[1];
                    ctrlControl[FORCE_Z] = forces[2];
                    ctrlControl[TORQUE_X] = torques[0];
                    ctrlControl[TORQUE_Y] = torques[1];
                    ctrlControl[TORQUE_Z] = torques[2];
                    ctrlMixWLoc(&firing_times, ctrlControl, ctrlState, min_pulse, 20.0
                        f, FORCE_FRAME_BODY);
                }
                else
                {
                    ctrlMixWLoc(&firing_times, ctrlControl, ctrlState, min_pulse, 20.0
                        f, FORCE_FRAME_INERTIAL);//Changed from 40.0f to 20.0f
                }
                propSetThrusterTimes(&firing_times);
        }

        //*********************************Termination Conditions
            *********************************
        //Determine length of this maneuver
        switch(test_number){
            case 1://  Test 1: SPH2 (Target) moves toward INSP, then moves in Z-
                direction
                MAN4_TIME_LIMIT = 240000.0f;
            break;
            case 2://  Test 2: SPH1 (Inspector) moves in 3-D path
                MAN4_TIME_LIMIT = 300000.0f;
            break;
            case 3://  Test 3: SPH1 performs 10-min inspection
                MAN4_TIME_LIMIT = 600000.0f;
            break;
            default://  Test 4: SPH1 inspects using SPH2 rotation information
                MAN4_TIME_LIMIT = 360000.0f;
            break;
        }

        if (sysIdentityGet() == SPHERE1)
            padsGlobalPeriodSetAndWait(200,205);
        if (MAN4_TIME_LIMIT <= (float)maneuver_time)
        {
            initTest = 0;
            ctrlTestTerminate(TEST_RESULT_NORMAL);
        }
        break;
    default:
        initTest = 0;
        ctrlTestTerminate(TEST_RESULT_ERROR);
    break;
}
//Check watchdog
if ((test_time % 5000) < 1000)
{
    expv2_uart_send(SERIALPORT_TESTPROG,sizeof(msgTP),(unsigned char*) &msgTP);
}

//%%%%%%%%%%%%%%%%%%% DEBUG %%%%%%%%%%%%%%%%%%%
    /*
    DebugVecFloat[0] = ctrlState[POS_X];
    DebugVecFloat[1] = ctrlState[POS_Y];
    DebugVecFloat[2] = ctrlState[POS_Z];
    DebugVecFloat[3] = ctrlState[VEL_X];
```

```
        DebugVecFloat[4] = ctrlState[VEL_Y];
        DebugVecFloat[5] = ctrlState[VEL_Z];
        DebugVecFloat[6] = (float)test_time/1000;
        DebugVecFloat[7] = (float)maneuver_time/1000;
        commSendPacket(COMM_CHANNEL_STL, GROUND, 0, COMM_CMD_DBG_FLOAT, (unsigned char *)
            DebugVecFloat, 0);

        DebugVecShort[0] = (short) maneuver_number;
        DebugVecShort[1] = (short) (ctrlStateError[POS_X]*10000);
        DebugVecShort[2] = (short) (ctrlStateError[POS_Y]*10000);
        DebugVecShort[3] = (short) (ctrlStateError[POS_Z]*10000);
        DebugVecShort[4] = (short) (ctrlStateError[RATE_X]*10000);
        DebugVecShort[5] = (short) (ctrlStateError[RATE_Y]*10000);
        DebugVecShort[6] = (short) (ctrlStateError[RATE_Z]*10000);
        DebugVecShort[7] = (short) (GogglesAttached);
        commSendPacket(COMM_CHANNEL_STL,GROUND,0, COMM_CMD_DBG_SHORT_SIGNED, (unsigned
            char *) DebugVecShort, 0);

        dbgThrusterTimesPackFull(&DebugVecUShort[0], firing_times);
        commSendPacket(COMM_CHANNEL_STL,GROUND,0, COMM_CMD_DBG_SHORT, (unsigned char *)
            DebugVecUShort, 0);
        */
}

void gspVERTIGOManeuver_ProcessRXData(default_comm_packet packet)
{
    //send to daemon serial port
    expv2_uart_send(SERIALPORT_DAEMON,37,packet);
}

void gspProcessUART_GogglesDaemon(unsigned char source,unsigned char *dataPacket,unsigned
    int length)
{
    dbg_ushort_packet dbg = {0};
    unsigned char datamsg[32] = {0};
    msg_spheres_id msg = {0};

    if ((length == 1) && (*dataPacket == 0xA1)) {
        //message requests spheres id
        msg.to = ANY_GOGGLES;
        msg.from = commHWAddrGet();
        msg.ID= SPHERE_ID_REQUEST;
        msg.spheresLogicID = (unsigned char) sysIdentityGet();
        msg.programID = PROG_ID;
        expv2_uart_send(SERIALPORT_DAEMON,sizeof(msg),(unsigned char*) &msg);

        //send debug vector
        memcpy(&dbg,&msg, sizeof(msg));
        commSendRFMPacket(COMM_CHANNEL_STL, GROUND, COMM_CMD_DBG_SHORT_UNSIGNED, (unsigned
            char *) dbg, 0);
    }
    else {
        /* Send the packet to GROUND over the RF */
        memcpy(datamsg, dataPacket, length <= 32 ? length: 32);
        commSendRFMPacket(COMM_CHANNEL_STL, GROUND, COMM_CMD_GOGGLES_PAYLOAD, datamsg, 0);
    }
}

void gspProcessUART_TestProgram(unsigned char source,unsigned char *dataPacket,unsigned
    int length)
{
    int counter = 0;

    if (initTest != 1)
    {
        for (counter = 0;counter<length;counter++)
        {
            if ((dataPacket[counter] == START_BYTE) && (!packet_buffer_length))
```

```
            {
                packet_buffer[0] = dataPacket[counter];
                packet_buffer_length++;
            }
            else if (packet_buffer_length)
            {
                packet_buffer[packet_buffer_length++] = dataPacket[counter];
            }

            if ((packet_buffer_length >= 2) && (packet_buffer_length == (int)packet_buffer
                [1] + sizeof(msg_header)))
            {
                parsePacket(packet_buffer);
                packet_buffer_length = 0;
            }
            else if (packet_buffer_length >= max_length)
            {
                packet_buffer_length = 0;
            }
        }
    }

}

void parsePacket(unsigned char *dataPacket)
{
    msg_header *msg;
    msg_body_forces_torques *msgData;
    msg_body_tgt_location *msgLoc;
    msg_terminate_test *msgTerm;
    dbg_ushort_packet dbg = {0};

    msg = (msg_header *)dataPacket;

        if ((msg->startByte == START_BYTE) && (msg->from == FROM_GOGGLES))
        {
            switch (msg->ID){
            case TERMINATE_TEST:
                    msgTerm = (msg_terminate_test *)&dataPacket[sizeof(msg_header)];
                    initTest = 0;
                    ctrlTestTerminate(msgTerm->return_code);
                    //send debug vector
                    memcpy(&dbg,&msg, sizeof(msg));
                    commSendRFMPacket(COMM_CHANNEL_STL, GROUND,
                        COMM_CMD_DBG_SHORT_UNSIGNED, (unsigned char *) dbg, 0);
                break;
            case FORCES_TORQUES:
                    msgData = (msg_body_forces_torques *)&dataPacket[sizeof(msg_header)];
                    //copy forces and torques
                    memcpy(forces, msgData->forces,sizeof(float)*3);
                    memcpy(torques, msgData->torques,sizeof(float)*3);
                    //send debug vector
                    memcpy(&dbg,&msg, sizeof(msg));
                    commSendRFMPacket(COMM_CHANNEL_STL, GROUND,
                        COMM_CMD_DBG_SHORT_UNSIGNED, (unsigned char *) dbg, 0);
                break;
            case TGT_POSITION:
                    msgLoc = (msg_body_tgt_location *)&dataPacket[sizeof(msg_header)];
                    memcpy(position, msgLoc->xyzPos,sizeof(float)*3);
                    memcpy(velocity, msgLoc->xyzVel,sizeof(float)*3);
                    memcpy(&dbg,&msg, sizeof(msg));
                    commSendRFMPacket(COMM_CHANNEL_STL, GROUND,
                        COMM_CMD_DBG_SHORT_UNSIGNED, (unsigned char *) dbg, 0);
                break;
            case WATCHDOG_REPLY:
                //Reset watchdog timer
                GogglesAttached = 1;
                watchdog_flag = 0;
```

```
                break;
            }

    }
}


void changetoBodyFrame(state_vector TargetState, state_vector InspectorState, float *
    vectorOut, unsigned int vectorType)
{
    /*  TargetState and InspectorState begins in global frame
    *   ...convert to body frame:
    *  POS are in global
    *  VEL are in global
    *  QUAT are from global frame to body frame
    *  RATE are in body
    * We will use the quaternions to take the postion and velocity vectors
    * from the global frame to the body frame
    */

    float R_temp[3];
    float RBody[3];
    float cross[3];
    float V_temp[3];
    float mat[3][3];

    switch (vectorType){
    case POSITION_VECTOR:
        //Make measurements relative:
        //Moves about point at center of volume (0,0,0)
        R_temp[0] = TargetState[POS_X] - InspectorState[POS_X];
        R_temp[1] = TargetState[POS_Y] - InspectorState[POS_Y];
        R_temp[2] = TargetState[POS_Z] - InspectorState[POS_Z];
        //Move to INSP Body Frame
        quat2matrixIn(mat, &InspectorState[QUAT_1]);//MAT <= rotation matrix from global
            to INSP body
        mathMatVecMult(RBody, (float**)mat, R_temp, 3, 3);
        vectorOut[0] = RBody[0];//POS_X
        vectorOut[1] = RBody[1];//POS_Y
        vectorOut[2] = RBody[2];//POS_Z
        break;
    case VELOCITY_VECTOR:
        //V = Rot*(r') - wx(Rot(r)))
        InspectorState[VEL_X]  = TargetState[VEL_X] - InspectorState[VEL_X];
        InspectorState[VEL_Y]  = TargetState[VEL_Y] - InspectorState[VEL_Y];
        InspectorState[VEL_Z]  = TargetState[VEL_Z] - InspectorState[VEL_Z];
        mathMatVecMult(V_temp, (float**)mat, &InspectorState[VEL_X], 3, 3);
        mathVecCross(cross, &InspectorState[RATE_X], &InspectorState[POS_X]);
        vectorOut[0] = V_temp[0] - cross[0];//VEL_X
        vectorOut[1] = V_temp[1] - cross[1];//VEL_Y
        vectorOut[2] = V_temp[2] - cross[2];//VEL_Z
        break;
    case ACCEL_VECTOR:
        vectorOut[0] = 0.0f;
        vectorOut[1] = 0.0f;
        vectorOut[2] = 0.0f;
        break;
    case ROTATION_VECTOR:
        //Move TGT Rot in TGT Body to INSP Body
        R_temp[0] = TargetState[RATE_X];//Get TGT Rotation Rates in TGT Body Frame
        R_temp[1] = TargetState[RATE_Y];
        R_temp[2] = TargetState[RATE_Z];
        quat2matrixOut(mat, &TargetState[QUAT_1]);//MAT <= rotation matrix from TGT Body
            to Global
        mathMatVecMult(RBody, (float**)mat, R_temp, 3, 3); //TGT Body to Global
        R_temp[0] = RBody[0];
        R_temp[1] = RBody[1];
        R_temp[2] = RBody[2];
```

```
        memset(RBody,0,sizeof(float)*3);
        quat2matrixIn(mat, &InspectorState[QUAT_1]);//MAT <= rotation matrix from global
            to INSP body
        mathMatVecMult(RBody, (float**)mat, R_temp, 3, 3); //Global to INSP Body
        //vectorOut = ROT_RATE_DIR[0-2]
        vectorOut[0] = RBody[0];//X.
        vectorOut[1] = RBody[1];//Y
        vectorOut[2] = RBody[2];//Z
        //Find Magnitude
        //ROT_RATE_TGT
        vectorOut[3] = (float)sqrt(vectorOut[0]*vectorOut[0] + vectorOut[1]*vectorOut[1] +
            vectorOut[2]*vectorOut[2]);
        break;
    default:
        initTest = 0;
        ctrlTestTerminate(13);//ERROR: Incorrect call to changetoBodyFrame
        break;
    }
}
```

THIS PAGE INTENTIONALLY LEFT BLANK

# Appendix B

# VERTIGO System Requirements

## The VERTIGO Project

VERTIGO is a DARPA-funded project which combines the knowledge of the MIT Space Systems Laboratory with the flight hardware experience of Aurora Flight Sciences in a partnership to upgrade the current SPHERES testbed on the International Space Station. Launched in 2006, SPHERES is a 6-degree of freedom control and navigation testbed which has proved invaluable to scientists and engineers seeking to test algorithms in a microgravity environment. VERTIGO seeks to add visual navigation to the capabilities of SPHERES by adding a set of "Goggles" which combine a pair of cameras for stereo vision with processing and communications hardware upgrades. Individually, these two items are called the camera and avionics stack.

## Primary Mission Objectives

The Primary Mission Objective of the VERTIGO Program is to upgrade the SPHERES satellites to enable the rapid and flexible research and development (R&D) of Vision-Based Navigation (VBN) Algorithms in a "shirt-sleeve micro-gravity environment" inside the International Space Station. Specifically, VERTIGO will allow one or two SPHERES satellites to construct a 3D model of an unknown object (possibly moving and tumbling) without any *a priori* state knowledge. Two inspector SPHERES satellites will perform relative navigation solely by sensory reference to the target object. The performance of this algorithm will be verified using the SPHERES Global Metrology System and a CAD model of the target object. [PMO]

This can be summarized as follows:

1. Develop an algorithm to construct a 3D map of an object and use the map for relative navigation. [MO 1]
2. Rapid Research and Development of Vision-Based Navigation. [MO 2]
3. Flexible Research and Development of Vision-Based Navigation. [MO 3]

## Definitions

1. "**Rapid**" – in the context of R&D for VBN, rapid implies that algorithms should be able to be developed by a small research team working during an academic year with results obtained within an academic semester.
2. "**Flexible**" – The VERTIGO System must allow different types of vision-based navigation algorithms to test the relative advantages and disadvantages of each approach.
3. **The VERTIGO System (the System)**: comprises the SPHERES satellite(s), attached Goggles, the Flight GUI on the Space Station/Express Rack Computer (SSC/ERC), and support equipment.
4. **SPHERESCore Software**: that software which exists within the SPHERES Satellites, independent of any peripheral hardware.
5. **The Flight GUI**: the software onboard the SSC/ERC which allows astronauts onboard the ISS to interact with the SPHERES testbed and related hardware.
6. **The Goggles Onboard Software**: the software which is loaded onto the Goggles and exists independent of the SPHERE that the Goggles are attached to.

## Reference Documents

*Reference documents will be used in their current state as of 12 April 2011.*

1. **SSP 57000**, Pressurized Payloads Interface Requirements Document, International Space Station Program
2. **SSP 50313**, Display and Graphics Commonality Standard (DGCS)
3. **SSP 50835**, ISS Pressurized Volume Hardware, Common Interface Requirements Document
4. **SSP 51700**, Payload Safety Policy and Requirements for the International Space Station
5. **JSC 20793**, Crewed Space Vehicle Battery Safety Requirements

## System Requirements

1. The VERTIGO System must use cameras to estimate the structure of an object with no *a priori* knowledge of that object. [SR 10]
   *Rationale: this derives from Mission Objective (MO) 1.*
2. The VERTIGO System must use cameras to estimate the angular and translational velocities of the inspected object. [SR 20]
   *Rationale: this derives from MO 1.*
3. Two inspector SPHERES must navigate around the inspected object using its estimated structure and velocities. [SR 30]
   *Rationale: this derives from MO 1.*
4. The System must be able to upload and run new tests and download data from tests. [SR 40]
   *Rationale: this derives from MO 3.*
5. The VERTIGO Goggles must attach to the existing SPHERES Satellites and be compatible with the SPHERES Flight GUI. [SR 50]
   *Rationale: this derives from the Primary Mission Objectives (PMO) and MO 2.*
6. The VERTIGO System must be operated by astronauts inside the International Space Station. [SR 60].
   *Rationale: this derives from the PMO.*

## Functional Requirements

1. The VERTIGO System must use cameras to estimate in 3 dimensions the structure of an object with no *a priori* knowledge of that object.
    a. An observing SPHERES satellite must use only onboard cameras, accelerometers, gyroscopes, and knowledge of its own dynamics in constructing the estimated structure. [FR 10]
        *Rationale: These restrictions are from the PMO.*
    b. The algorithm must use one or two SPHERES satellites in the development of the 3D model. [FR 20]
        *Rationale: this requirement flows directly from the PMO.*
    c. The System must sense depth and light intensity of scenes including the target object. [FR 30]
    d. The System must process the sensor information to obtain depth and light information. [FR 40]
    e. The System must store the 3D structure representation of the inspected object. [FR 50]
2. The VERTIGO System must use cameras to estimate the angular and translational velocities of the inspected object.
    a. The System must be able to identify features. [FR 60]
    b. The System must be capable of tracking features on the object at TBD ms intervals as the object moves at no more than TBD radians per second and TBD meters per second. [FR 70].
    c. The system must store estimated angular and translational velocities of the inspected object. [FR 80]
3. Two inspector SPHERES must navigate around the inspected object using the knowledge of its structure and velocities.
    a. The 3D model must be accurate enough to safely navigate around another satellite (TPM 01: 5cm). [FR 90]
    b. Inspecting SPHERES satellites must be able to share real-time video between their attached Goggles with no loss of pixel information. [FR 100]
        *Rationale: in order to develop a map jointly, known vision-based navigation algorithms require this information to be shared between the two inspectors.*
    c. The VERTIGO Team must supply at least two (2) SPHERES Goggles for launch to the International Space Station. [FR 110]
        *Rationale: the requirement to use 2 SPHERES as inspectors implies a need for at least 2 Goggles to be launched.*
4. The System must be able to upload and run new tests and download data from tests.
    a. The VERTIGO System must provide methods for new algorithms to be programmed. [FR 120]
        *Rationale: this is to support the flexibility MO.*
    b. THE VERTIGO System must provide a method for new programs to be uploaded to the ISS compatible with the existing SPHERES upload procedures. [FR 130]
    c. The VERTIGO System aboard the ISS must be able to load the new programs in a method compatible with the existing SPHERES loading procedures. [FR 140]
    d. Data must be stored onboard the VERTIGO System until it can be downloaded to Ground. [FR 150]
    e. Data must be stored in files that can be downloaded using existing ISS wireless communications infrastructure. [FR 160]

*Rationale: this allows rapid testing MO.*

5. The VERTIGO Goggles must attach to the existing SPHERES Satellites and be compatible with the SPHERES Flight GUI.
    a. The Goggles must connect electrically and mechanically to the SPHERES satellite only via the expansion port (CSAC launched). [FR 170]
    b. The center of mass of the SPHERES-Goggles system must not shift more than 5 cm from the center of mass of the SPHERE as per the SPHERES Expansion Port ICD. [FR 180]
    c. The Goggles must not obstruct the SPHERES thrusters as per the SPHERES Expansion Port ICD. [FR 190]
    d. The SPHERES-Goggles system must retain the ability to use the ultrasound system as a truth sensor. [FR 200]

        *Rationale: this is necessary for navigation, timing, and for determining the fidelity of the navigation using relative navigation. Need for truth sensor comes from PMO.*
    e. The Goggles must be capable of interfacing across the SPHERES serial interface ports in order to share data, timing and status information between the SPHERES satellites and the Goggles. [FR 210]

        *Rationale: Goggles are a sensor and SPHERES satellite has the actuators.*
    f. A VERTIGO visualization tool must be added to the Flight GUI visualization area to display image data from the Goggles. No other graphical elements of the Flight GUI can change. [FR 220]
    g. The VERTIGO System must use the same test management as the SPHERES Flight GUI. [FR 230]
    h. The VERTIGO Team must develop software that runs onboard the Goggles and allows for communication between the Goggles and the VERTIGO visualization tool. [FR 240]
6. The VERTIGO System must be operated by astronauts inside the International Space Station.
    a. Tests using the SPHERES Goggles must be able to be conducted within a 3 hour test session. [FR 250]

        *Rationale: To support MO 2, it must be possible to schedule test sessions that fit in the ISS schedule. Historically, these must be within 2-3 hours of science time.*
    b. The Goggles must have an Astronaut interface panel that complies with NASA safety requirements. [FR 260]

        *Rationale: these safety requirements are defined by SSP 57000 HFIT (Human Factors Interface Team) requirements. Crew interface must be approved by the IPLAT (ISS Payload Label Approval Team).*
    c. Goggles must be capable of surviving transportation and launch loads to reach the ISS as defined by SSP 50835. [FR 270]
    d. Goggles must be capable of surviving environmental conditions onboard the ISS as defined by SSP 50835. [FR 280]
    e. The System must comply with safety requirements enumerated for free-flying payloads for human spaceflight onboard the International Space Station in SSP 51700. [FR 290]
    f. Astronauts must be able to view live video or algorithm output from the Goggles during operation. [FR 300]

## Subsystem Requirements

1. The VERTIGO System must use cameras to estimate in 3 dimensions the structure of an object with no *a priori* knowledge of that object.
    a. An observing SPHERES satellite must use only onboard cameras, accelerometers, gyroscopes, and knowledge of its own dynamics in constructing the estimated structure.
    b. The algorithm must use one or two SPHERES satellites in the development of the 3D model.
        i. The SPHERES Goggles must be able to pass sensor data between them. [SSR 10]
        ii. The SPHERES Goggles must be able to provide accurate timestamps for shared information. [SSR 20]
    c. The System must sense depth and light intensity of scenes including the target object.
        i. The System must use stereo cameras. [SSR 30]
            *Rationale: trinocular cameras offer the same benefits as stereo cameras, but do so at a mass cost which conflicts with the mass requirement levied by the requirement to attach to SPHERES.*
            1. Lenses selected for the cameras must be capable of surviving the launch environment such that software correction allows for 1-pixel accuracy. [SSR 30.10]
                *Rationale: it is unlikely that the lenses will remain fully calibrated on orbit, and therefore there is a need to provide some sort of calibration method after delivery to ISS.*
        ii. The onboard Goggles must have a wide view angle lens of 45 degrees (half-cone) or greater. [SSR 40]
    d. The System must process the sensor information to obtain depth and light information.
        i. Goggles must have its own processor independent of SPHERES. [SSR 50]
            *Rationale: the SPHERES processor is insufficient for running visual navigation algorithms and the related peripherals, including the cameras.*
            1. The processor must have greater than 2GB of RAM. [SSR 50.10]
    e. The System must store the 3D structure representation of the inspected object.
        i. The 3D model must be compared to the actual target offline to determine the accuracy of the mapping algorithm. [SSR 60]
            *Rationale: required to meet the PMO.*
2. The VERTIGO System must use cameras to estimate the angular and translational velocities of the inspected object.
    a. The System must be able to identify features.
        i. The Goggles must be able to resolve objects of 5 cm on the inspected object. [SSR 70]
    b. The System must be capable of tracking features on the object at TBD ms intervals as the object moves at no more than TBD radians per second and TBD meters per second.
        i. The Goggles must be able to capture and process images at TBD fps or greater. [SSR 80]
    c. The system must store estimated angular and translational velocities of the inspected object.
3. Two inspector SPHERES must navigate around the inspected object using the knowledge of its structure and velocities.
    a. The 3D model must be accurate enough to safely navigate around another satellite (TPM 01: 5cm).

i. The estimated trajectory must be compared to the ultrasonic time-of-flight "ground truth" provided by the global metrology system. [SSR 90]
ii. Cameras must be able to track 5 cm point features in the image and compute stereo disparity in ISS interior lighting conditions for motion of less than 5 cm/s and 6 deg/s at distances between 50 cm and 3 m. [SSR 100]

*Rationale: Numbers are based on a 1 meter diameter circle in 60 seconds. Lighting conditions are defined in reference documents (SSPs).*

1. Cameras must have a minimum of 640x480 resolution for use in the developed algorithms. [SSR 100.10]
2. If optical testing of the algorithms show it to be necessary, the Goggles must include an illuminating LED light which meets SSP 51700 and SSP 57000, with the appropriate power regulators. [SSR 100.20]

b. Inspecting SPHERES satellites must be able to share real-time video between their attached Goggles with no loss of pixel information.
i. The data transfer method between inspector SPHERES must operate with a latency of TBD ms or less. [SSR 110]
ii. A wireless data link of at least 70 Mbps within the test volume must be available between the two inspector SPHERES. [SSR 130]

*Rationale: a minimum link of 35 Mbps (bidirectionally) is needed to share the expected amount of real-time video coming from the Goggles. This is derived from 10fps, 640x480 8-bit grayscale images that are losslessly compressed. Wireless is necessary because wires running to a SPHERE would severely inhibit its ability to build a 3D map and maneuver around the test volume.*

1. The Goggles must use 802.11n or similar architectures to communicate. [SSR 130.10]

*Rationale: 802.11n is the only currently available 802.11 standard which allows for bi-directional rates at or above 70 Mbps.*

c. The VERTIGO Team must supply at least two (2) SPHERES Goggles for launch to the International Space Station.

4. The System must be able to upload and run new tests and download data from tests.
a. The VERTIGO System must provide methods for new algorithms to be programmed.
b. THE VERTIGO System must provide a method for new programs to be uploaded to the ISS compatible with the existing SPHERES upload procedures.
i. There must be a method for libraries installed on the Goggles to be updated while on station. [SSR 140]

*Rationale: to meet MO 3 while satisfying MO 2, as new open source libraries become available, updating those on the ISS should be possible.*

ii. The Goggles disk image must be able to be completely replaced. [SSR 150]
1. The disk image must be able to be connected directly to the SSC/ERC. [SSR 150.10]
2. The Flight GUI must provide a mechanism for reimaging a disk that is connected to the SSC/ERC. [SSR 150.20]

c. The VERTIGO System aboard the ISS must be able to load the new programs in a method compatible with the existing SPHERES loading procedures.
i. The VERTIGO Goggles must have a method of receiving new programs from the SSC/ERC. [SSR 160]

d. Data must be stored onboard the VERTIGO System until it can be downloaded to Ground.
    i. Goggles must have a hard disk (HD) of at least 16GB. [SSR 170]
        *Rationale: During a test session, at least 13GB of data is expected to be generated. This is computed based on four (4) 640x480 8-bit images at 10 fps for 20 minutes.*
e. Data must be stored in files that can be downloaded using existing ISS wireless communications infrastructure.
    i. Data from SPHERES must reside in an acceptable file format as per Ground Rules & Constraints document. [SSR 180]
    ii. Files must be of an acceptable file size as per Ground Rules & Constraints document. [SSR 190]

5. The VERTIGO Goggles must attach to the existing SPHERES.
    a. The Goggles must connect electrically and mechanically to the SPHERES satellite only via the expansion port (CSAC launched).
        i. Goggles power must be provided by the Goggles system. [SSR 200]
            *Rationale: the power that can be supplied through the expansion port is insufficient for the Goggles processing needs.*
    b. The center of mass of the SPHERES-Goggles system must not shift more than 5 cm from the center of mass of the SPHERE as per the SPHERES Expansion Port ICD.
        i. SPHERES Goggles hardware must have a mass less than 1.5 kg. [SSR 210]
            *Rationale: based on the dry mass distribution, a mass of more than 1.5 kg will shift the center of mass beyond the 5 cm limit enumerated above.*
    c. SPHERES thrusters must be unobstructed by the Goggles as per the SPHERES Expansion Port ICD.
        i. The Goggles must remain outside of a TBD volume around the SPHERES Thrusters. [SSR 220]
        ii. Communication within the VERTIGO System must be wireless. [SSR 230]
            *Rationale: wires connected to the satellites will impede control. Need this requirement to support rapid MO.*
    d. The SPHERES-Goggles system must retain the ability to use the ultrasound system as a truth sensor.
        i. The Goggles must remain outside of a TBD volume around SPHERES ultrasonic microphones as per the SPHERES Expansion Port ICD. [SSR 240]
        ii. The Goggles must remain outside of a TBD volume around the SPHERES IR beacon as per the SPHERES Expansion Port ICD. [SSR 250]
    e. The Goggles must be capable of interfacing across the SPHERES serial interface ports in order to share data, timing and status information between the SPHERES satellites and the Goggles.
        i. Attached Goggles must be capable of accepting IMU data transmitted from SPHERES at a rate of at least 20 Hz and with a timestamp that is accurate to at least TBD ms. [SSR 260]
            *Rationale: these standards are already able to be met by SPHERES, acting in concert with the ultrasonic global metrology system. Delays greater than TBD ms are expected to impact the fusion of the IMU and vision data.*
        ii. IMU data must have a latency of no more than 5 ms or no more than 2 ms latency added on top of transmission time. [SSR 270]

*Rationale: greater latency severely limits the controllability of SPHERES.*

iii. Goggles onboard software must be able to command thruster firings on SPHERES. [SSR 280]

*Rationale: because the VBN algorithm will be supplying much of the information required to navigate and processing that information is computationally intensive, commands using that information will have to come from the Goggles.*

f. A VERTIGO visualization tool must be added to the Flight GUI visualization area to display image data from the Goggles. No other graphical elements of the Flight GUI can change.

i. The Flight GUI must include software to interface with the Goggles over a communications link of at least 70 Mbps. [SSR 290]

*Rationale: to download information at the end of a test session and to allow for streaming of video from inspector Goggles, the communications link should be at least 70 Mbps for the reasons listed elsewhere. The Software must be able to support that rate.*

ii. The visualization tool must meet SSP 50313, Display and Graphics Commonality Standard (DGCS). [SSR 300]

g. The VERTIGO System must use the same test management as the SPHERES Flight GUI.

i. Flight Software must be capable of stopping a test program in conjunction with commands from the Flight GUI relayed through the SPHERES satellite. [SSR 310

ii. Commands running between SPHERES and the Goggles must be transmitted at a speed of at least 115.2 kbps. [SSR 320]

h. The VERTIGO Team must develop software that runs onboard the Goggles and allows for communication between the Goggles and the VERTIGO visualization tool.

6. The VERTIGO System must be operated by astronauts inside the International Space Station.

a. Tests using the SPHERES Goggles must be able to be conducted within a 3 hour test session.

i. The onboard Goggles must be capable of running for TBD hour(s) or more using onboard battery power. [SSR 330]

*Rationale: to meet MO 3, battery life must be sufficiently long that 3-4 hour test sessions can deliver results. Batteries lasting less than this limit restrict that mission.*

ii. The Goggles must use a battery system that is rechargeable on station. [SSR 340]

iii. The Goggles must use a battery system that meets SSP 51700, SSP 57000, and JSC-20793. [SSR 350]

iv. The Goggles must communicate with the SSC/ERC and other Goggles using a high speed wireless link such as 802.11n. [SSR 360]

*Rationale: the need to transmit large amounts of data at the end of a test session requires a rate of at least 70 Mbps in order to download data in 15 minutes or less. This rate will be necessary to keep overhead low during an allotted test session. Further, the connection must be wireless to increase astronaut effectiveness and to eliminate disturbances during maneuvers.*

b. The Goggles must have an astronaut interface panel that complies with NASA safety requirements.

i. **The astronaut interface panel must have an on/off switch. [SSR 370]**
ii. **The astronaut interface panel must have a reset button. [SSR 380]**

c. Goggles must be capable of surviving transportation and launch loads to reach the ISS as defined by SSP 50835.
d. Goggles must be capable of surviving environmental conditions onboard the ISS as defined by SSP 50835.
e. The System must comply with safety requirements enumerated for free-flying payloads for human spaceflight onboard the International Space Station in SSP 51700.
f. Astronauts must be able to view live video or algorithm output from the Goggles during operation.
    i. **The Goggles onboard software must provide a low resolution/low bandwidth video display of the Goggles Algorithms for the astronauts to monitor using the VERTIGO visualization tool. [SSR 390]**

        ***Rationale: video output from the Goggles allows algorithm performance feedback from astronauts.***

# Bibliography


[1] R. R. Britt. Is Hubble Worth the Upgrade Mission's Risk and Cost? `http://www.livescience.com/3579-hubble-worth-upgrade-mission-risk-cost.html`, 2011. [online periodical].

[2] D. Leone. NASA: James Webb Telescope Expected to Cost $8.7 Billion. `http://spacenews.com/civil/110826-jwst-cost-billion.html`, 2009. [online periodical].

[3] A. E. Turner. Cost-Effective Spacecraft Dependent Upon Frequent Non-Intrusive Servicing. AIAA, August 28-30 2001.

[4] Broad Agency Announcement: Phoenix Technologies. DARPA-BAA-12-02, 2011. DARPA-BAA-12-02.

[5] J. L. Ruiz and C. H. Frey. Geosynchronous Satellite Use of GPS. pages 1227–1232, 2005.

[6] Global Positioning System Standard Positioning Service Performance Standard, 2008.

[7] I. Nygren and M. Jansson. Terrain navigation for underwater vehicles using the correlator method. *Oceanic Engineering, IEEE Journal of*, 29(3):906 – 915, july 2004.

[8] K Machida. Space test of sensor-fused telerobotics for high-precision tasks. *Journal of Spacecraft and Rockets*, 41(1):132–139, 2004.

[9] Deborah Meduna. *Terrain relative navigation for sensor-limited systems with application to underwater vehicles*. Phd, Stanford University, 08/2011 2011.

[10] J. P. Curran D. S. Moyer R. L. Strachan I. Mills D. P. Goodwin, L. E. Hembree and J.-S. Valois. Orbiter space vision system on space shuttle flight sts-80. *SPIE*, 3074:18–28, 1997.

[11] R.T. Howard, A.F. Heaton, R.M. Pinson, and C.K. Carrington. Orbital Express Advanced Video Guidance Sensor. In *Aerospace Conference, 2008 IEEE*, pages 1 –10, march 2008.

[12] Daniel Sheinfeld and Stephen M. Rock. Rigid Body Inertia Estimation with Applications to the Capture of a Tumbling Satellite. February 2009.

[13] Peter Kimball. *Iceberg-Relative Navigation for Autonomous Underwater Vehicles*. Phd, Stanford University, Stanford, CA, 08/2011 2011.

[14] Peter Kimball and Stephen M. Rock. Sonar-based iceberg-relative navigation for autonomous underwater vehicles. *Deep Sea Research Part II: Topical Studies in Oceanography*, 58(11-12):1301 – 1310, 2011. Free-Drifting Icebergs in the Southern Ocean.

[15] Kiran Murthy and Stephen M. Rock. Navigation for Performing Visual Surveys of Non-Planar Surfaces. In *Proceedings of AIAA Guidance, Navigation, and Control Conference*, 2009.

[16] Kiran Murthy and Stephen M. Rock. Spline-based Trajectory Planning Techniques for Benthic AUV Operations. In *Proceedings of IEEE Autonomous Underwater Vehicles Conference*, 2010.

[17] O. Yakimenko G. Boyarko and M. Romano. Optimal Rendezvous Trajectories of a Controlled Spacecraft and a Tumbling Object. *AIAA Journal of Guidance, Control, and Dynamics*, 34(4):1239–1252, July-August 2011.

[18] J. L. Crassidis R. Linares and Y. Cheng. Constrained Relative Attitude Determination for Two-Vehicle Formations. *AIAA Journal of Guidance, Control, and Dynamics*, 34(2):543–553, March-April 2011.

[19] H. B. Hablani. Autonomous Inertial Relative Navigation with Sight-Line-Stabilized Integrated Sensors for Spacecraft Rendezvous. *AIAA Journal of Guidance, Control, and Dynamics*, 32(1):172–183, January-February 2009.

[20] A. Weichbrod J. DiMatteo, D. Florakis and M. Milam. Proximity Operations Testing with a Rotating and Translating Resident Space Object. August 10-13 2009.

[21] Kiran Murthy. A Trajectory Optimization Method for Close Range Surveys of Non-Planar Surfaces. Master's thesis, Stanford University, 03/2012 2012.

[22] B. K. P. Horn. *Robot Vision*. MIT Press, 1998.

[23] David G. Lowe. Distinctive Image Features from Scale-Invariant Keypoints. *Int. J. Comput. Vision*, 60(2):91–110, November 2004.

[24] Allen Chen. Propulsion System Characterization for the SPHERES Formation Flight and Docking Testbed. Master's thesis, Massachusetts Institute of Technology, May 2002. S.M. Thesis.

[25] Reaction Control System. `http://science.ksc.nasa.gov/shuttle/technology/sts-newsref/sts-rcs.html`, 1988/2000.

[26] V. Zalgaller. Shortest Inspection Curves for the Sphere. *Journal of Mathematical Sciences*, 131:5307–5320, 2005. 10.1007/s10958-005-0403-9.

[27] Paul Bourke. Baseball seam curve. `http://paulbourke.net/geometry/baseball/`, January 2001.

[28] Simon Nolet. *Development of a Guidance, Navigation and Control Architecture and Validation Process Enabling Autonomous Docking to a Tumbling Satellite*. Scd, Department of Aeronautics and Astronautics, Massachusetts Institute of Technology, Cambridge, MA, 2007.

[29] Simon Nolet. The SPHERES Navigation System: from Early Development to On-Orbit Testing. *AIAA Guidance, Navigation and Control Conference and Exhibit*, August 20-23 2007.

[30] Brent E Tweddle, Alvar Saenz-Otero, and David W Miller. Design and Development of a Visual Navigation Testbed for Spacecraft Proximity Operations. In *AIAA SPACE 2009 Conference Exposition*, number September. American Institute of Aeronautics and Astronautics, 2009.

[31] Bill Triggs, Philip McLauchlan, Richard Hartley, and Andrew Fitzgibbon. Bundle Adjustment — A Modern Synthesis. In Bill Triggs, Andrew Zisserman, and Richard Szeliski, editors, *Vision Algorithms: Theory and Practice*, volume 1883 of *Lecture Notes in Computer Science*, pages 153–177. Springer Berlin / Heidelberg, 2000.

[32] R. Smith, M. Self, and P. Cheeseman. Autonomous robot vehicles. chapter Estimating uncertain spatial relationships in robotics, pages 167–193. Springer-Verlag New York, Inc., New York, NY, USA, 1990.

[33] Brent Tweddle. Relative Computer Vision Based Navigation for Small Inspection Spacecraft. Aug 8-11 2011.

[34] Brent Tweddle. Computer Vision Based Navigation for Spacecraft Proximity Operations. Master's thesis, Department of Aeronautics and Astronautics, Massachusetts Institute of Technology, 2010. S.M. Thesis.

[35] Oliver J. Woodman. An introduction to inertial navigation. Technical Report 696, University of Cambridge Computer Laboratory, 15 JJ Thomson Avenue, Cambridge CB3 0FD, United Kingdom, August 2007.

[36] SPHERES Fact Sheet, May 20 2007.